University of Wisconsin Milwaukee

UWM Digital Commons

December 2021

Transport and Fate of Phosphorus in the Nearshore Zone of Lake Michigan

NATHAN VAN EE
University of Wisconsin-Milwaukee

Follow this and additional works at: https://dc.uwm.edu/etd

Part of the Ecology and Evolutionary Biology Commons, Environmental Sciences Commons, and the Fresh Water Studies Commons

TRANSPORT AND FATE OF PHOSPHORUS IN THE NEARSHORE ZONE OF LAKE MICHIGAN

by

Nathan Van Ee

A Thesis Submitted in

Partial Fulfillment of the

Requirements for the Degree of

Master of Science

in Freshwater Sciences

at

The University of Wisconsin-Milwaukee

December 2021

ABSTRACT

TRANSPORT AND FATE OF PHOSPHORUS IN THE NEARSHORE ZONE OF LAKE MICHIGAN

by

Nathan Van Ee

The University of Wisconsin-Milwaukee, 2021
Under the Supervision of Professor Harvey Bootsma

Bioavailable phosphorus loads exported to Lake Michigan from the Milwaukee and Sheboygan River Watersheds appear to have increased in the last 40 years despite meeting total phosphorus (TP) loading goals set by the Great Lakes Water Quality Agreement (GLWQA).

Overall, bioavailability of P delivered from the Milwaukee and Sheboygan Rivers was highest during the warmer months, which coincides with the nearshore nuisance algae growth season. However, first order loss rates of SRP calculated during baseflow recession were also greatest during the summer, suggesting that increased river residence time during the summer could reduce export of bioavailable P.

Observations of phosphorus partitioning combined with historic USGS monitoring data parallels trends seen in several Lake Erie watersheds with an increase in soluble reactive phosphorus (SRP) and decreases in particulate phosphorus (PP) export. Suspended sediment loads from the Milwaukee and Sheboygan watersheds are relatively P rich (mean 2.3 ± 0.66 ugP/mg) and relatively bioavailable at 39% and 33% respectively (using NaOH-extractable P as

an index of bioavailability). Incubation experiments showed that over time river PP, and in particular NaOH-extractable P, releases P to the SRP pool.

A seasonal increase in the PP:SRP ratio parallels increases in the percent bioavailability within the particulate P pool due to an increased contribution of NaOH-extractable P. This pattern coincides somewhat with prevalent midwest land use practices such as harvest of grain corn, but may also be driven by a combination of temperature and pH dependent coprecipitation and sorption phosphate buffering mechanisms on fine-grained particles that move SRP to the PP pool. However, this phosphate buffering mechanism may be offset by land use practices that increase soil P-Content, reducing the number of SRP sorption sites on particles. Moreover, P-rich fine-grained particles that do not settle in harbors but are discharged to the nearshore may desorb phosphate due to changes in equilibrium kinetics.

Upon entering the lake, fine-grained P-rich particles can be intercepted by invasive mussel filtration, potentially releasing SRP to nearshore nuisance algae and thereby increasing the retention of P within the nearshore zone. Nearshore lake sediments were collected to test this hypothesis by examining lake sediments for fine-grained particles with high sorption capacity. Sorption experiments revealed that particles with high sorption capacity were present in the sediments. P-content saturation kinetics were modeled as a function of initial P-content, initial SRP concentration, and time. Results indicate that, though multiple size fractions of sediment exist in the lake sediment, it is the small (< 30 μm) fine-grained particles that have the highest sorption capacity.

Invasive quagga mussels were "fed" a variety of PP sources including algae culture, lake sediments (bulk and fine-grained), and river water in laboratory experiments. Mussel filtration rates did not appear to be affected by food source "quality". Likewise, with the exception of P-rich fine-grained particles, food source quality did not seem to affect mussel excretion rates. Throughout mussel experiments, excretion rates rarely differed from baseline (i.e. control) rates. However, feeding on fine-grained particles resulted in significantly greater SRP excretion rates, which may be due to release of loosely sorbed P on these particles. Bulk egestion (i.e. the production of feces and pseudofeces), was regulated by initial TSS concentrations within the feeding chamber.

The initial P-content of particulates fed to mussels was compared with the P-content in egested material. For most food groups, P content declined following passage through the mussel gut. The percent change in P-content varied from 15 – 75 % depending on food source. The only exception was bulk lake sediments, which had a very low initial P-content (i.e. ~0.8 µg/mg).

This work provides more evidence that supports the nearshore shunt hypothesis and suggests that tighter restrictions of non-point source P loading may be necessary. River restoration projects that increase river residence time and phosphate assimilation are likely valuable and may be quantifiable with calculations of first order SRP loss rates. Natural phosphate buffering mechanisms such as coprecipitation and sorption may provide a phosphate management tool, but should be paired with management actions that reduce upstream soil P-content and enhance in-route particle settling through increased residence

time. Mussels continue to pose a management challenge, but better mechanistic understanding of processes affecting PP quality, transport, and mussel digestion may inform modeling efforts that identify optimal management strategies for the nearshore zone.

DEDICATION

This work is dedicated in loving memory of my grandparents,

Alvin and Helen Smit.

TABLE OF CONTENTS

LIST OF FIGURES

LIST OF TABLES

LIST OF EQUATIONS

ACKNOWLEDGEMENTS

To my advisor Harvey Bootsma, thank you for your flexibility, patience, and guidance throughout this project. I appreciate your professional insight, but also your curious spirit and love for adventure. When I remember you it will always be backflips off the Osprey, pizza on the grill, and that video of the humpback whale (again and again…).

To my committee members, Jim Waples and Qian Liao, thank you for your invaluable advice and expertise. Jim, you have gone above and beyond what your role required, thank you for remaining creative, curious, and generous.

To the technical staff at UW-Milwaukee School of Freshwater Sciences, thank you. You keep things running and do so much more than people may realize. I need to give special thanks to Geoff Anderson, Jeff Houghton, Maxwell Morgan, Mark Lausten, Jessie Grow, and Tim Wahl. You all taught me patiently and were gracious with me when I made mistakes, thank you.

To the janitorial staff, and especially Mary, thank you for your consistent kindness.

To the graduate students in other labs, especially Hui Lin, Max Spehlmann, and Eric Ostovich, thank you for your friendship.

To my friends in the Bootsma Laboratory, thank you for your expertise and assistance, but more for your friendship. Emily, Graceanne, Philip, and Rae-Ann, I am sure you will all succeed at whatever you put your minds to. Sam and Gary, I'll never forget that jousting match! Tyler, I'm pretty sure the basketball tally ended in my favor. Kathryn, what can I say… You rock girl!

To Noelle, Nicholas, Noah, Justin and Jordan, my blood and adopted siblings, I should have called more. You gave good advice, provided a welcome distraction, listened, laughed, and reminded me of what mattered most.

To my parents, who have helped care for my children and provided me and my family with countless meals and weekend activities. I do not think this would have been possible without your love, support, and friendship. Thank you.

To my wife, Alison, who supported me throughout this process. Thank you for being my loving wife and a great mother to our children. From the lows of the pandemic and lost loved ones, to the highs of a birth and a new job, you've been there. I hope this next phase of our lives will have fewer tears and more joy.

Chapter 1: General Introduction

Phosphorus

Phosphorus is an extremely reactive element that is never found as a free element, but rather incorporates into a variety of compounds. The phosphate ion, PO_4^{3-}, is an essential nutrient for life found abundantly in DNA, RNA, ATP, and cellular membrane phospholipids. Because of its ubiquity for life and chemical reactivity, environmental P takes a multitude of forms which can be subdivided into a variety of operationally defined categories including organic/inorganic, particulate/dissolved, reactive/unreactive, and biologically available/ unavailable (James & Barko, 2005; Lin & Guo, 2016). Each of these operational classifications can be combined to create narrower combinatory definitions such as particulate organic, particulate inorganic, dissolved reactive, dissolved unreactive, etc. On its journey from land, to stream, down river, and into the lake ecosystem, a single atom of P may take on a multitude of forms. The form of a P atom shapes both its transport and fate.

Transport and Fate

The transport and fate of nutrients through an aquatic ecosystem can be viewed as a complex network directed by a combination of physical, chemical, and biological interactions. Physical forces promote entropy, acting to redistribute, mix, and ultimately homogenize nutrient inputs throughout the system. Chemical distribution within a waterbody is largely subject to physical forces such as advection and dispersion. However, chemicals, including nutrients, are also distributed by species specific chemical equilibria that are not homogenous or random, but dynamically predictable based on conditions of the surrounding physical/chemical environment. Biological forces are quite different, acting in the opposite

direction of entropy, negentropy. Lifeforms actively gather, organize, and store nutrients as biomass. However, due to the second law of thermodynamics, within a closed system, entropy ultimately wins out. Life in aquatic ecosystems and on earth more generally, perseveres only because the system is not closed. The sun provides a consistent external energy source that allows biological life to thrive but also sets into motion powerful physical forces such as evaporation, atmospheric deposition, and wind due to differential heating of the earth's surface. These forces tend to dominate the transport and fate of nutrients in aquatic ecosystems. Throughout this entire complex matrix of connections, the law of conservation of mass states that mass cannot be created or destroyed within the system.

Transport

Precipitation and Infiltration

Atmospheric moisture that reaches the ground in the form of rainfall can infiltrate into pervious soils where it may eventually be used by vegetation, returned to the atmosphere via evapotranspiration, or reach the water table where it contributes to groundwater baseflow. This mechanism maintains a dynamic reservoir or "stock" of water critical for maintaining streamflow and freshwater ecosystems between precipitation events (Fetter, 2001). Infiltration rates and total capacity vary significantly with land use. Urbanized impervious surfaces have poor to no infiltration capacity and cropland has a reduced infiltration capacity compared to natural landscapes like forest, shrub, and wetland. Infiltration capacity can also vary for the same soil depending on antecedent conditions affecting soil moisture and compaction. Generally, dry, coarse, well vegetated, well aerated soils have the highest infiltration capacity (Fetter, 2001).

Overland Flow

Atmospheric deposition that either falls on impervious surfaces or meets a full reservoir flows horizontally across the ground following the local gradient. This horizontal transport, called overland flow (Horton, 1933, 1940) also occurs if deposition outpaces infiltration by saturating soil moisture capacity. Any case of overland flow can mobilize P stocks that have accumulated on the surface of the land since the last precipitation event.

For a given watershed, one can estimate the number of expected days of overland flow following a precipitation event with the empirically derived equation (Linsley et al., 1975):

$$D = A^{0.2} \tag{1}$$

where

D = the number of days between the hydrograph peak and end of overland flow

A = the drainage basin area in square miles

0.2 is an empirical constant.

Stream Hydrographs

Overland flow leaves a distinctive "handprint" on the hydrograph that roughly resembles the back of one's right hand held up with the index finger pointed skyward while the other fingers form a fist. The left-side upward slope of the finger is referred to as the rising limb, the top of the finger is the peak, and then the right side of the index finger and remaining folded fingers make up the failing limb and recession respectively.

The height and width of this finger provides information about the watershed, with a taller skinnier "finger" generally associated with either steep gradients and/or poor infiltration

3

rates. Within the same watershed, comparisons between hygrographs through time can also reveal information. The steepness with which the finger rises gives information on the precipitation:infiltration ratio, while the width of the finger gives information about the duration of the precipitation event. The pre-storm baseflow height reveals antecedent conditions of the groundwater reservoir and the folded fingers, or falling limb, give the baseflow recession. Baseflow recessions show changes in groundwater storage and can be fit with the following exponential decay function (Fetter, 2001):

$$Q = Q_0 e^{-at} \tag{2}$$

where

Q = the flow at time t after the recession started (L^3/T)

Q_0 = the flow at the start of the recession (L^3/T)

a = the recession constant for the basin (1/T)

t = the time since the start of the recession (T)

L = Length

T = Time

Particulate transport is generally maximized at the hydrograph peak as both land surface and streambed stocks are caught up by turbulent flow. The region of the hydrograph from the peak to the start of baseflow recession is called the quick flow recession, which has a different recession constant. The equation above can be modified to find this constant as well.

River

Once transported from a watershed and to a river, a single P atom moving downstream is subjected to a variety of physical, chemical, and biological forces. The physical force dominating transport in river systems is streamflow discharge, which is affected by seasonal patterns in rainfall, natural gradients of the watershed, land use, and stored stocks in groundwater. As the dominant force, flow ultimately transports P from the land, downriver to its receiving waterbody.

Along the way, however, a P atom is subject to chemical and biologic forces as well. A P atom may be assimilated by a primary producer or bacteria for growth, sorbed to small mineral crystals or fine-grained sediment particles suspended in the flowing water, or chemically precipitated out of solution. Most of these transformations act as detours that slow the delivery rate of P to the receiving waterbody, however other transformations, such as uptake by and harvest of aquatic vegetation, can divert P out of the aquatic system, changing its long term fate (Rezania et al., 2021).

A key determinant of P transformation and fate throughout the transport process is residence time, the average amount of time an ion or particle is likely to stay within a designated boundary. Steady state residence time is defined as the following:

$$\text{when } F_{in} = F_{out}, \tau = \frac{V_z}{F_{out}} \tag{3}$$

where

F_{in} = Volumetric flow in (L^3/t)

F_{out} = Volumetric flow out (L^3/t)

V_z = Volume of the zone of interest (L^3)

τ = Residence time of $V_z(t)$

Within a river system, increased residence time allows greater in-route processing via natural P loss vectors such as biological uptake, chemical precipitation, sorption, and sedimentation. These natural environmental processes play a key role diverting P out of the aquatic ecosystem, delaying and buffering P delivery to a lake, and transforming soluble reactive phosphorus (SRP) into less reactive particulate phosphorus (PP) forms.

Lake

Once delivered to the lake, a similar dynamic path will unfold, again directed by the relative strength of physical, chemical and biological forces. In terms of P, lakes are generally P deficient, with ambient concentrations of P far below that of the river.

Thus, if particulate P in the river is at equilibrium with a relatively high concentration of dissolved P, the P atom may be released from that particle in order to reach a new equilibrium with the lower dissolved P concentrations of the lake. Aquatic microbes may colonize the particle, recycling the P, or P could be captured by filter feeding organisms. Eventually, depending largely on particle size, and hydrodynamics forcing, P may travel to a lake's outflow to continue the downstream journey, or come to rest and burial in sediments.

Soluble P forms, especially inorganic forms, are extremely reactive in the P limited lake ecosystem and tend to have short residency in their soluble reactive phosphorus (SRP) form as they are quickly assimilated by algae. This reactive propensity can produce deleterious effects near tributary outflows by promoting nuisance levels of algal growth and impairing water quality. Much of P management within the Great Lakes is concerned with reducing these

beneficial use impairments (BUIs) while still maintaining a high enough level of P inputs to support a stable and productive ecosystem (Hecky & DePinto, 2020).

Again in the lake system, residence time can play a critical role in determining the path a P atom may take. In this case, however, long residency of river plume water in a nearshore zone can produce negative effects. Continued P delivery and extended river plume residence in a lakes nearshore zone can increase dissolved P concentration and may directly impact human beneficial use through algae blooms that cause beach marring and closures, elevated levels of bacteria, anoxic waters, lower food web instability, and fish kills (Carpenter et al., 1998; Dillon, 1974; Paerl et al., 2001). Thus, hydrodynamics that promote nearshore nutrient flushing can be important mechanisms that dilute plume footprints (Huang et al., 2019).

River and lake systems are intimately coupled, and the residence time and assimilation rate of P in the river directly affects its receiving lake partner. Increased flow rates associated with episodic storms decrease water residence times, which can overwhelm a receiving water body's assimilation rate. Nutrients mobilized in overland flow can be transported much faster and much further in the case of particulate bound nutrients, than under baseflow conditions, increasing the intensity of nutrient plumes at the river-lake interface. Man-made structures common to the lakefront such as harbors and break walls generally act to delay and process nutrients prior to lake entry via settling and biologic assimilation. However, a large enough plume can overwhelm and largely bypass these structures. The result is that a storm event often delivers a large "pulse" or "plug" of nutrient laden water to a nutrient limited nearshore zone. Once the plume has exited a river mouth or harbor gap and entered the lake, the

7

momentum of the river quickly diminishes. Now the fate of the plume nutrients is dominated by complex nearshore hydrodynamics and biogeochemistry.

Sometimes, the same atmospheric forcing patterns that initiated the nutrient plug through rainfall can control the fate of the nutrients in the lake, dictating its path through wind driven currents. However, large lake hydrodynamics are not ephemeral phenomena alone, but a complex convolution of myriad signals preserved over time by the powerful momentum of fluid water. Depending on the hydrodynamic forcing of the day, combined with weeks to months of antecedent conditions, nutrients could be advected to the hypolimnion by down-welling, readily mixed and assimilated near the point of entry, transported by longshore currents to settle and assimilate elsewhere in the nearshore zone, or transported from nearshore to pelagic by upwelling or horizontal mixing.

Fate

While the residence time shapes the timing and path of transport, the ultimate fate is determined by the innate, ever evolving, structure of the ecosystem. Not all paths lead to the same destination, and some paths could be dead ends. This ecosystem structure is determined by the strength of physical, chemical, and biological processes acting to direct the flow of nutrients within the system. Generally, ecosystem structures are strengthened and stabilized by having a multitude of connections, promoted by biodiversity, and natural negative feedback loop buffering mechanisms (Landi et al., 2018). However, certain negative feedback systems can become overwhelmed if critical thresholds are breached. Additionally, impaired systems with few or weak connections are prone to instability and leave open niche space for ecosystem invaders (i.e. invasive species).

Species that modify ecosystem conditions, directly or indirectly modulating the availability energy and nutrients are referred to as ecosystem engineers (Emery-Butcher et al., 2020). Aside from changing the magnitude of nutrient and energy pathways, some ecosystem engineers may have the ability to establish reinforcing, or positive feedback loops, in which nutrients and energy become coupled to the ecology of the invader. In this case, a paradigm shift can occur as the system becomes destabilized and moves to a new steady state. Such changes to the original structure of the ecosystem network ultimately affect nutrient fate.

Problem Statement

Cultural Eutrophication

Cultural eutrophication is widely regarded as one of the greatest threats to aquatic ecosystem health. Urbanization, agricultural practices, and other anthropogenic activities contribute to excess nutrient loads in waterways (Paul & Meyer, 2001). Excess nutrients can promote rapid growth of nuisance algae and toxic cyanobacteria, eventually leading to die-offs, decomposition, oxygen deficiency, deteriorating water quality and loss of invertebrates and fish. (Carpenter et al., 1998; Dillon, 1974; Paerl et al., 2001). The primary elemental nutrients associated with eutrophication are nitrogen and phosphorous. Historically, algal production in many marine systems has been found to be limited by nitrogen (N) due to low concentrations of metal cofactors (Wu et al., 2000) and selective loss of N due to denitrification, whereas most freshwater lakes are limited by phosphorus (P) (D W Schindler, 1971). This study was located on the P limited Lake Michigan and deals primarily with P dynamics affecting Lake Michigan.

Aquatic Invasive Species

Research and public interest in aquatic invasive species has increased greatly in the last two decades (Kovalenko et al., 2021). Increased attention is merited since globally aquatic invasive species have been shown to significantly impact invaded waters reducing native species abundance, transforming habitats, and exacerbating issues of eutrophication (Gallardo et al., 2016). A particularly successful aquatic ecosystem invader is the bivalve mussel of the genus *Dreissena*, which has invaded and negatively impacted aquatic ecosystems in the United States from the Hudson (Strayer et al., 1999) to the Colorado (Nalepa, 2010) River. Two *Dreissenid* invaders in the Great Lakes Region, the zebra (*Dreissena polymorpha)* and quagga (*Dreissena rostriformis bugensis)* mussels have produced large economic and ecological costs (Stone, 2005) by altering food web interactions (Vanderploeg et al., 2015), re-engineering abiotic habitat (Emery-Butcher et al., 2020), and altering internal nutrient recycling dynamics (Bootsma & Liao, 2013).

Change in Transport and Fate of Phosphorus in the Great Lakes

In recent decades, it has become apparent that nearshore zones of the Great Lakes are again experiencing impairments due to eutrophication (Auer et al., 2010a). However, while the nearshore experiences eutrophication, some offshore regions are experiencing hyper-oligotrophy (R. Hecky & DePinto, 2020). This creates a nutrient management conundrum that is not easily resolved. Additionally, there is uncertainty about the root cause of this issue.

Changes in land use practices, such as the adoption of no-till soil conservation, may have instigated eutrophication issues in the Great Lakes by inadvertently increasing the export of bioavailable phosphorus forms from watersheds dominated by agricultural land use (Baker et

al., 2014). However, other work has suggested that it is increased inputs from urban areas that have enriched nearshore waters (Howell & Benoit, 2020).

But external inputs are not the only source of nutrients within large lake systems such as the Great Lakes. The Great Lakes also have large internal nutrient stores in sediments (Eadie et al., 1984) and internal loading mechanisms, such as sediment resuspension during large winter-spring storms (Eadie et al., 2008), can promote internal recycling of nutrients within the lake ecosystem (Ji et al., 2002). Thus, some have suggested that it is largely physical forces, which affect the dynamics of large internal stores, combined with internal biogeochemical controls that ultimately affect the trophic status of the lakes (Brooks & Edgington, 1994).

Another important change concurrent with re-eutrophication issues was the invasion and proliferation of *Dreissenid* mussels starting in the late 1980s. Hecky et al., (2004) hypothesized that invasive mussel could re-engineer the nearshore environment, capturing and sequestering energy and nutrients in the nearshore zone and limiting export of nutrients to the offshore. In addition to promoting the retention of river-borne nutrients in the nearshore zone, nearshore dreissenids may serve as a sink for particulate P advected from offshore waters (Waples et al., 2017). Recent modeling work suggests that invasive mussels now dominate the regulation of internal phosphorus dynamics within the Great Lakes, reducing the importance of external inputs and limiting the effectiveness of traditional management strategies (J. Li et al., 2020).

Objectives

The primary purpose of this research was to gain a greater understanding of the mechanisms and processes that currently dictate transport and fate of phosphorus in Lake Michigan's nearshore zone. The three basic questions that drive this research are:

1) How much P is going into the lake, and in what forms?

2) Where does it go?

3) What happens to it?

Informed by the current literature, this work can be further focused on three main study areas that help address the larger basic questions.

1) Changes to and comparisons between phosphorus loading from agricultural and urban landscapes

2) Sediment phosphorus interactions

3) Mussel phosphorus interaction

Thesis Outline

Chapter 2 provides historical background of eutrophication and phosphorus management in the Great Lakes and discusses models that have been used to address these issues. In the methods section, I borrowed a simple linear algebra algorithm from the fields of economics and population modeling and adapted it for use in mass balance transport and fate modeling. I applied the algorithm to a model system with similar structure to the nearshore lake system. This model system was then used to explore several scenarios that relate to real transport and fate questions, with the hope of further exploring the three main study areas of

this thesis. A graphical user interface (GUI) for the nutrient model, NutriModeler, is available online for user exploration.

Chapter 3 primarily deals with the first study area, agricultural and urbanized landscape contributions to P loading. Informed by the exploratory modeling, it also investigated mechanisms that may modulate P delivery rates. The chapter relied heavily on data collected from field work conducted on the Milwaukee and Sheboygan rivers from July – November2020. These watersheds were chosen since they both deliver similar total P loads to Lake Michigan, but come from landscapes that primarily differ in agricultural vs urban land use. At each river mouth, I used automated ISCO samplers to collect daily phosphorus fractionation data for SRP, dissolved organic phosphorus (DOP), PP, and NaOH extractable P (NaOH-P) as well as total suspended solids (TSS). Sonde's were deployed at each station to collect ancillary data. Critical questions included how much of the load was bioavailable and how was the load transported and transformed through time. Comparisons were made between the two rivers and by nutrient groups including bioavailable, particulate, and dissolved. Field data was combined with external data sources in a data aggregation, visualization and analysis App called LimnoExplorer that was created to help contextualize the samples.

Chapter 4 combines the next 2 research areas and explores interactions between phosphorus, sediment, and mussels. Thus, the research moved away from the river, to the nearshore zone, and 20 meters underwater in the lake where I collected benthic sediment samples and quagga mussels for laboratory experiments. A series of experiments were performed on both sediments and mussels. Key parameters of interest for sediments were P-

content (i.e. µgP/mgTSS) and SRP sorption rate and capacity. I also examined particle settling rates with 2 methods.

1) Analytically calculated settling rates using Stoke's Law, a high powered microscope, and image processing software to estimate particle radius.

2) Empirically derived particle loss rates using a transmissometer and settling column.

For mussels, the key parameters of interest were phosphorus filtration, excretion, and egestion rates. The expectation was that these rates might be modulated by food source quantity and quality. Rates were compared between several food sources including cultured algae, river water suspended sediment, and lake sediments (both bulk and fine-grained).

Chapter 5 provides a summary of the key findings, discusses their implications, and provides suggestions for future research.

Chapter 2: Models in the Great Lakes and Exploratory Modeling

Introduction

Mathematical models help lake managers distill the myriad pathways and connections of a real ecosystem into smaller more generalized parts. This allows for the exploration of system responses to proposed management and/or threat scenarios without incurring the cost or possibly deleterious consequences of real world action. Mechanistic models can also be used to make predictions of past conditions, hindcasts, or future events, forecasts. Physical model forecasts such as wave models not only help managers understand the physical nature of the lake, but can also warn the public of dangerous conditions and save lives. Chemical and biological models that are connected to a physical model are referred to as coupled physical-biogeochemical models. These models allow for the prediction of state variables (measureable properties that describe the state of a dynamic system) through time and space.

Models became an integral part of nutrient management in the Great Lakes during the 1970s in response to issues of eutrophication. Early models were derived from simple statistical relationships between algae concentrations and phosphorus loadings. However, "system" models soon followed that helped translate these statistical relationships to make predictions in time and space. Though simple, the models were effective management tools that united managers and helped inform internationally agreed upon lake loading targets. Efforts were largely successful as the targets helped reduce eutrophication in the Great Lakes (Dolan & Chapra, 2012).

However, increasing anthropogenic influence, both from intensified land use and the inadvertent introduction of invasive filter feeding mussels, may have undermined this success.

By the early 2000s, nuisance algae had reemerged and nearshore waters were again impaired. This time, however, a fundamental shift in structure, likely due to dreissenid ecosystem engineering, appeared to have altered energy and nutrient pathways, directing excess energy and nutrients to the nearshore benthos (Turschak & Bootsma, 2015). While the nearshore was increasingly eutrophic and impaired, the pelagic was becoming hyper-oligotrophic with a reduced capacity to support upper level food web dynamics. This nutrient management conundrum has been labelled the "Duel Challenge" (Zhou et al., 2021).

Today, Great Lakes nutrient management faces a large challenge. Although scientists and managers have much more powerful modeling tools than they did in the 1970s, different tools have suggested different underlying causes of the Duel Challange and thus different management paths forward. There is no manifest consensus (Bootsma et al., 2015; Bravo et al., 2019; Huang et al., 2019; Kuczynski et al., 2016; Pilcher et al., 2017; Rowe et al., 2017; Warner & Lesht, 2015; Zhou et al., 2021). A least part of this uncertainty can be attributed to the growing complexity of models which can increase the number none unique solutions, model assumptions, and complexity of sensitivity analyses. Transparent communication of such modelling efforts in the limited space of an academic journal is challenging, and the lack of a full picture can hinder model interpretation. Perhaps the best path forward is a step back. Model complexity does not equate model utility.

This chapter provides a brief review of nutrient management in the Great Lakes as well as my thoughts and critiques on current modeling efforts. In the methods section, I introduce a revised linear algebra "input-output" based modeling framework adapted from the work of

1973 Nobel Prize winner in Economic Sciences, W.W. Leontief. The model is introduced

formally, and then more practically through engagement in a stock flux analysis of a River →

Harbor → Nearshore → Pelagic system. Each major stock, aside from the river, has a paired

benthic stock to represent nutrient settling, assimilation, and/or burial in sediments. The

method is normalized as proportional flux to decouple the model from time and space, allowing

for greater flexibility. Constraints are imposed on the model to ensure mass balance is

maintained. I have named this algorithm "the Proportional Mass Flux Algorithm".

In the results section, I apply the model to an analysis of 3 theoretical scenarios with

implications that inform and contextualize the additional work contained in this thesis. In the

conclusion I discuss these results briefly and use them as a context for the research presented

in the following chapters of the thesis. Further, I suggest that the simple, yet elegant

application of transition matrix algebra could compliment current modeling efforts within the

Great Lakes and more generally is well suited for mass balance models anywhere.

Background

Review of Nutrient Management in Great Lakes

Early research and modeling efforts of the 1960s and 1970s aimed to reduce

eutrophication throughout the entire Great Lakes basin. As such, they tended towards large

spatial and temporal scales such as lake-wide and yearly averages (Chapra, 1977). Such broad

spatial and temporal constraints afforded these early models with simplifying assumptions such

as chemical conservatism, constant nutrient delivery rate, and instantaneous mixing within the

lake. This type of model is often referred to as continuously stirred tank reactor (CSTR) (Biffi,

1963; Rainey, 1967). While these assumptions appear egregious, they were reasonable given

17

the spatial/temporal scope of the models, nature of the point source pollution issue at that time, and shared goal of lake managers.

An idealized CSTR seems less obtuse when one considers the various forces acting to mix a lake over the course of an entire year. Similarly, since most pollution sources at that time were point sources from wastewater treatment plants and other industries, fueled by nearly constant human use, a constant nutrient delivery rate was also reasonable. Another important simplifying assumption afforded by early models' coarse spatial/temporal scale was that total phosphorus (TP) was a suitable predictor for Chl *a*, and thus algae abundance. This assumption may be true over a large time span; however, it is known that not all forms of P are readily algal-available and some argued that a more precise and cost effective model would focus on P forms that promote immediate algae growth (Lee et al., 1980).

Despite their simplifications and what some may consider shortcomings, the early loading/eutrophication models proved useful. A suite of models (i.e. Chapra, 1975; Dillon & Rigler, 1974; Vollenweider, 1969; Vollenweider, 1975) helped set loading targets for each lake designed to bring Chl *a*, and thus eutrophication status to the optimum level that would reduce nuisance algae while still maintaining a healthy fishery. These targets were adopted in the 1978 amendment to the Great Lake Water Quality Agreement (GLWQA) (Bruce & Higgins, 1978) and eventually proved effective in meeting basin-wide eutrophication targets as measured by Chl *a* (Dolan & Chapra, 2012).

Although these early loading models were primarily statistical in nature, they were soon complemented by a series of ecosystem models (Scavia, 1980; Scavia & Fahnenstiel, 1987;

18

Thomann et al., 1975) that sought to bring a deeper mechanistic understanding of in-lake physical-biogeochemical processes. Despite their relative simplicity, post audit reviews of these early models in the late 1980s proved that they were effective in both predicting lake responses to target loads and simulating in-lake chemical processes and biological dynamics such as phytoplankton successional patterns (Bieiman & Dolan, 1986; Di Toro et al., 1987; Lam & Schertzer, 1987; Lam et al., 1987a). Annual reports of TP loads showed declining trends that were near or on track to meet the 1978 loading targets and in 1991, formal reports of TP loadings were discontinued (Dolan & Chapra, 2012).

Current Issues: The Same Problem with a New Twist

With the exception of select areas of Lake Erie, eutrophication in the Great Lakes appeared to have been solved by the late 1980s and modelers focused attention toward improvement of hydrodynamics. Spatially explicit hydrodynamic modeling was revolutionized with the advent of the Princeton Ocean Model (POM) (Blumberg, A. F.; Mellor, 1987) which was soon adapted by Great Lakes modeler's for predicting the transport and fate of toxic substances (Schwab & Beletsky, 2000; Schwab & Beletsky, 1998). Later, the Finite Volume Community Ocean Model (FVCOM) (Chen et al., 2003) improved upon the POM through the use of a more flexible unstructured grid, better suited to modeling complex coastal morphologies and high resolution nearshore hydrodynamics.

Despite the reduced attention given to nutrients in the 1990s, nutrient management progress was being undermined by two latent threats:

1)   Increased levels of bioavailable P loading from non-point tributaries due to changes in agricultural practices and the continued buildup and saturation of legacy P-stocks in soils (Logan and Adams, 1981; Baker et al., 2014).

2)   In-lake nutrient cycling dynamics re-engineered by the inadvertent introduction of two bivalve mussel species, zebra mussels (*Dreissena polymorpha*), and quagga mussels (*Dreissena rostriformis bugensis*) in the late 1980s (Hebert et al., 1989; Mills et al., 1993).

While increased bioavailability snuck under the noses of traditional TP monitoring programs, invasive mussel stowaways hitchhiked their way to the Great Lakes in ship ballast water. The largely invisible changes in load dynamics and reengineering of the lake ecosystem by mussels initiated changes favorable for the resurgence of nuisance algae in the nearshore zone (Hecky et al., 2004; Auer et al. 2010), refocusing nearshore research efforts back to eutrophication and P management (Bootsma et al., 2005). Today, increased bioavailability and dreissenids continue to tip the scales in favor of nuisance algae similarly by delivering readily assimilated nutrients and enhancing the local light environment. These mechanisms are briefly described in the following:

1. Increased loads of bioavailable P are transported and readily mixed in nearshore areas near tributaries where they can be assimilated for algae growth.

2. A decrease in the PP:SRP ratio may reflect lower suspended sediment loading, which may create clearer nearshore waters allowing the frequently light limited algae to grow rapidly.

3. Mussel filtration of particulate matter from the water column allows light to penetrate to areas previously un-colonized by the benthic nuisance algae (Auer et al., 2010; Kuczynski et al., 2016).

4. Mussel digestion/egestion/excretion converts PP forms, typically unavailable for algae growth, into soluble forms (i.e. PP → SRP) that can be assimilated by algae for growth (Bootsma et al., 2015).

Additionally, mussels bias interactions between nearshore and offshore nutrient exchanges, potentially trapping river-borne P in the nearshore via the incorporation of P into nearshore benthic biomass and sediments (R. E. Hecky et al., 2004; Turschak et al., 2014), while sequestering offshore nutrients made available to them through convective mixing (Waples et al., 2017) and altering the forms, and thus fate of P exported from nearshore to offshore. In particular, P attached to nutrient-rich fine-grained sediments that historically would have had short residency in the nearshore zone before being exported to the pelagic zone may now be captured by mussel filtration and retained in the nearshore for extended periods (Hecky et al., 2004). The end result is a double-edged sword of excess nuisance algae production and deteriorating water quality in the nearshore (Auer et al., 2010; Bootsma et al., 2015; Higgins et al., 2006), and a nutrient depleted offshore that may prove unable to sustain Great Lakes fisheries (Bunnell et al., 2014; IJC, 2020; Vanderploeg et al., 2010).

Despite these important effects, only a few ecosystem models have explicitly accounted for mussel grazing and nutrient recycling (Bravo et al., 2019; Rowe et al., 2015; Shen et al., 2020; Valipour et al., 2016; Zhou et al., 2021) and nutrient management programs, such as total

maximum daily load (TMDL), still use TP as their primary metric. Moreover, there is still uncertainty associated with how efficiently mussels capture and metabolize allochthonous P sources such as runoff from tributaries or resuspended sediments within the lake. Additionally, previous loading models calibrated for lake-wide yearly averages lack the spatial/temporal time scales required to inform localized/seasonal decisions and did not include mechanistic representations of ecosystem processes. Without this finer resolution and mechanistic understanding it is difficult to resolve questions about ecosystem drivers and potential effects of various management scenarios.

The Path Forward

Better Models, Definitions, and Observations

From an engineering perspective, the nutrient concentration of a given water body can be modelled as a function of the nutrient loading rate, as well as the physics, chemistry, and biology of the system. Together, the specific physics, chemistry, and biology, of a waterbody defines its assimilative capacity such that $c = \frac{1}{a}W$ were c = concentration, a = assimilative capacity, and W = the nutrient loading rate. From a management perspective, this leaves only a few options for lowering a water body's concentration 1) lower the nutrient loading rate, and 2) enhance the waterbody's assimilative capacity. However, from an ecological point of view, the above equation and proposed mitigation strategies appear overly simplistic. It is the metaphorical equivalent of simply counting calories in your diet and making sure you exercise without paying attention which foods are in your diet and what types of exercises you're doing. In the same way different diet and exercise regimes with the same net calories can have vastly different impacts on personal health, different forms of P-loading and assimilative capacity

pathways may net the same final average P concentration, but with drastically different impacts on ecosystem health and beneficial uses. In other words, mind not only the amount and destination, but the quality and the journey.

To address current water quality issues, a single lake-wide target concentration is no longer tenable. Instead, effective models must meaningfully define a management area's boundaries and accurately measure this potentially dynamic area's assimilative capacity while mechanistically partitioning nutrient transport, transformation, and fate through its various ecosystem compartments. This complex task is often accomplished with the coupling of ecosystem models to spatially explicit hydrodynamic models such as POM and FVCOM. An example of this is the work of Bravo et al., (2019) in which researchers bounded their definition of the lake's assimilative capacity to relevant spatial (i.e. a 100m grid resolution along a 45.5 km of the nearshore zone out to the 30m isobath) and temporal (i.e. the *Cladophora* growing season) scales, allowing them to explore different management outcomes related to moderating the P concentration of a specific WWTP's effluent. The work relied heavily on a previous nearshore model (Fillingham, 2015) that includes both mussel grazing/recycling and *Cladophora* growth (Tomlinson et al., 2010) sub models. Bravo et al. nested Fillingham's biogeochemical model within a 3D hydrodynamic model to create a coupled physical biogeochemical model. Though labor and data intensive, this type of management directed high resolution modeling has become the gold standard and a frequent contributor to Great Lakes research (Bootsma et al., 2015; Fillingham, 2015; Huang et al., 2019; Khazaei, 2020; Pilcher et. al, 2015; Pilcher et al., 2017; Rowe et al., 2015; Rowe et al., 2017, 2017; Shen, 2016; Shen et al., 2018; Shen et al., 2020; Zhou, Auer, & Xue, 2021).

The Bravo et al. (2019) adaptation of Fillingham's (2015) model was focused on the fate

of P from a point source and did not account for the influence of non-point tributary loading.

Tributary loading is important because it ultimately drives long-term lake-wide nutrient

averages. And although tributary loading may play a minor role in subsidizing the coastal

benthos compared to larger in-lake nutrient recycling processes (Waples et al., 2017), short

term and localized effects may still be important for informing nearshore management

decisions. Additionally, there is evidence that tributary mouths, harbor areas, and river plumes

have become biological hotspots (B. J. Smith & Simpkins, 2018), host charismatic species (Dow,

2018), and are important for fish recruitment (Carreon-Martinez et al., 2015). Wildlife and

recreational uses can be important factors in influencing public perception and stakeholder

investment. Thus, it is important to have models that are refined enough to simulate the effects

of nutrient loading on both the near and offshore regions, with the goal of reducing nuisance

algae in the nearshore while still providing enough nutrients to support plankton and fishery

production in the offshore (Hecky & DePinto, 2020).

The Need for Model Transparency

The final need is model transparency and clear honest communication among

researchers and stakeholders. As models become more and more complex their implicit

assumptions can become less apparent. There is a need for standardization in how models are

presented, communicated, and shared in academic journals with an emphasis on clearly stating

model assumptions and parameterizations. With dozens to hundreds of model parameters to

tune and a high computational cost to running each simulation, thorough model sensitivity

analysis has become increasingly challenging (IJC, 2019). Moreover, many mechanistic models

have either not been constrained by available empirical data, or the data to constrain them does not exist (Arhonditsis et al., 2019). Thus, increasing *in situ* or experimental observations that can better constrain model parameters should be prioritized. Finally, it should become standard practice to share model parameterization methodology along with annotated scripts of model execution, output extraction, and analysis. Such efforts may reduce the "black box" nature of current modeling practices contributing to greater model transparency and instigating future collaboration across modeling groups.

In the preface of his book "Surface Water Quality Modeling" (1997), Steven Chapra speaks of the computer-modeling revolution with excitement, but also issues the following warning:

"On the down side, wide-spread and easy use of models could lead to their being applied without insight as `black boxes`. The main thesis of this book is that models must be applied with insight and with regard to their underlying assumptions" –Steven Chapra

Though he appears to be speaking of model use/abuse by non-experts in this quote, none are free from absolution. Good modeling comes at a cost. Part of that cost is taking the time to lay bare model assumptions and their related implications. We must all remain vigilantly skeptical of results and mindful of our biases. Furthermore, since complexity does not necessarily trend with utility (Arhonditsis & Brett, 2004), we should not use a more complex model if a simpler one would do.

Methods

Matrix Models

A simple and elegant representation of a complex network, such as the movement of nutrients, energy, or pollutants, through an ecosystem, can be contained in a matrix. Using linear algebra, this matrix can be solved for its steady state outcome either iteratively, through matrix multiplication, or directly through retrieval of its Eigen vectors. This modeling method is common in the field of population modeling (Caswell, 2002), and has been applied extensively for analysis of large social networks on the internet (Hanneman & Riddle, 2005). However, credit for this "*input-output*" modelling method's development belongs to W. W. Leontiff, winner of the 1973 Nobel Prize for economics who used his model to analyze complex interactions in economic systems by mapping the flow of goods from producers to consumers (Leontief, 1936).

An adaption of this "systems" based modeling method has been applied to water quality modeling efforts of the past. Thomann & Sobel, (1964) applied this modeling framework for pollution abatement within the Delaware estuary. The methods developed during the study helped develop the control-volume method, led to the development of the steady state response matrix model, and in general helped promote "systems" based thinking in water quality management (R V Thomann, 1974). In a brief subchapter of his book "*Surface Water Quality Modeling*", S.C. Chapra introduces the steady-state system response matrix, and more broadly the efficiency of matrix multiplication and inversion for solving linear systems of equations. However, the discussion is primarily one of concentrations, not mass flux, and as

such a simple yet elegant property of "input-out" models was thus `diluted` by the addition of volume.

The Proportional Mass Flux Algorithm

A Formal Introduction

Consider the evolution of nutrients in an empty and closed aquatic system with river, harbor, nearshore, and pelagic zones. This system can be represented by 4 water column stocks for the 4 zones mentioned above, with 3 additional stocks denoting nutrients within the benthos of the harbor, nearshore, or pelagic zones. Each of the 7 stocks shall be indexed by i. Let A denote the total mass of the nutrients in the system, with $\mathbf{p_{it}}$ as the proportion of the loading that is in stock i at time t, and $\mathbf{p_t} = (\mathbf{p_1}, \mathbf{p_2}, ..., \mathbf{p_7})$ a vector of those proportions with $\mathbf{p_0}$ being the initial allocation vector. By the law of conservation of mass, we must have $\sum_{i=1}^{7} \mathbf{p_{it}} = 1$ for any time t. Within this system, the nutrients are transferred between the stocks over time until they meet a steady state. If we let $\mathbf{T}$ denote the time at which the system reaches the steady state, we know that $\mathbf{p_{t_1}} = \mathbf{p_{t_2}}$ for all $\mathbf{t_1}, \mathbf{t_2} \geq \mathbf{T}$; that is, once the system reaches steady state, the proportion of nutrients in each stock remains constant. If all stocks are connected to the system by an inflow, no more than 1 stock lacks an outflow, and the transfer rate between the stocks remains constant, than for any loading A and initial allocation $\mathbf{p_0}$, the system will converge to the same steady state nutrient allocation denoted by $\mathbf{p^\star}$. However, the time $\mathbf{T}$ to reach steady state will vary with $\mathbf{p_0}$.

We can write an algorithm to model this evolution of nutrients in a system. To do this, we discretize nutrient transfer to time intervals l. The inputs to the algorithm are A, total loading of nutrients in the system, and $\mathbf{p_0}$, the initial proportional allocation of that loading. We

evolve the allocation of nutrients in the system by means of matrix multiplication with $\mathbf{M}$,

where $\mathbf{M}$ is a square matrix that specifies each relationship between each stock, i.e. the

constant proportional flux rate associated with time interval l. To maintain mass balance

throughout the evolution, $\mathbf{M}$ must be constrained such that the row sums each equal 1. Then,

the proportional mass flux algorithm is defined by the following equation: $\mathbf{p_l} = \mathbf{M} \times \mathbf{p_{l-1}}$. We

define the algorithm to have reached steady state when $\mathbf{p_{l+1}} = \mathbf{p_l}$. The algorithm will converge

to $\mathbf{p}^\star$ for any inputs A and $\mathbf{p_0}$, but certain inputs will require more iterations to converge, and

the nutrient histories/trajectories $\{\mathbf{p_1}, \mathbf{p_2}, \dots, \mathbf{p_L}\}$ will be unique to the initial conditions.

However, a change to $\mathbf{M}$, either in structure i.e. the loss or addition of connections, or

modification of proportional flux rates, can result in a nutrient paradigm shift, creating a new

steady state.

A Concrete Example

Let us now move from the abstract to the concrete. Consider the following 7 X 7 matrix

$\mathbf{M}$ (Table 1: shown here in less formal spreadsheet format for ease of interpretation)

representing the proportional fluxes associated with time interval l that dictates the transport

and fate of phosphorus within a River → Harbor → Nearshore → Pelagic system.

Table 1: Labelled 7 X 7 matrix of proportional nutrient flux.

Rows are indexed with capital letters and columns lowercase letter, each derived from the first letter(s) of the corresponding P stock that they represent (i.e. location column, River – P. Benthos). Upper case letters show where the flux is coming from, while lower case letters show where the flux is going to.

location	id	r	h	n	p	hb	nb	pb	mass balance
River	R	0.00	1.00	0.00	0.00	0.00	0.00	0.00	1.00
Harbor	H	0.00	0.36	0.24	0.00	0.40	0.00	0.00	1.00
Nearshore	N	0.00	0.09	0.27	0.44	0.00	0.20	0.00	1.00
Pelagic	P	0.00	0.00	0.44	0.36	0.00	0.00	0.20	1.00
H. Benthos	HB	0.00	0.40	0.00	0.00	0.60	0.00	0.00	1.00
N. Benthos	NB	0.00	0.00	0.10	0.00	0.00	0.90	0.00	1.00
P. Benthos	PB	0.00	0.00	0.00	0.00	0.00	0.00	1.00	1.00

This matrix maps inputs, designated by the named row vectors, to outputs (i.e. the column vectors). More specifically, as a P loading transport and fate model, it represents the proportional mass flux of P from one named stock to another or back to itself. For example, the top row reads in plain English as `the river delivers 100% of its load to h in 1 time step of $l$` (i.e. the harbor). To concretize this further imagine $l = 1$ day. In this case, the loading of the river to the harbor may represent an episodic summer storm that delivers a pulse injection load from the river to the harbor in a single day. Continuing with this line of thought, in row two, the harbor retains 36% of its stock per day, which can be related to the half-life of a nutrient unit within the harbor's water column by solving the exponential decay function $\frac{\ln(0.5)}{-0.36\ d^{-1}} =$ ~1.93 days. This should make it clear that the diagonals of the matrix are directly related to each stock's residence time in units of l, which in this example is days, but could be any time increment. The harbor exports 24% d^{-1} of its stock to the nearshore, and 40% d^{-1} settle to the harbor benthos. Other than the river stock, in row 1, each other major stock has an associated

benthic stock that represents either settling or biological assimilation in the benthos.

Permanent burial of nutrients in the sediments can be represented as a benthic stock that has a

proportional return flux of 1 (i.e. the stock returns only to itself). By inspecting the diagonals of

the matrix, it is apparent that this matrix includes that case at $\mathbf{M}$[7, 7], in the benthic stock of

the pelagic zone. This is not an attempt to realistically model the actual process of P burial in

the benthos, but an example that illustrates the sensitivity of the model to a "dead-end" stock.

Because mass flux is represented proportionally, it is unit less. This makes calculating a

mass balance for the model as simple as ensuring that the row sum is equal to 1, which can be

seen on the right side of the matrix in Table 1. Although only 16 of the 49 cells of matrix $\mathbf{M}$

contain a number other than zero, this is already a complete model capable of predicting

steady state outcomes by extracting the right-hand-side (rhs) Eigen vectors. In this case, solving

for the rhs Eigen vectors of matrix $\mathbf{M}$ returns a 1 X 7 vector $\mathbf{p}^{\star}$ with the values (0, 0, 0, 0, 0, 0, 1).

Again in plain English, the output vector states that at steady state, no nutrients are left in the

river, harbor nearshore, etc. but all of the nutrients in this system, for this matrix, go to the

benthos of the pelagic. The model structure can be visualized with a simple box model diagram

(Figure 1).
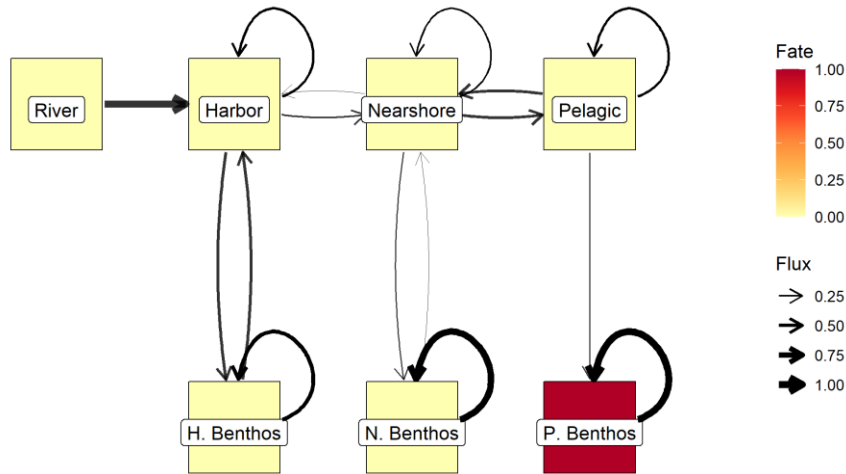
Figure 1: Box Model Diagram of Nutrient Flux and Fate.

Weight of arrow shows proportional flux of nutrients. Color saturation shows ultimate proportional fate of nutrients at steady state. In this model, 100% of nutrient fate rests in the benthos of the pelagic zone.

But steady state outcomes alone do not tell the whole story. The transient portion of this model, i.e. $\{\mathbf{p_1}, \mathbf{p_2}, \ldots, \mathbf{p_L}\}$, can also be recovered and analyzed through iterative matrix multiplication with the proportional mass flux algorithm defined earlier. This model can either be run for l_{max} iterations, where l_{max} is a user defined threshold value designating the maximum number of iterations allowed, or more formally constructed to run until the model reaches asymptotic convergence as seen in the previous section. In order to run an iterative solution, the scaler load A is multiplied by the initial proportional allocation of nutrients, $\mathbf{p_0}$. Thus, a pulse injection into an empty lake system as seen in this example can be modelled by allocating the entire load to the river slot of the initial vector. Since the river is the first column of the loading vector river this can be defined as $\mathbf{p_{0_1}} = 1$ and $\mathbf{p_0} = A \times \mathbf{p_0}$. Now the proportional mass flux algorithm can be initiated by $\mathbf{p_l} = \mathbf{M} \times \mathbf{p_{l-1}}$ and the model output

values contained in $\{\mathbf{p_1}, \mathbf{p_2}, \dots, \mathbf{p_L}\}$ associated with this pulse injection scenario can be

visualized as a time series (Figure 2).
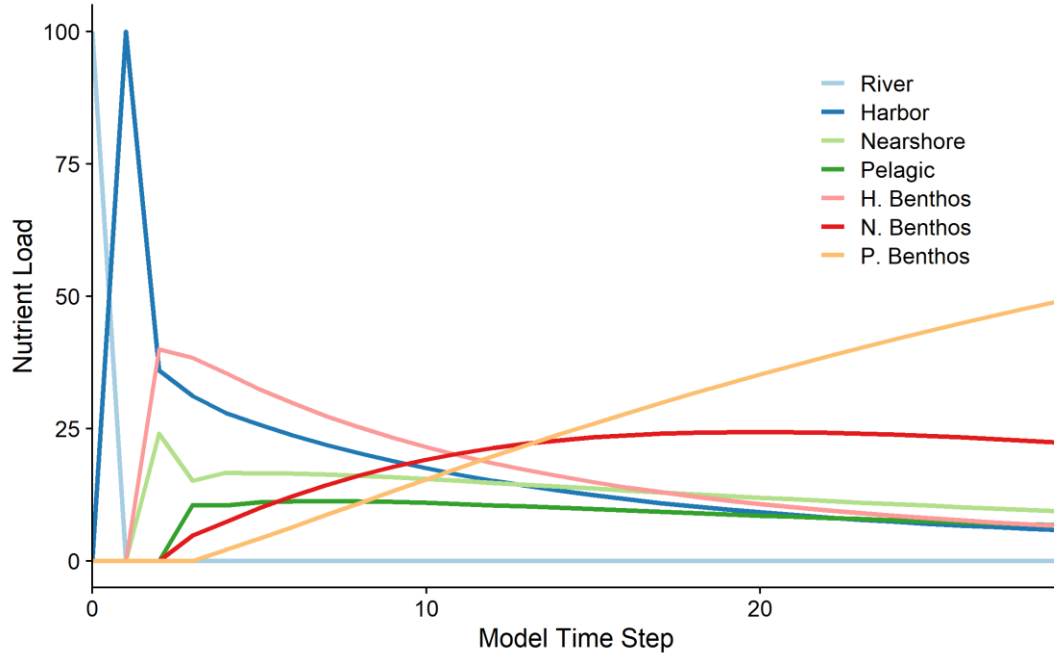
Figure 2: Iterative Output from Nutrient Loading Model.

Results shown for M, l_{max} = 30, A = 100, and $\mathbf{p_{0_1}} = 1$. Note the system responses to a nutrient pulse that is delivered quickly to the harbor, delayed for a short time as some nutrients settle to the harbor benthos. Other nutrients make it to the nearshore zone and the nearshore benthos before nutrients are finally exported to the pelagic where they settle. Due to resuspension, the harbor and nearshore benthos continue to act as a slow nutrient source to the water columns. At l_{max}= 30, the system has not yet reached steady state.

Exploratory Modeling Scenarios

With a working, albeit simple model, it is now possible to explore the model system's

response to various management, seasonal, or threat scenarios that relate to the real system.

With respect to the transport and fate questions of this thesis, three simple scenarios beyond

the previously illustrated pulse injection scenario come to mind.

1. Management reduces nutrient delivery rate to keep nutrient load below a critical

   nearshore threshold.

2. Seasonal resuspension of lake sediments releases and recycles P.

3. Mussel filtration reduces nearshore → pelagic nutrient transport by increasing the effective settling rate to the nearshore benthos.

Results

Model Baseline: Pulse Injection to an Empty System

A

B

C
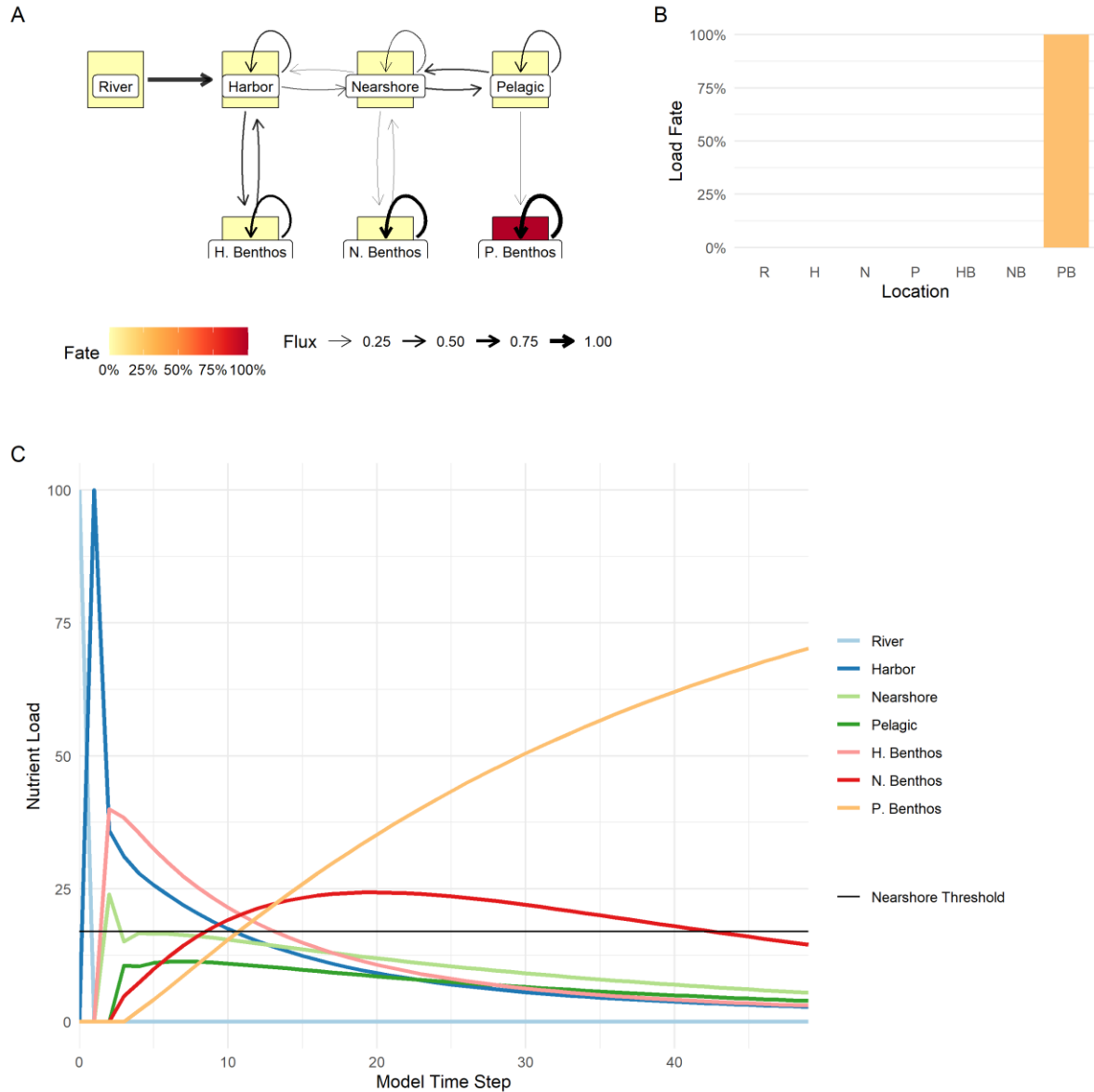
Figure 3: Pulse injection into an empty system.

Changes: No changes to original 7x7 matrix.

A) Shows structure of the model. B) Shows nutrient fate. In this model, all of the nutrients end up in P. benthos. C) Transient portion of the model shows the nutrient pulse moving through the system. Note the black line representing a nearshore management threshold that is initially breached in this pulse injection scenario. At time step 50, the model has not reached steady state.

Model scenario 1: Increased River Residence Time
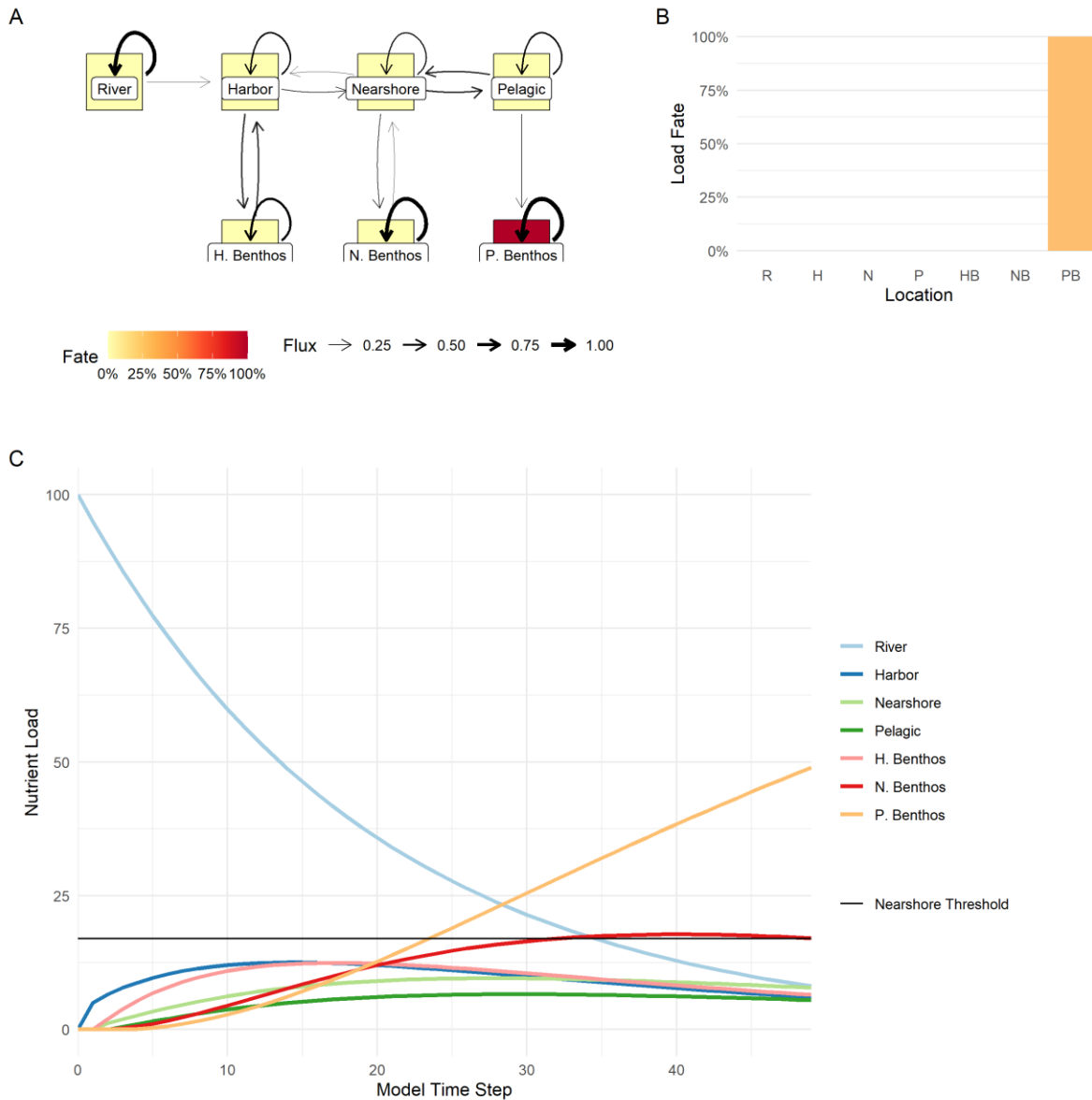
Figure 4: Scenario 1 - Reduced Nutrient Delivery Rate.

Changes: Increase proportion of flux returned to river from 0 →0.95, reducing flux to harbor from 1 → 0.05.

A) Model structure – note that the only change to model structure is a self-return arrow within the river stock. B) Steady state outcomes are not changed by the management actions. C) Transient model – Note that the black "Nearshore Target" line is not breached in this scenario i.e. management action appears to be successful. However, this may not have been true for a case in which residence time was only increased slightly. At time step 50, the model has not yet reached steady state.

Model scenario 2: Seasonal Resuspension of Pelagic Sediments
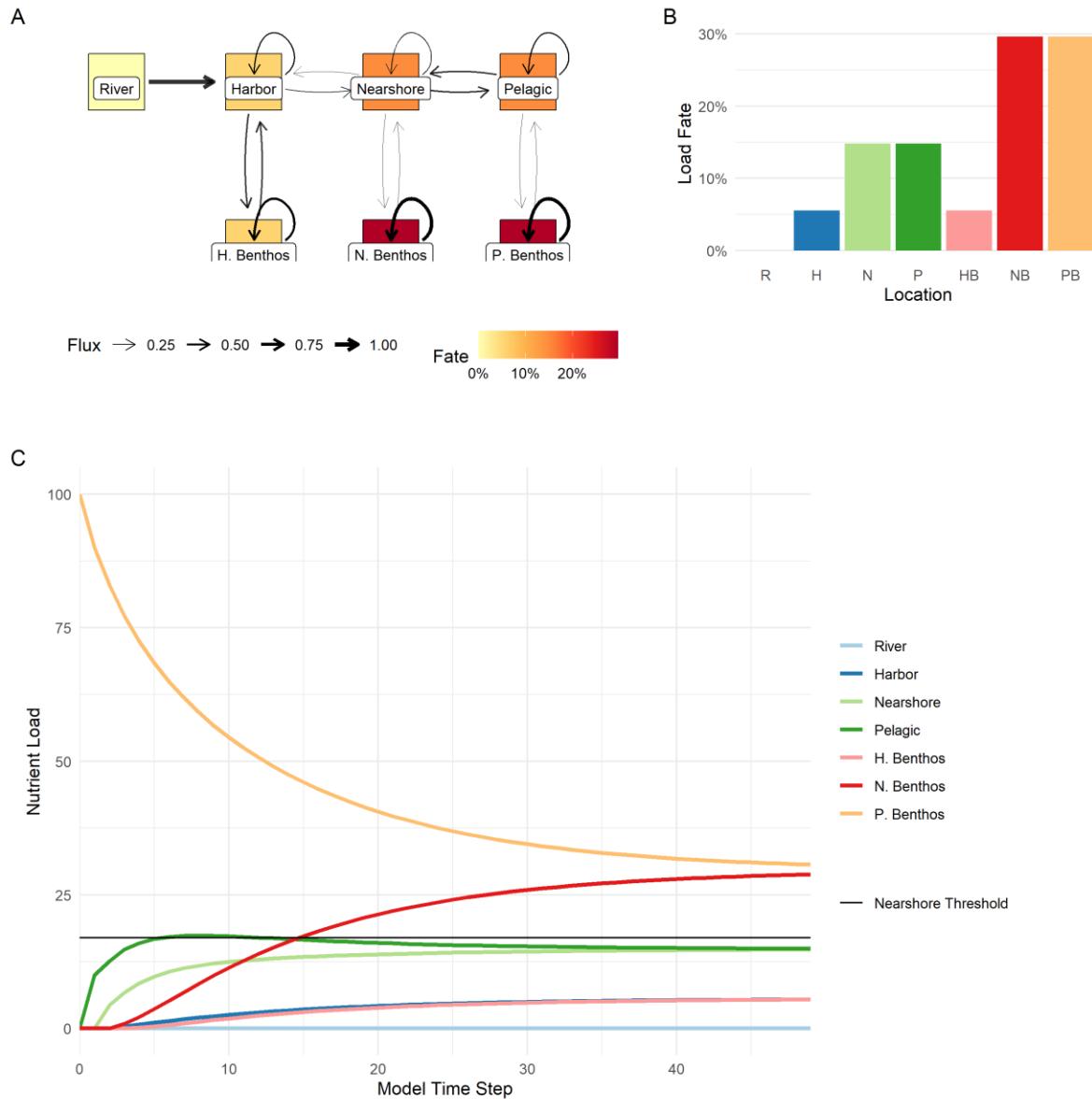
Figure 5: Scenario 2 - Seasonal Resuspension of Pelagic Sediments.

Changes: Increase flux from pelagic benthos to pelagic 0 → 0.1, reducing benthic residence time from 1 → 0.9. Change direction of loading by allocating the full load to p. benthos for the initial conditions.

A) Model structure is the same as in the baseline condition except now a small flux of nutrients is returned from the sediments to the water column. B) Steady state outcomes have changed drastically due to this small modification. Eventually, most nutrients end up in the sediments, but they are balanced between the nearshore and offshore. Similarly, the pelagic and nearshore zones also have equal distributions of nutrients in the water column. C) Transient model shows that the nearshore threshold is met. At time step 50, the model looks to be near steady state convergence.

Model scenario 3: Increased Settling to Nearshore Benthos Reduces Export to Pelagic
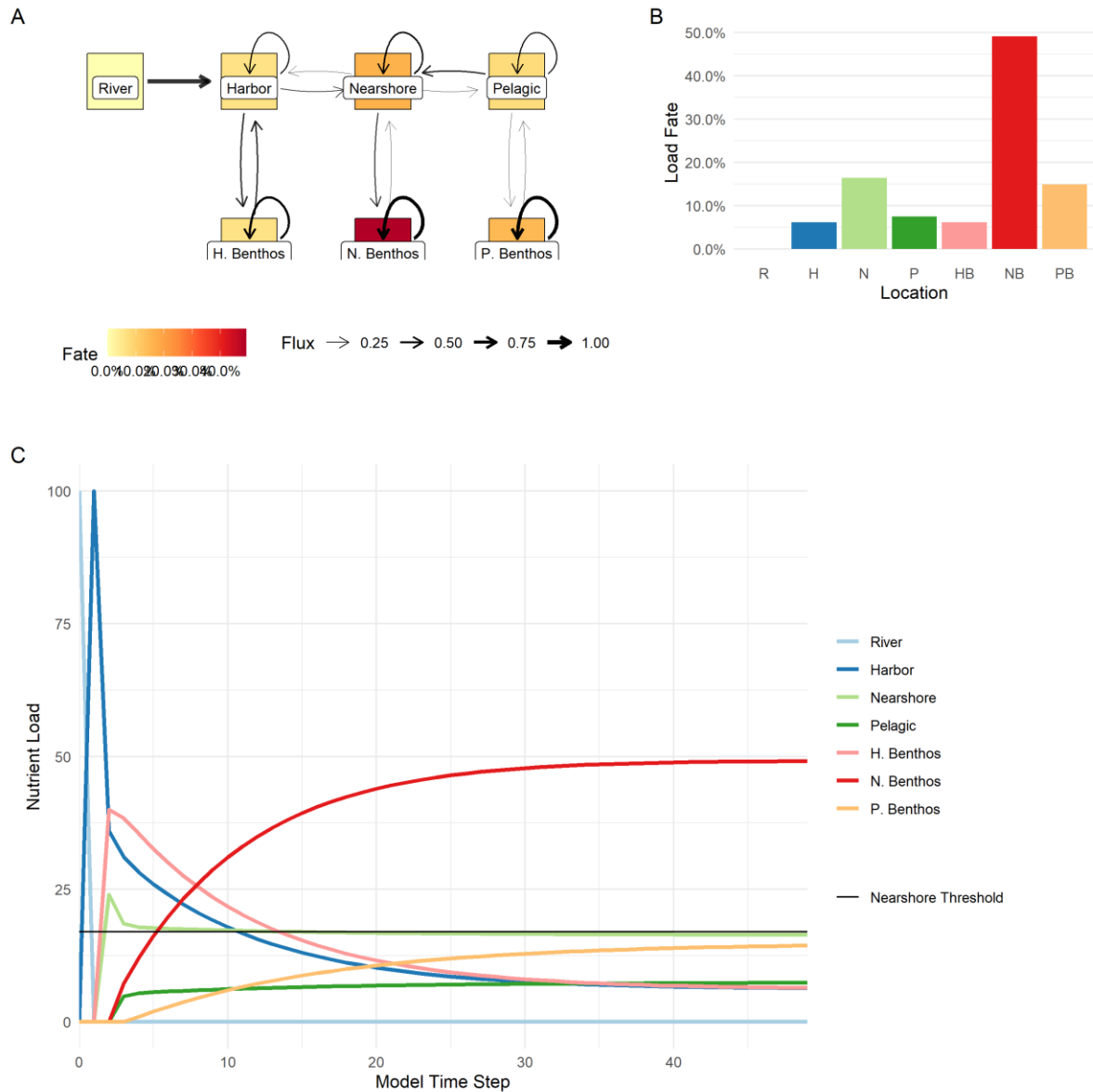
Figure 6: Scenario 3 - Increased Settling to Nearshore Benthos Reduces Export to Pelagic.

Changes: Increase flux from p. benthos to pelagic 0 → 0.1, reducing benthic residence time from 1 → 0.9. Increase settling to nearshore benthos from 0.2 → 0.3. Reduce nearshore to pelagic export 0.44 → 0.2. Increase nearshore residence time from 0.27 → 0.41.

A) Model structure has changed to show increased flux to the benthos, reduced transport to the pelagic, and increased nearshore residence time. B) Steady state outcomes show a shift toward nearshore dominance with ~50% of nutrients fated for the nearshore benthos. The nearshore management threshold is breached initially by the pulse injection, but remains near the threshold due to a shift in nearshore steady state. Additionally, the steady state in the pelagic has been reduced.

Summary of Scenario Results

 Below is an outline that summarizes the results from the 3 exploratory modeling

scenarios. Though these results are "wrong" in that they fail to represent any specific time or

actual place, they may still be useful for gathering intuition about how the real system may

function/dysfunction under different scenarios. Thus, interpretations of the model contain

language about potential real world outcomes.

1) **Model Modification**: Increase river residence time.

 a. **Outcome**: Nutrient delivery rate slows and smooths transitions from river, to harbor,

  to nearshore, potentially mitigating nuisance algae blooms. The steady state

  outcomes are not changed by changes in river residence time.

2) **Model Modification**: Allow resuspension and release of nutrients from sediments in the

 benthos to the pelagic.

 a. **Outcome**: Enhanced nutrient recycling throughout the rest of the lake occurs,

  changing steady state outcomes and underscoring the importance of seasonal

  resuspension and internal loading. A slow release of nutrients from the sediments

  keeps the nearshore threshold from being breached.

3) **Model Modifications**: Increase settling to nearshore benthos. Reduce nearshore export to

 pelagic.

 a. **Outcome:** Invasive mussel filtration combined with high nearshore benthic algae

  biomass increases the effective settling rate, sequestering nutrients in the nearshore

  benthos reducing the export to the pelagic. Nearshore and pelagic zones diverge i.e.

a paradigm shift. The new steady state is near the nearshore threshold, while the offshore is nutrient starved.

Discussion

This simple exploratory modelling reveals a few important things about our theoretical system that may be related to real processes in the Lake Michigan system.

1. Dead end stocks play a disproportionately large role in determining steady state outcomes.

While we may not consider any stock to be a true "dead end" in real life, there are times, such as summer stratification, when an internal stock of nutrients may be less available to the rest of the system (e.g. nutrients in the profundal zone). Additionally, some researchers have regarded invasive mussels as a "dead end" stock for nutrients, due to low predation rates. However, recent shifts in Lake Whitefish feeding behavior have changed this view somewhat (Madenjian et al., 2010).

2. Not all changes to the system affect the steady state outcome.

This was the case for changes to river residence time. However, in this case the change did affect the transient state enough to avoid unwanted outcomes. While it may be difficult to solve an issue like non-point source pollution, perhaps there are intermediate solutions or existing mechanisms in nature that can still help mitigate impairments.

3. Resuspension and internal recycling in general is important.

Without resuspension, or some other flux out, a benthic stock becomes a "dead end". In the model, even a slow flux rate out of a benthic stock had a large impact over time. So what are the mechanisms at work in this critical zone?

4. Changes in flux rates between stocks can have a large impact, especially if the residence time of the receiving stock is long.

This was the case for the benthic stocks in the model which had longer residence times and slower release rates. Thus, even a small increase of a flux into a benthic stock (e.g. increased settling, mussel filtration, benthic algae assimilation etc.) had a disproportionally large impact on study state outcomes.

Additional Thoughts

Since the matrix contains proportional mass flux, stocks are shown in mass, not concentration. However, concentrations can be estimated easily. In this case, all that is needed is an estimate of river, harbor, nearshore, and pelagic zones volumes as well as the areas of harbor, nearshore, and pelagic zone's benthos for calculating the areal density of sediment P. Then, one could estimate residence times, take field measurements of flux rates, and begin to tune the proportional flux parameters of the matrix to a real time and place. If greater spatial resolution is needed, one may simply chain a number of stocks together. However the purpose of this modeling was not to accurately depict a real place and time, but to explore a model system that has some of the same components as the research system.

So while we have not modelled a specific time or place explicitly in this chapter, we have learned things about our model system that may exist in the real world. For example, in a real

river system, movement of nutrients from the river to the lake can be delayed by increased residence time, which can allow for greater biological assimilation and changes in P forms. In chapter 3, I compare two large river systems; investigating trends that may affect P residence time, assimilation, and transformation. Similarly, in the real nearshore zone, movement of P from the water column to the benthos or vice-versa is as important as it was in the exploratory model. Again, the form of P is important for determining nutrient fate. So in chapter 4, I conduct a series of experiments with benthic lake sediments to see what impact they may have on movement between dissolved and particulate forms. Additionally, I investigate mussel filtration, digestion, and egestion/excretion in a series of laboratory experiments to see how mussels may have changed nearshore phosphorus transport and fate in Lake Michigan.

Given the results from exploratory modeling, it seems likely that mussels are the principle driver of the Lake Michigan nutrient paradigm shift. Mussels themselves may act as a partial "dead end" sequestering nutrients in their tissues and shells, but moreover alter nutrient flux rates between the nearshore and the nearshore benthos, which also alters flux between the nearshore and offshore water columns. In the model system, these changes produced a distinct divide between the nearshore and offshore nutrient stores. It seems plausible that mussels may produce a similar effect in the real world.

Chapter 3: River Loading and Phosphate Buffering Mechanisms

Introduction

Land Use and Non-Point Influences on Surface Waters

Agricultural landscapes are known to contribute excess nutrients to surface waters causing beneficial use impairments (BUIs) both worldwide (FAO & IWMI, 2017), and in the Great Lakes Region (Kerr et al., 2016). Similarly, impervious surfaces and other land use characteristics associated with highly developed and industrialized area can negatively impact surface water quality by increasing runoff, reducing residence time, and adding thermal (Herb et al., 2008), toxic metal (Hwang et al., 2016), bacterial (Newton & McLellan, 2015), pharmaceutical & nanoparticle (Boxall et al., 2012), as well as nutrient pollutants (Paul & Meyer, 2001).

Both landscapes are well known, frequently studied stressors of surface water quality, presenting a large challenge for water policy and management due to the complexities of their non-point source nature. Traditional monitoring programs performed by federal agencies such as the USGS and local state agencies have experienced budget cuts, layoffs, and reduced sampling effort (USGS, 1999), adding to this challenge. While there appears to be a renewed public interest in water quality issues evidenced by an increase in citizen science and public engagement, volunteer efforts are not an effective substitute for professionally trained scientists informed and directed by interagency coordination (Woolley et al., 2016). As a result, we lack the temporal resolution, monitoring continuity, and quality of observations needed to answer specific questions about the mechanisms driving and/or mitigating BUIs.

The need for better mechanistic understanding of processes affecting both external and internal nutrient loads is especially apparent in the Great Lakes Region, where renewed issued of eutrophication (Auer et al., 2010b) have been coupled with decreasing offshore productivity (R. Hecky & DePinto, 2020), creating a challenging management conundrum. This chapter deals primarily with non-point source external (i.e. river) loads from two Lake Michigan tributaries. The next chapter will look at internal loading mechanisms.

Phosphorus Loading and Nutrient Processing in the Great Lakes

Determining Loads

Basic non-point load calculations require two primary estimates, 1) stream flow discharge and 2) concentration. The product of these two estimates creates the load with units of mass/unit time. In the Great Lakes Region, streamflow discharge data is available for most large rivers on the American side via the United States Geological Survey's (USGS) National Water Information Service (NWIS) and in Canada from the Hydrometric Data (HYDAT) database maintained by Environment Canada, Water Survey Canada. Concentration estimates from various field monitoring programs are available in STORET, the U.S. EPA database for water quality data. In the days following the adoption of loading targets set by the GLWQA (1978), TP concentrations were monitored and reported regularly to ensure that loading targets were being met. However, formal reporting of TP ceased in 1991 (Dolan & Chapra, 2012), and the number of Great Lakes tributaries monitored with enough frequency and consistency to create accurate loads diminished (Alexander et al., 1996).

In response to the eutrophication issues of the early 2000's, Dolan and Chapra, (2012) used the available government data sources to update TP loading for the Great Lakes Region.

They employed mathematical estimators such as Beal's Ratio Estimator (Beale, 1964; Dolan et al., 1981) and Maximum Likelihood Estimation (El-Shaarawi & Dolan, 1989) to account for stratified and missing data, and had to extrapolate their results from nearby tributaries in areas that were unmonitored. Thus areas that lacked monitoring, such as much of Lake Superior, had greater uncertainty associated with their load estimates. However, estimates can also be derived from the land use characteristics of the watershed. Robertson & Saad, (2011) implimented SPAtially Referenced Regressions On Watershed attributes (SPARROW) models for the Great Lakes to allow for load predictions where available data was sparse as well as compare watershed contributions to load at various spatial scales.

Load estimates were and continue to be an important contribution to Great Lakes modeling efforts. Since the river load is an external input into a lake physical-biogeochemical model, it is often referred to as a forcing variable. Changes to model forcing (i.e. input) will directly affect the response of the model (i.e. output). Thus, determining the size of a river load and how that load is delivered temporally is a critical first step in accurately modeling how that load will be received by the nearshore waters of a lake. Since high frequency temporal resolution is often lacking, modelers must choose how to distribute estimated annual loads. One approach is to assume a constant nutrient concentration and then distribute the mass flux load as a percentage of annual discharge (Rowe et al., 2017). While this assumption may be appropriate or even necessary for large "full lake" scale modeling, it underestimates the variance of a real watershed and may not be able to reproduce real-world phenomena that promote localized BUIs.

Gauging Stations

In the Great Lakes, field measurements made to determine load typically come from stream gauge stations well upstream of the river – lake interface. This is done intentionally to reduce the influence of large lake effects such as seiche and upwelling (Larson et al., 2016). However, this choice means that important in-route processing and transformation of P-species in these dynamic zones are overlooked. In order to quantify these effects, Larson et al., (2016) conducted surveys of 23 river mouth sites along with their upstream and nearshore partners. Then, using stable oxygen isotopes and a water mixing model he was able to determine that 8 of the 23 river mouth sites significantly altered nutrient concentrations beyond what would have been expected from conservative mixing alone, indicating that river mouth processing effects were at work. Each of the 8 "high effect" sites was correlated with a high proportion of upstream cropland, indicating that watershed land use may be an important determinant in downstream fractionation and assimilation patterns at the river-mouth. In another river-mouth study Larson et al., (2019), measured the 'first order loss rate' of dissolved inorganic N and P with a method similar to that of (Reisinger et al., 2015), short term *in situ* water column incubation experiments that measured an initial and final inorganic nutrient concentration from within the water column incubation chamber. The results from these short-term incubation experiments varied widely, predicting dissolved inorganic nutrient losses from 0 – 99% without any clear correlation with ancillary measurements including TSS, Chl *a*, light, temperature etc. So while the study did not identify the clear environmental covariates or driving mechanisms of nutrient loss rates, it did show that the assumption of "no change" between river gauge and lake delivery was not tenable. Moreover it was able to identify residence time as the key

hydrologic factor in modulating water column processing rates with increased residence times

due to low flow allowing for greater nutrient processing.

The estimation of first order loss rates, with the understanding that loss rates may vary

with land use, season, temperature, pH, and other factors, would be of great benefit to current

modeling efforts. Aside from improving the accuracy of current loading models, accounting for

changes to nutrient transport, transformation, and delivery due to first order loss rates may

even help to quantify the value of 'ecosystem services' and restoration projects, by providing a

comparable and quantifiable metric (Larson et al., 2013). Moreover, first order loss rates are

mathematically desirable and easy to incorporate into models and algorithms such as the ones

presented in the previous chapter. So the question becomes, what are the specific biological,

physical, and chemical, factors that modulate nutrient loss rates?

In Route Phosphorus Buffering Mechanisms

P that is transported from a watershed downstream in ionic, i.e. phosphate PO_4^{3-}, form

is reactive and can be assimilated by stream biota such as riparian vegetation, phytoplankton,

and biofilms. Biological assimilation moves P from the soluble reactive phosphorus (SRP) pool

to the particulate phosphorus (PP) pool, which can delay the delivery of SRP to the P-limited

lake, helping to mitigate nuisance algae blooms and other BUIs. Stream restoration projects

have tried to enhance this assimilative pathway by increasing river residence time through

methods such as stream meanders, which allow plants more time to take up nutrients, as well

as increasing floodplain areas, and planting vegetation capable of sequestering SRP

((Newcomer Johnson et al., 2016)). However, phosphate can also be subject to physical and

chemical reactions that move P from the SRP to PP pool. Examples of this include

adsorption/desorption of phosphate on charged fine-grained particles and precipitation/dissolution reactions dependent on species specific chemical equilibria. Together, these physical and chemical mechanisms that regulate P delivery are called the "phosphate buffer mechanism" (Richardson, 1985). Finding and quantifying assimilation pathways and existing buffering mechanisms at the watershed scale could greatly enhance our understanding of in-route processing, improving modeling efforts, and helping managers develop localized P mitigation strategies.

Moving Forward with Management

Within the Great Lakes Region, managers continue to debate which loading factors have contributed the most to nearshore re-eutrophication. Some point to the mischaracterizations of total load due to exclusion of small but many direct lake drainage tributaries (Marcarelli et al., 2019), others point to systematic changes in the "quality" of the load due to increases in the bioavailability (Baker et al., 2014), while still others believe that it is not the magnitude, but the specific timing of the load delivery that matters most (Hui et al., 2021). Additionally, it may not be changes to the external load that are critical, but changes to within lake nutrient recycling induced by invasive Dreissenids (Bootsma & Liao, 2013). There is likely truth in each argument and dealing with BUIs induced from non-point loading sources may require a combination of high level federal oversight (e.g. changes to current loading targets) as well site specific monitoring and management efforts to identify stressors and solutions at the local level.

One thing is certain, with the manifest and impending increase of episodic storm events in the Great Lakes region (Wuebbles et al., 2019), we need a better understanding of how watersheds are reacting to the intensification of atmospheric and hydrologic forcing. This need

47

is especially true for urban and agricultural watersheds, which are known stressors to surface water quality. Due to the complex, interactive, and often localized nature of the non-point source problem, efforts must be made to increase the frequency and quality of nutrient observations. This should be paired with efforts to gather, curate, and analyze the necessary ancillary data to contextualize nutrient observations. Given improvements in government data curation and storage, it is now possible for this type of data processing pipeline to be automated, flexible, and scalable. Increased nutrient observations combined with contextualization can aide federal management and inform policy and may also provide valuable insight into important nutrient buffering mechanisms, improving modeling efforts, and giving managers the tools they need to mitigate BUIs at the local level.

Outline of Research Questions

The goal of this study was to collect and compare high frequency (i.e. daily) phosphorus samples from the Milwaukee and Sheboygan Rivers. The watersheds associated with these rivers are similar in total load, but different in their land use, with Milwaukee having a higher percentage of urbanized land and Sheboygan a larger percentage dedicated to agriculture. Recognizing the potential importance of in-route processing and interactive lake effects, observations for this study were taken at the tributary mouth of each river where river, harbor, and lake dynamics intermingle. Additionally, to account for potential changes in load bioavailability, P samples were fractionated into two dissolved and two particulate groups for a total of four groups:

1) Soluble reactive phosphorus (SRP)

2) Dissolved organic phosphorus (DOP)

3) NaOH-extractable particulate phosphorus (NaOH-P)

4) Non-NaOH extractable particulate phosphorus (Other-PP)

Phosphorus observations were complimented and contextualized by the collection of a variety of ancillary data including data from *in situ* Sondes, buoy data, NOAA weather data, historic USGS data, and load estimations from a variety of federal and state agencies. The following are important questions I considered when comparing and contrasting loads mobilized from these landscapes moving from general to particular:

1. How large is the load?

    a. How large is loading relative to watershed area?

2. How much of the load is bioavailable?

    a. How is loading partitioned among various P pools?

3. Is P partitioning relatively stable or dynamic?

    a. If dynamic, is there a generalizable pattern?

    b. What mechanisms might drive partitioning patterns?

4. Are there detectable P assimilation and buffering mechanisms?

    a. If so, how might one heal, restore, or enhance them?

Background

Overview of Study Area
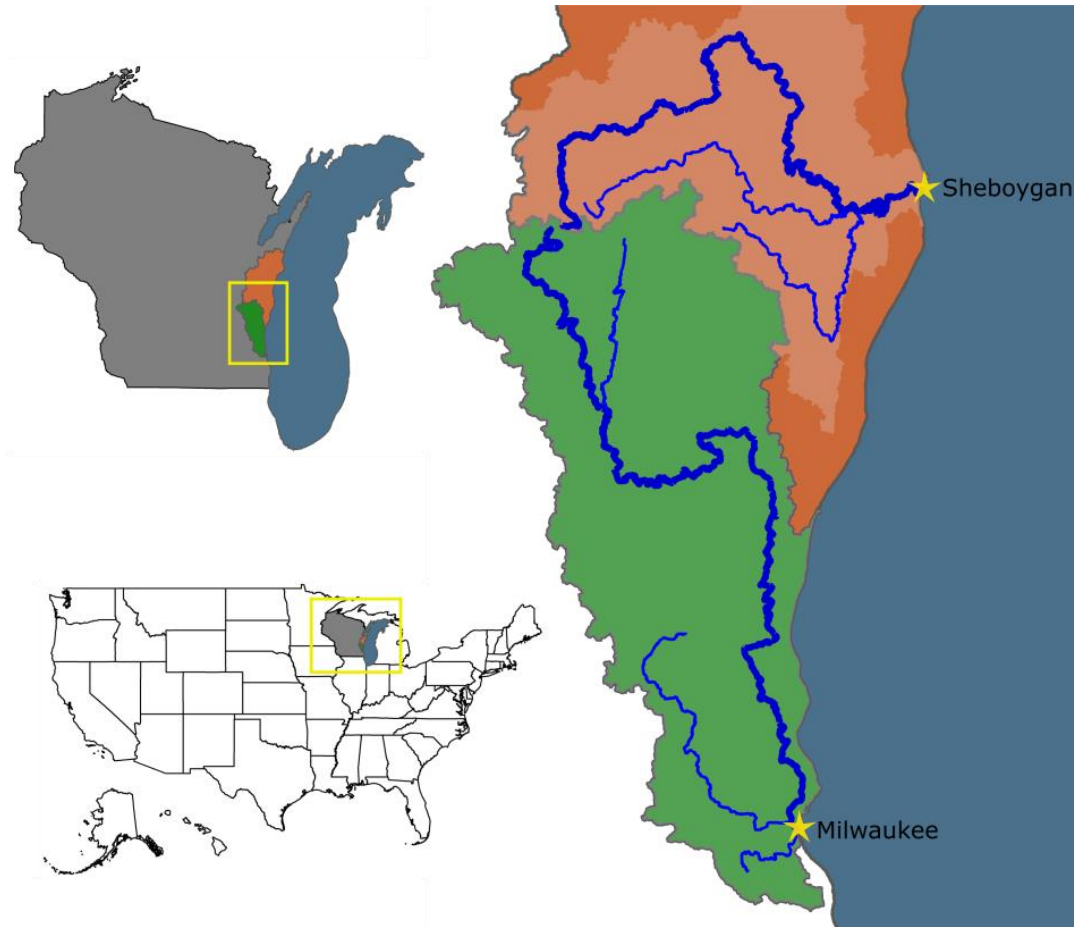
Figure 7: Study Region

The Milwaukee (green) and Manitowoc-Sheboygan (sienna) watersheds located in southeastern Wisconsin on the Western side of Lake Michigan. Note that lighter shade of sienna is drainage associated with the Sheboygan River and its tributaries. Darker sienna shades indicate Manitowoc or direct lake drainage. Thick blue lines represent the Milwaukee and Sheboygan Rivers, while thinner lines represent their major tributaries (i.e. South to North, the Kinnicknic, Menomonee, E. Branch Milwaukee, Onion, and Mullet Rivers). Figure created with data from USGS's National Hydrography Dataset.

Comparison of Watersheds, Rivers, and Harbors

The Milwaukee and Manitowoc-Sheboygan Watersheds (Figure 7) rest on the eastern

side of Lake Michigan in South-eastern Wisconsin. The Milwaukee River drains 2,259 km^2 of

mixed-use land that includes urban runoff from the city of Milwaukee and has been estimated

to contribute a median of 66.7 MTA of P loading to Lake Michigan. The Sheboygan River drains

1,089 km² of primarily agricultural land and has been estimated to contribute a median of 54.4

MTA to P loading (Dolan & Chapra, 2012).

Although point source loading to the lake declined following the implementation

GLWQA, nonpoint source loading from these rivers has remained relatively stable since the

1980s and recent observations show the two rivers trending together (Figure 8).
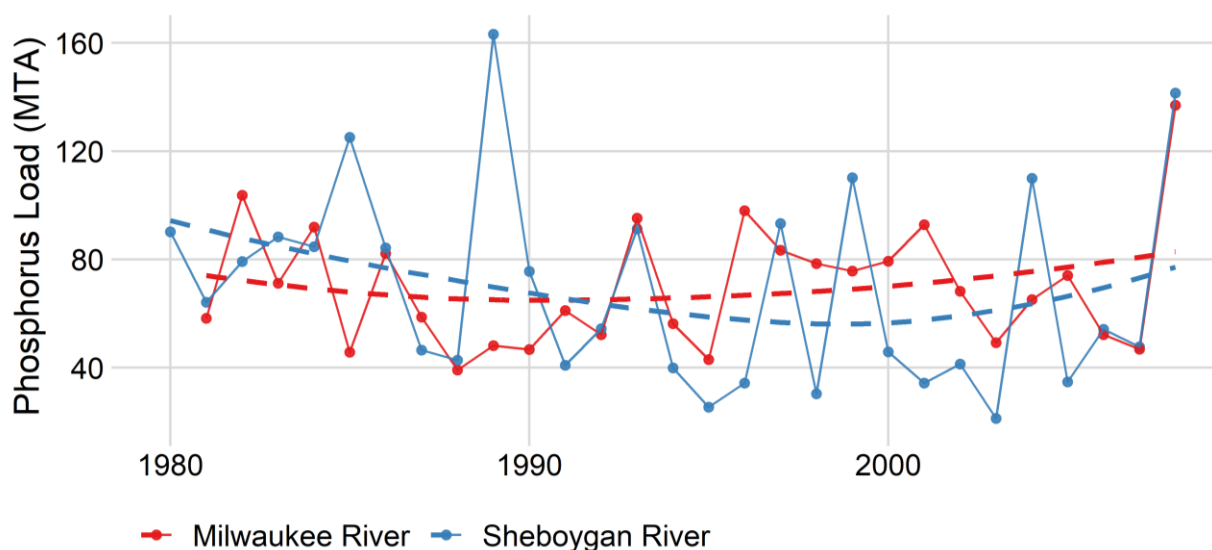
Figure 8: Historic Phosphorus Loads by Watershed

Annual phosphorus loads by watershed, 1980-2008 (data from Dolan and Chapra (2012)). Dashed lines show loess
smoothing. Nonpoint source loading from these rivers has remained relatively stable since the 1980s and recent
observations show the two rivers trending together.

Site Dynamics

River

At their headwaters, the Milwaukee and Sheboygan Rivers appear quite similar, with

tributaries stemming from a mix of inland lakes, farm, forest, and marsh land. However, as you

travel downstream, a bifurcation becomes apparent. The Sheboygan continues to meander

through rural Wisconsin's farm and marsh land until reaching its channelized and armored

harbor at < 3.2 km from Lake Michigan. The Milwaukee River, on the other hand begins to

experience the effects of urbanization as early as Saukville, > 40 km upstream of its mouth at

Milwaukee Harbor. There are also several dams between Saukville and the harbor, which can

reduce particle transport through sedimentation, and may shift phosphorus fractionation

patters. Starting at Lincoln creek, the river's channel is stabilized with rip-rap. Shortly thereafter

near Caesar park, the channel is armored 6.4 km away from the river's nearest exit to Lake

Michigan through Milwaukee Harbor Middle Gap.

Despite many similarities, the proportion of the Sheboygan River's developed land use is only 1/3 that of the Milwaukee River (Figure 9). Because of this, one may expect the Milwaukee to act "flashier", with a shorter river residence time following a precipitation event. River residence time can have a
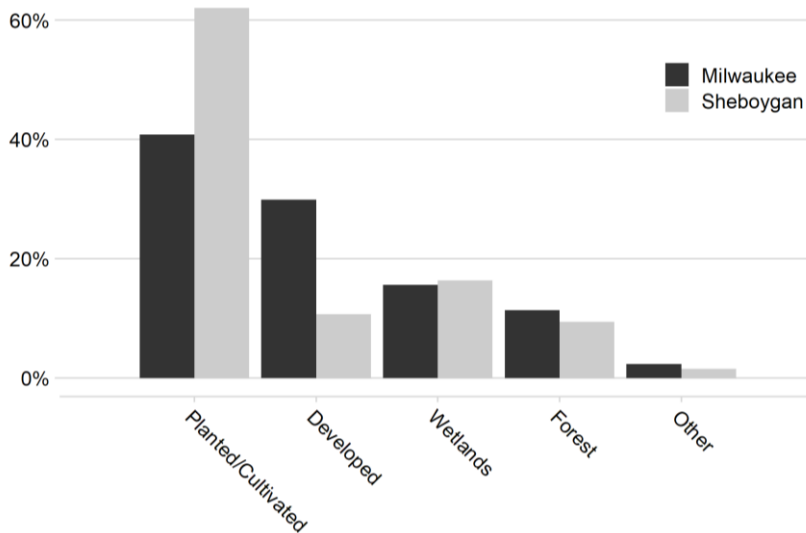
Figure 9: Land Use by Watershed

The primary differences between the Sheboygan and Milwaukee watersheds is the percentage of land use in agricultural (i.e. "planted cultivated") vs developed. Milwaukee has a higher percentage of developed land and Sheboygan a larger percentage dedicated to agriculture.

large impact on nutrient delivery and fractionation. However, there are other land use factors

that impact nutrients, such as agriculture. A study in upstate New York found evidence that P

loads from a primarily agricultural landscape contained a higher mean fraction of bioavailable

phosphorus than other land uses (Prestigiacomo et al., 2016). If this observation holds true in

Sheboygan's watershed, which has 1.5x more agricultural land than Milwaukee's (Figure 9), this excess of bioavailable P could perturb Sheboygan's nearshore zone and may be more important than river residence time.

Harbor

Another important factor that can modulate nutrient delivery rates and fractionation patterns is the size and unique structure of each river's harbor. The Milwaukee river estuary is quite large, a total area of 7.49 km^2 that includes the confluence of three major rivers, as well as an inner and outer harbor area (Dow, 2018). In contrast, the Sheboygan River's inner and outer harbors are a fraction of the size, with a combined area of 0.4 km^2 (Bzdusek et al., 2006). Physical aspects of a harbor such as sharp corners, bends, and hydrodynamic "dead zones" can also impact residence time. Due to its large size, complex layout, and extended residence times, previous work has suggested that the Milwaukee harbor acts as an effective P sink, with losses to harbor sediments and biologic activity estimated to be -45% within the particulate pool and -39% within soluble pool (Bannerman et al., 1979; Bootsma et al., 2005).

In 2016, a systematic survey of P speciation between the Milwaukee River and a pelagic station showed monotonic declines in both dissolved inorganic phosphorus (DIP, primarily as phosphate, PO_4^{3-}) and particulate inorganic phosphorous (PIP). Interestingly, the smaller area between the Milwaukee River and harbor mouth saw substantial increases in dissolved organic phosphorus (DOP) during May and June (Lin & Guo, 2016). While the harbor likely functions as an overall P sink, it is not an indiscriminate one. The harbor may function similarly to a waste water treatment plant, with increased residence times affording particle settling and within-

53

harbor biologic activity transforming P species, ultimately affecting the proportion of

bioavailable phosphorus (BAP) discharged to Milwaukee's nearshore.

Bannerman et al., (1979) estimated Milwaukee's mean outer harbor residence time to

be 6 days, however, a more recent study using medically-derived iodine-131 as a tracer

estimated that Milwaukee's outer harbor water column residence time was only 3.1 days

(Montenero et al., 2017). On the opposite end of the spectrum, the natural residence time, as

calculated with Equation 3, was closer to 21 days. Since Sheboygan's harbor is a fraction of the

size of Milwaukee's, we can estimate that its natural residence time will be much shorter.

Sheboygan's harbor has an average depth of 6.4 m making for an estimated volume of 2.56

$x10^6$ m^3, and a mean flowrate near 12 m^{3}s^{-1}. If we assume steady state, and ignore

channel/harbor morphology residence time can be estimated with harbor volume/in-flow.

Thus, we can estimate that Sheboygan Harbor has a mean residence time of 2.7 days. However,

given that other estimation methods estimated residence times much shorter than the natural

residence time for Milwaukee's harbor, it is possible that Sheboygan harbor has a much shorter

residence time as well on the order of hours. This shorter residence time may reduce the

effects of particulate settling and within-harbor P species transformation. The final

consequence of these factors is that Sheboygan River may discharge a greater percentage of its

nutrient loads directly into the nearshore zone.

Methods

Field Data Collection

River water samples were collected from July through early November 2020 at the

mouths of the Sheboygan and Milwaukee Rivers using automated ISCO samplers (Figure 10).

Original plans to sample during the entire *Cladophora* growing season (May-October) had to be adjusted due to the Covid-19 pandemic and subsequent lockdown. Samples were collected as daily composites in acid washed polypropylene ISCO bottles, with 4 equal volume samples per bottle taken every 6 hours starting at midnight the day after deployment as was done in Baker et al., (2014). Thus, each bottle represented an estimate of the average P conditions for a single calendar day.
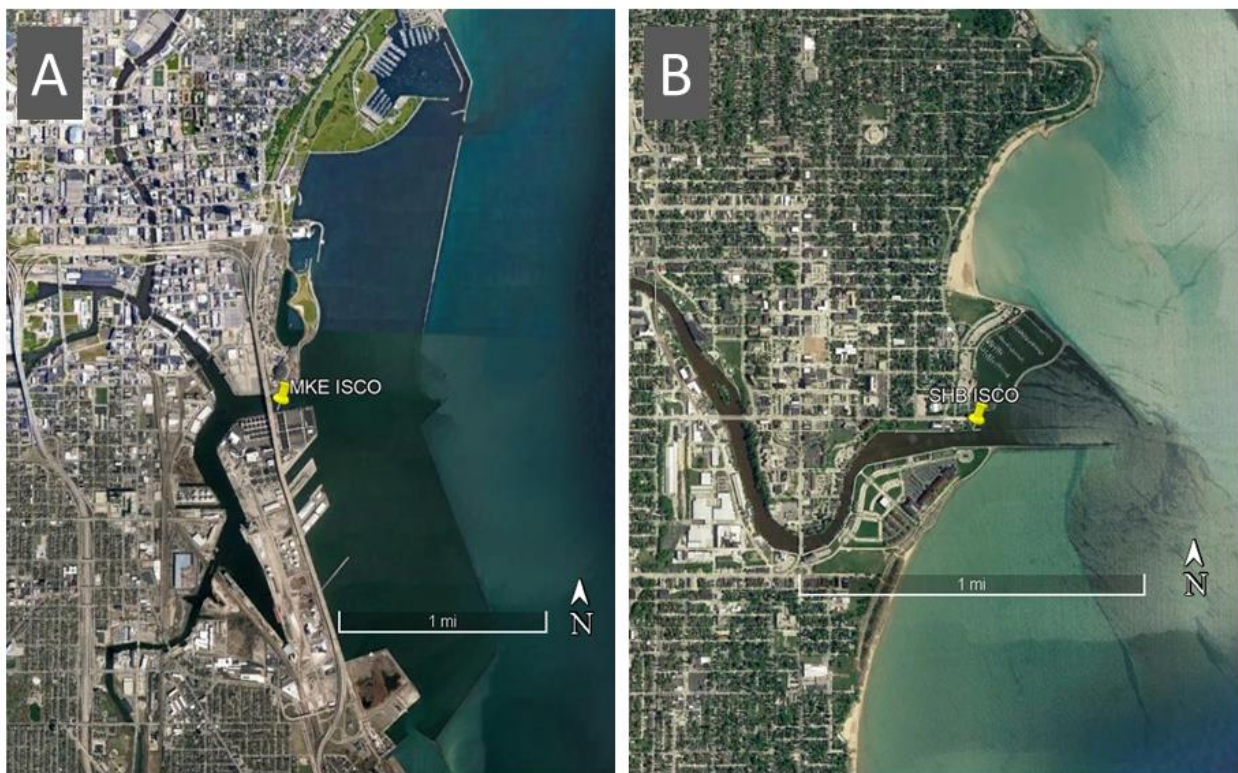
Figure 10: ISCO Sampler Locations

Yellow pin shows location of ISCO sampler. A) Milwaukee harbor area. B) Sheboygan harbor area. Milwaukee's harbor is much larger, and more complex than Sheboygan's.

Upon deployment and during each subsequent bottle collection trip, a manual ISCO sample of 1L of water was taken, homogenized in an acid washed, polypropylene bottle, and then subdivided into two 500 mL replicates. One of these replicates, "fresh", was immediately

packed on ice and taken to the lab for same day filtration and analysis while the other was left

on site in the final slot of the ISCO sampler (referred to as the "old" replicate. This process

allowed for estimation how partitioning among the various P pools may have altered in the

time between ISCO sampling and laboratory analysis, which at times was nearly 3 weeks. To

ensure that P fractionation was not induced by anoxic effects, periodic measurements of

dissolved oxygen in the "old" sample bottle were taken on site with a handheld oxygen sensor

and compared to ambient river concentrations prior to sample packaging and transport.

ISCO measurements were complemented by *in situ* sonde (6600 at SHB, and Exo2* at

MKE) deployments with measurements of pressure, temperature, conductivity, turbidity,

dissolved oxygen*, and pH* taken every 15 minutes at SHB, and every 10 minutes at MKE. The

SHB sonde received maintenance during each site visit, every 1-3 weeks. The MKE Sonde at

Jones Island is the property of USGS and calibrated/maintained on a monthly schedule

(personal correspondence with USGS). Sonde measurements were used to identify lake

backwater effects such as seiches and upwelling events and, when combined with NOAA

meteorological data and USGS discharge data, offered insight into disentangling the timing and

effects of episodic storm events, seasonal changes, and large lake processes. Having this

additional time series data also aided in data imputation of missing or compromised ISCO

samples and allowed me to test the efficacy of estimating P dynamics at each location via

surrogate variables such as turbidity (Grayson et al., 1996).

Chemical Analysis

All phosphorus fractions were analyzed by first converting, if necessary, the target P

fraction(s) to SRP followed by reduction with the 4:1 molybdate-ascorbid acid method of

Stainton et al. (1977) and measurement of absorbance at 885 nm on a spectrophotometer. The SRP detection limit for analysis on a 10 cm path length cuvette was 0.3 μg/L. Total dissolved phosphorus (TDP) samples were digested by adding dilute sulfuric acid and peroxide, followed by a 2-hour photo-oxidation digestion. DOP was derived by subtracting SRP from TDP. Total PP samples were first digested by high temperature combustion (i.e. 550 °C for 1 hour in a muffle furnace) followed by a 2-hour extraction in a dilute hydrochloric acid solution at 105 °C (Stainton et al. 1977). NaOH-P was measured following the 17-hour shaker sodium hydroxide extraction method described in Baker et al. (2014). NaOH-P is the particulate fraction that has been determined to be the most bioavailable to algae (DePinto et al., 1981). Non-NaOH-P or "Other-PP" was calculated by subtracting NaOH-P from Total PP. Only "fresh" samples were analyzed for Chl a, which was extracted with a 68:27:5 methanol–acetone–deionized water extraction solvent for 24 hours at −28 °C and then measured on a Turner Model 10 Series fluorometer. TSS was determined by filtering onto dried pre-weighed membrane filters, redrying at 60-70°C for >12 hours and reweighing. Weights were measured on a Sartorius 3-digit microbalance with an accuracy of 0.001 mg.

Additional Data Gathered

To add larger context to the samples, supplementary data including USGS discharge and NOAA meteorological data were gathered from each organization. USGS data is available online in tab-delimited (rbd) file format. Users can find and download the data using USGS's webpage GUI *https://waterdata.usgs.gov/nwis/* or automate retrievals using USGS's REST (i.e. URL friendly) web services *https://waterservices.usgs.gov/rest/*. NOAA climate data are available for download via a browser based GUI tool at *https://www.ncdc.noaa.gov/cdo-web/datasets*.

However, downloads can be automated by pulling directly from their public FTP server

https://www1.ncdc.noaa.gov/pub/data/. To approximate daily precipitation patterns at the

watershed scale, I used county level precipitation grids by month from NOAA's FTP server

https://www1.ncdc.noaa.gov/pub/data/daily-grids/beta/by-month/ .

Consistent meteorological observations including wind and air temperature were found

at the Sheboygan (Station ID "KSBM") and Milwaukee (Station ID "KMKE") airports and

retrieved using the synoptic data Mesonet API *https://developers.synopticdata.com/mesonet/*.

KMKE (42.9484 -87.9046) is located approximately 5.25 miles south of the MKE Jones Island

sampling station and KSBM (43.7639° -87.8520°) is located approximately 7.5 miles west of the

SHB sampling station.

For comparison, historic grab sample and loading estimates from the SHB river were

provided by the WDNR NE Lakeshore TMDL program Coordinator (personal communication),

and historic grab samples from MKE JI site were fetched from the USGS webpage

https://nwis.waterdata.usgs.gov/usa/nwis/qwdata.

Land use data for the contiguous United States and Alaska are available from the

National Land Cover Database (NLCD) and Multi-Resolution Land Characteristics Consortium

partnership via their viewer download tool *https://www.mrlc.gov/viewer/* . I used the 2016

land use raster data which is available in 30m resolution. Watershed boundary data came from

USGS's NHD data set. Both watershed and land use data were processed in R using the sf, rgdal,

and raster packages (Bivand et al., 2021; Hijmans, 2020; Pebesma, 2018). Data were

transformed to an appropriate equal area projection for SE Wisconsin, and specific land use for

each watershed was extracted by using the watershed boundaries as a mask over the land use data.

All of these data were compiled, cleaned, and merged with the *in situ* samples and have been made publicly available to view in an interactive web application "Limno Explorer" that was created as part of this project *https://nvanee.shinyapps.io/LimnoExplorer/*. Additionally, buoy data from UW-Milwaukee's Atw20m buoy (GLOS Buoy 45013) during the 2020 season have also been made available in for data exploration

https://nvanee.shinyapps.io/BuoyApp_2020/ .

Quality Assurance and Quality Control
ISCO sample preservation experiments

Samples tested for post storage oxygen levels were never more than 2 mg/L different from ambient river water and never below 7 mg/L suggesting that samples did not experience anoxia. Preservation experiments showed only small changes in total phosphorus with a mean difference between fresh and old samples of -3.34 µg/L for Milwaukee (sd = 4.59 µg/L) and -1.37 µg/L for Sheboygan (sd = 5.87 µg/L). Mass balances were also good with an average percent error of -3.64% for Milwaukee (sd = 5.70%) and -0.572% for Sheboygan (sd = 5.41%). Partitioning between the specific fractions of P were more dynamic, but generally showed moderate increases of SRP concentration for "old" samples with decreases in DOP, NaOH-P, and PP (Figure 11). Change in SRP while samples were in the ISCO was almost always positive and change in PP was mostly negative. Two notable exceptions to this trend were samples taken at SHB on 2020-07-30 and the other at MKE on 2020-11-02. This observation may

indicate that particulate material was actively scavenging soluble forms of P at the time of

sample collection.
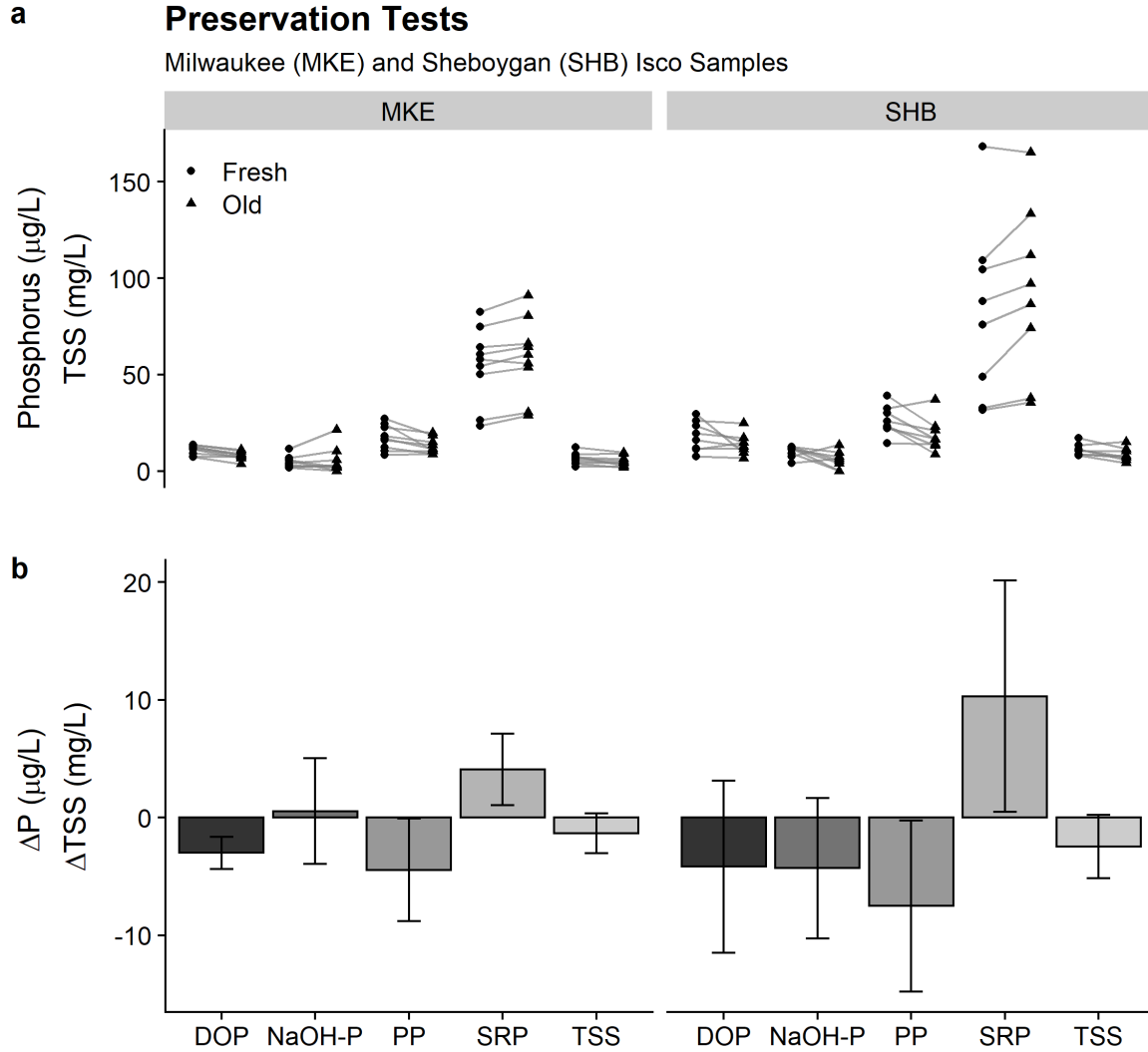
Figure 11: ISCO Preservation Experiments

Preservation experiments showed that in general, PP samples degraded to SRP. A) Plot shows paired "fresh" and "old" observations, note that SRP slopes are almost all positive and PP slopes are almost all negative. B) Barplot shows mean ± SD change between "old" and "fresh" samples.

Samples from the Sheboygan ISCO showed greater average change and higher variability

in each fraction (Figure 11 b). One plausible explanation for this variation is the difference in

ISCOs installations. The Sheboygan ISCO was installed outdoors to a chain-link fence at the US

Coast Guard Station where it was exposed to a wide range of environmental conditions. The

MKE ISCO, however, was protected from the elements inside the USGS gauging station on Jones

Island (04087170). It is also possible that variance in storage reflects differences in actual water

chemistry between the two rivers.

Other studies have also shown that the effects of one week of unrefrigerated storage

between sample collection and analysis have minimal impact on P loading calculations

(Johnson, 2013). Although our storage times were sometimes greater than a week, we too saw

relatively small effects on the order of ~5 µg/L. Since effects were small and there was no

evidence of sample bottles going anoxic, the data were analyzed "raw", rather than attempting

to adjust data for the effect of storage.

Imputation of lost and compromised samples
There were several occasions in which ISCO sample results were compromised. Reasons

varied from loss of battery power to technician error in sample processing. There were also

periods in which Sonde data collection was halted due to necessary maintenance. Though

missing data in WQ datasets is common, there is not a consensus on which imputation methods

are most appropriate. Generally, it is accepted that missing data require case by case

assessment based on the cause and patterns of data gaps (Hamzah, 2020). Since gaps in Sonde

data were usually short (< 1.5 hours) missing data were imputed with simple linear

interpolation. The same approach was taken for single missing samples from the ISCO.

However, for a few cases at the SHB ISCO, data gaps were longer and alternate imputation

methods had to be considered to achieve more realistic results (Figure 12).

Multivariate imputation models were all created in the R package tidymodels. First, a linear interpolation model was created as a baseline. Next, I created more sophisticated bagged tree and K-Nearest Neighbors (KNN) imputation models trained on the *in situ* Sonde and USGS discharge data.

The bagged tree method is a decision tree suite that splits data into smaller and smaller subsets based on the input from the available predictors. This process is iterated hundreds of times creating a forest of decision trees. Finally, the resulting "vote" from each tree is averaged and tested against a number of unseen observations that have been held out or "bagged" to help evaluate the model. The entire process is then rerun as parameters are adjusted to enhance model performance until some user defined threshold is met. Though it sounds computationally expensive, because each individual tree is independent of the others, trees and forests can be grown in parallel.

KNN is a distance-based method that predicts the missing value based off a weighted average of the k (in this case 5) nearest neighbors in a Gower's distance matrix.
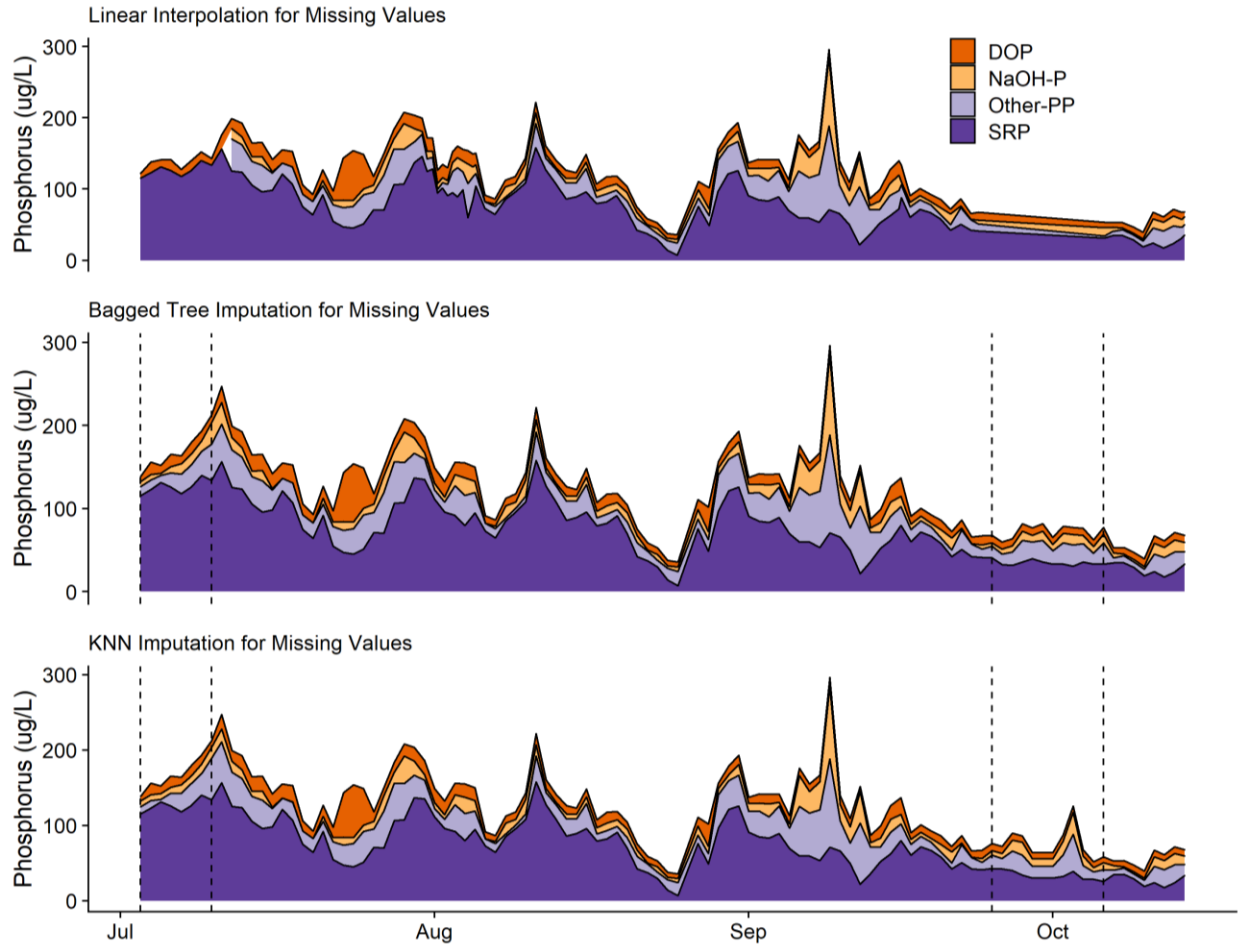
Figure 12: Multivariate Imputation for Missing Samples.

Top row = Linear Regression. Middle row = Bagged Tree. Bottom row = KNN.

Both bagged trees and KNN methods produced similar results (Figure 12) but ultimately,

I decided to proceed to analysis with the results from KNN imputation based on visual analysis

of the results alongside covariates such as discharge and turbidity. However, this visual

inspection method was somewhat subjective. A better method would have been to use cross

validation. Separating out a portion of the original data (i.e. test set), developing the imputation

models with the remaining data (i.e. training set), and testing the imputation models

performance on the unseen test set data.

63

Results

Answering Research Questions

How large is the load?

I multiplied the daily mean concentration of TP by mean daily discharge to attain daily TP load estimates. The mean daily load for Milwaukee was 168 ± 104 kg d^{-1}, whereas the mean daily load for Sheboygan was higher and more variable at 175 ± 267 kg d^{-1}. Controlling for the size of the watersheds and extrapolating the daily median loads to a year, Milwaukee had a median yield of 21.7 kg/km^2/yr and Sheboygan had a median yield of 31.4 kg/km^2/yr. These values are compared to the other available sources in Table 2.

Table 2: Comparison of Median Yield Estimates by Watershed

All Table numbers show Total Phosphorus Annual Yield (kg/km^2/yr).

Estimates from this study are lower than the other studies. This is likely a seasonal effect since a large proportion of load enters during the spring. Seasonally filtered data from WDNR produced a yield of 17.5 kg/km^2/yr for SHB.

Tributary	SPARROW	Dolan and Chapra	WDNR TMDL Draft	This Study
Sheboygan River	102.6	48.3	41	31.4
Milwaukee River	108.2	29.8	-	21.7

Yields calculated for this study are lower than the other three estimates. This is not surprising given that these data were collected from July – November and missed the early spring months typically associated with high loading. The WDNR produced modelled estimates of daily loads 1990 – 2019 curtesy of the North East Lakeshore Total Maximum Daily Load project. I was able to filter this data set to derive a median yield specific to my 2020 sampling schedule. This resulted in a new date specific estimated median yield of 17.5 kg/km^2/yr, suggesting that 2020's median yield for the same dates was nearly twice as high as the 1990 – 2019 seasonal median.

Loading patterns between the rivers were moderately correlated (Pearson's Correlation Coefficient (r) = 0.39). A time series plot shows Sheboygan's mean daily TP load was well below Milwaukee's from mid-August to late October, but peaked near 2500 kg/day on October 25 during a large precipitation event (Figure 13). However, on the same day, with a similar amount of precipitation, Milwaukee had a load near 320 kg/day.
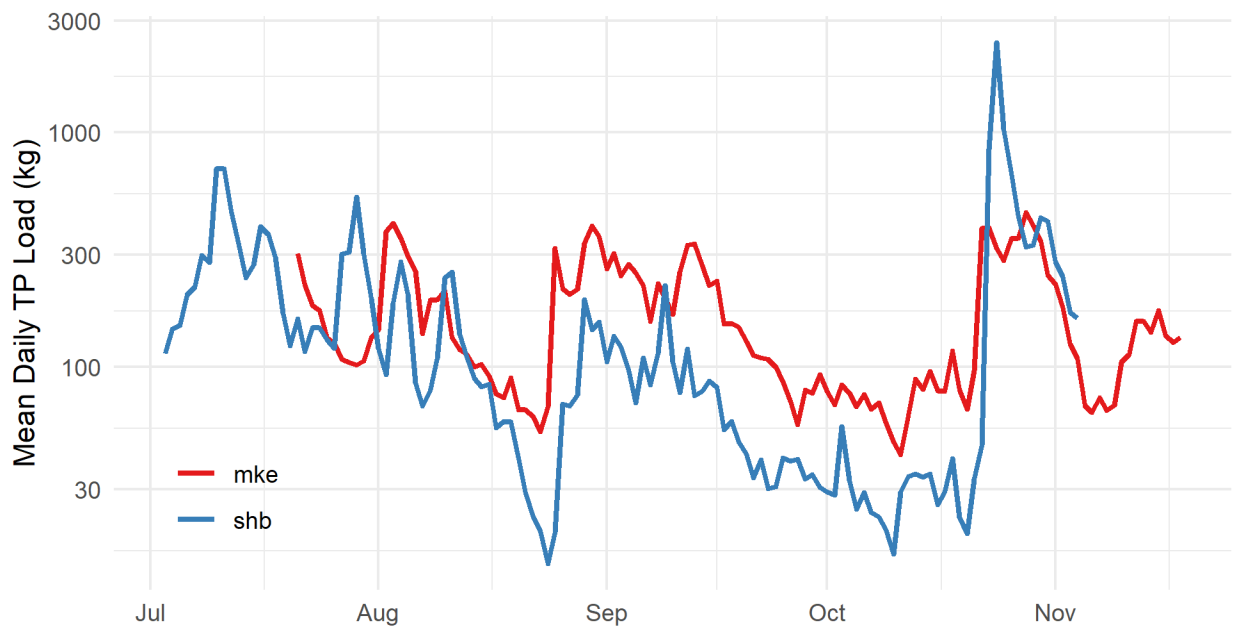
Figure 13: Mean Daily TP Loads (kg)

Milwaukee and Sheboygan loading patters were similar, but Sheboygan's load was more variable. Note the log10 scale on the Y-axis.

How much of the P is bioavailable?

Milwaukee and Sheboygan were similar in terms of bioavailability (i.e. SRP + NaOH-P), with average bioavailability concentrations near 70%. Within this bioavailable fraction SRP was the dominant contributor at 79% for Milwaukee and 85% for Sheboygan (Table 3). Sheboygan's mean daily concentration of bioavailable P was higher at 90 µg/L than Milwaukee's at 65 µg/L.

Table 3: Mean and Percent Daily Bioavailability by River

Milwaukee				Sheboygan			
95				130			
Less Available		Bioavailable		Less Available		Bioavailable	
30		65		40		90	
31%		69%		31%		69%	
DOP	Other PP	NaOH-P	SRP	DOP	Other PP	NaOH-P	SRP
8.8	20.8	13.4	51.5	13.3	27.2	13.6	76.0
30%	70%	21%	79%	33%	67%	15%	85%

*plain numbers are concentration µg/L and percentages relate to preceding upper level

Accounting for discharge, the mean bioavailable load for Milwaukee was 116 ± 74.5 kg d^{-1} and 121 ± 172 kg d^{-1} for Sheboygan. The daily percentage of the load that was bioavailable varied from 35 – 91% for Sheboygan, with less variance at Milwaukee from 46 – 82%. Aside from a large precipitation event on October 24, bioavailability generally seemed to decrease moving from summer to fall (Figure 14).
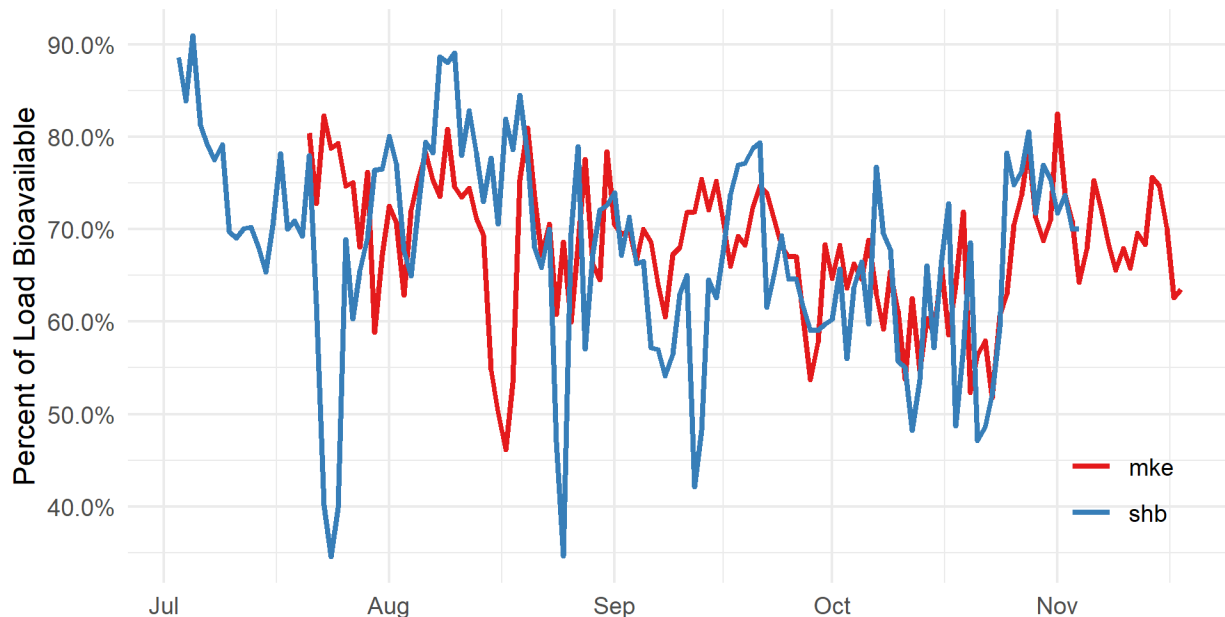
Figure 14: Percent of Load Bioavailable

Both rivers had loads with a mean bioavailability near 70%, but Sheboygan's bioavailability was more variable.

How is P partitioned across the various P pools?

On average, the Sheboygan River saw both greater mean daily concentrations and variation of P across all fractions tested (Figure 15 a). However, allocations of P fractions as a percentage were very similar between both rivers (Figure 15 b). Sina plots of P fraction concentration by location (Figure 15 c) show the dynamic spread of Sheboygan's data compared to Milwaukee's tighter distributions. Unsurprisingly, this translates into a more dynamic distribution of total phosphorus concentrations (Figure 15 d).
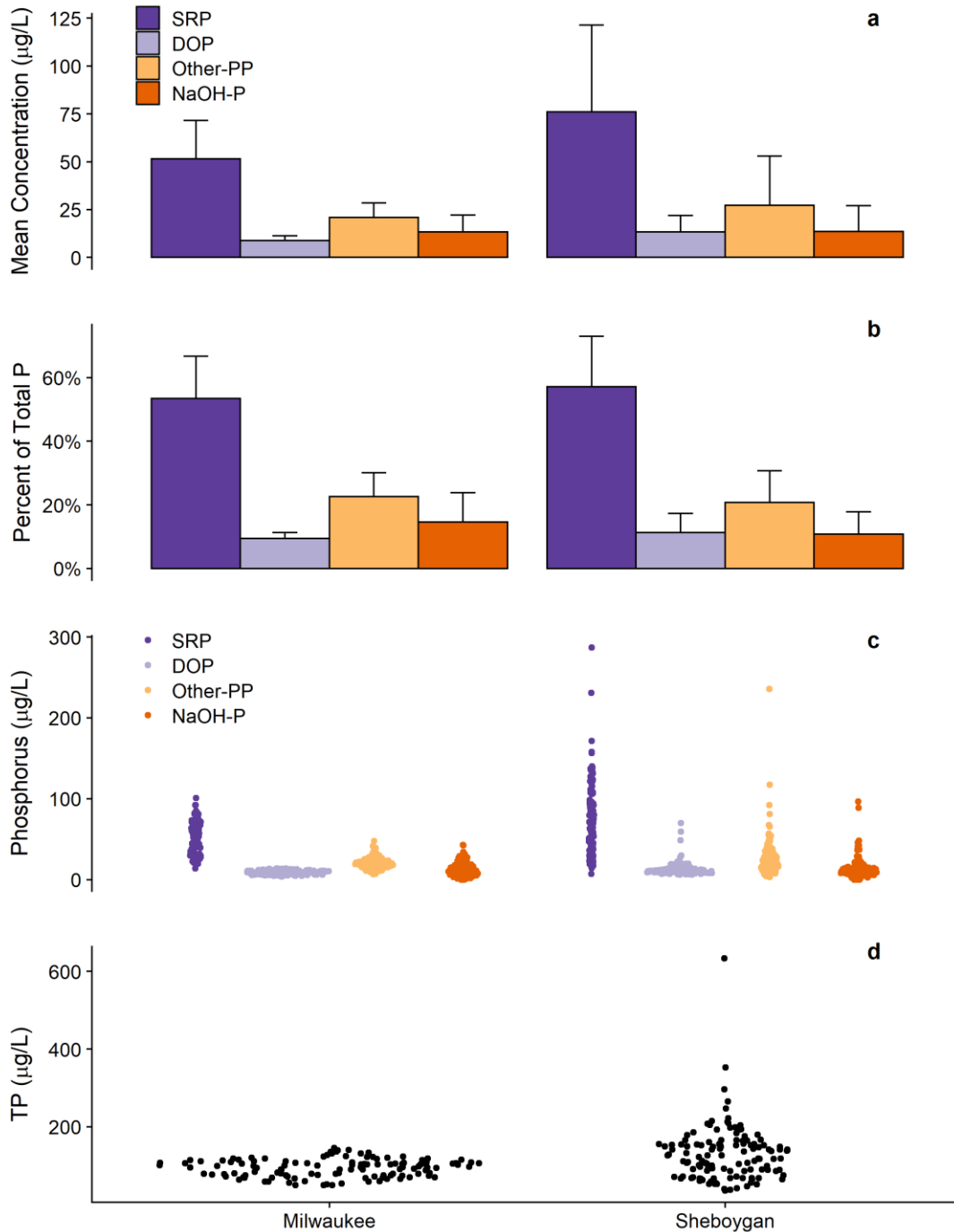
Figure 15: Variation in P Fractionation by River.

Mean concentration and percentages between the rivers were similar for all P fractions, though the Sheboygan River was more variable. Sina plots, C and D, help visualize the number of observations as well as their density distribution. Each point represents a unique observation. That point is then distributed along the x-axis according to its relative density. Thus, the widest portion of the plot shows the mode.
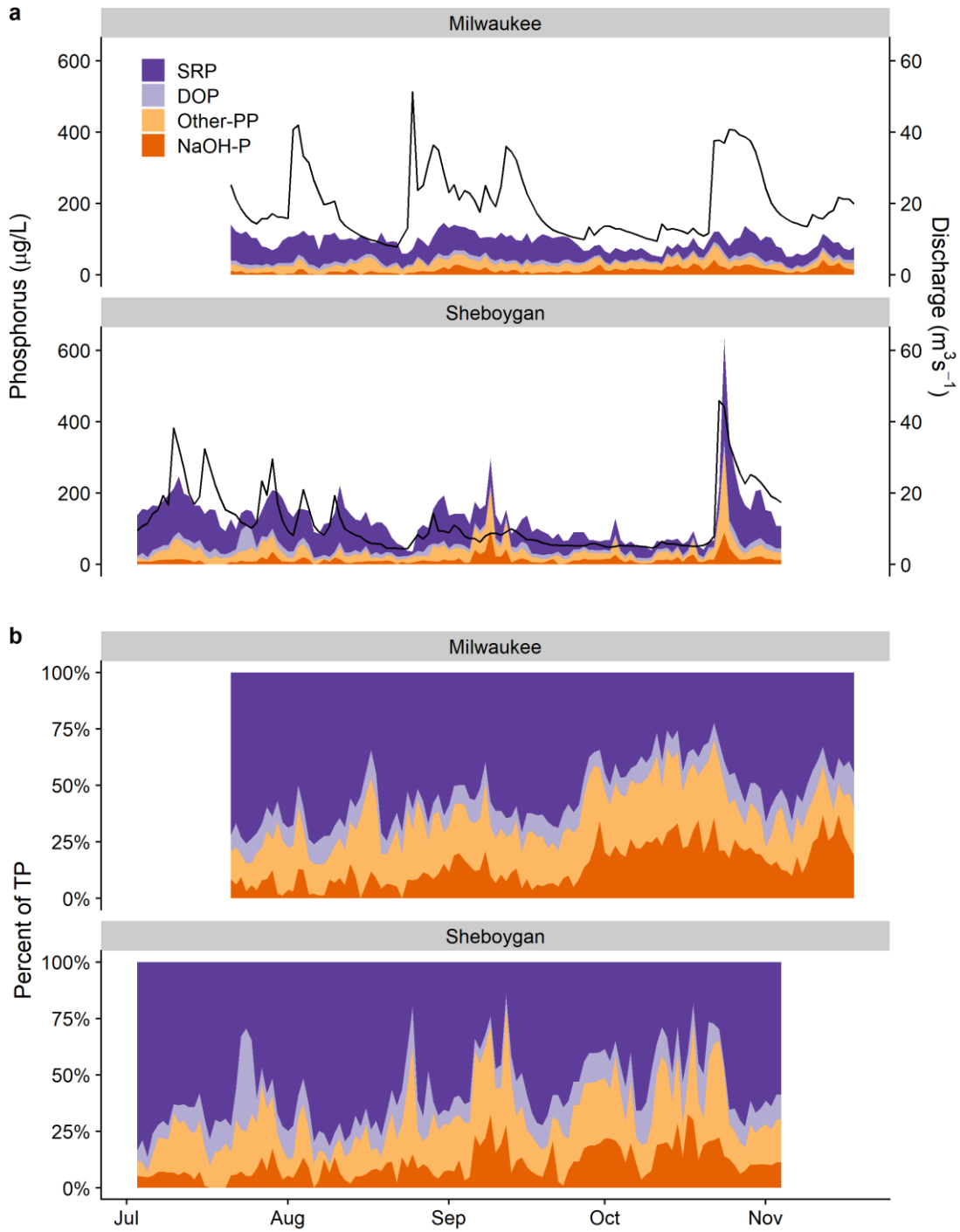
Figure 16: Time series of P fractions and proportions.

A) Changes in P at Sheboygan appear to be influenced by river discharge. B) Proportion of each fraction through time show increasing PP (tan colors) moving from summer to fall.
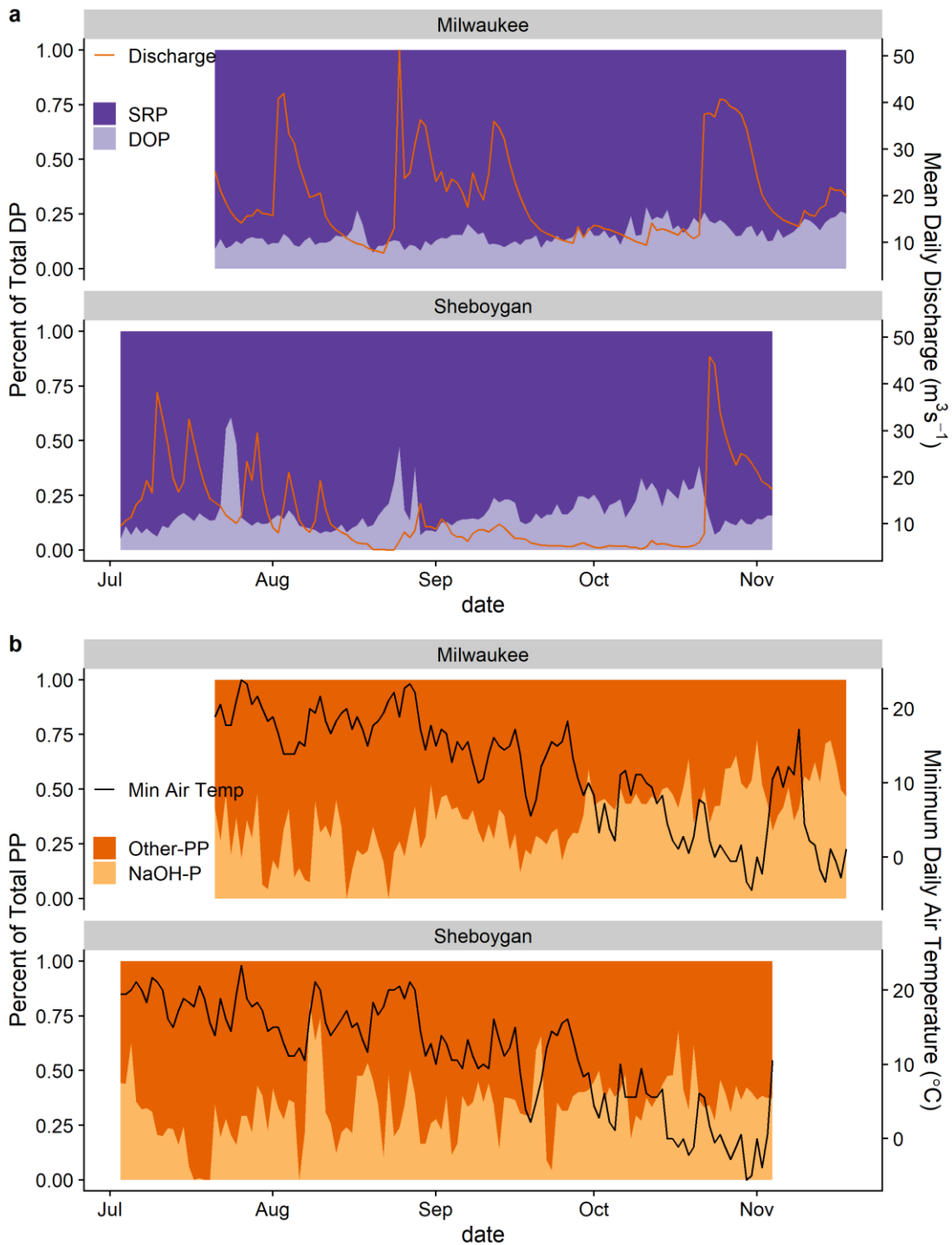
Figure 17: Stacked Area Chart Time Series by Soluble and Particulate Forms.

Soluble forms (a) show an increase in DOP contribution concurrent with a falling hydrograph. This trend is more apparent at SHB than MKE. Particulate forms (b) show an increase in NaOH-P contribution with time and/or falling temperature. This is more apparent at MKE than at SHB.

Do P fractions and bioavailability change over time?

Although mean load, concentration, and percentage values were similar between the two rivers, time series visualization of P fractionation patterns gives a better appreciation for the specific temporal locations of both similarities and differences between the two rivers P dynamics. Figure 16a depicts the change in total P and within P fractions over time, whereas Figure 16b, helps visualize the changes between P fractions through time while controlling for changes in total P.

Total Phosphorus
Regulation by River Discharge and Upwelling

Sheboygan's variability is apparent, and it seems that increases in total P are influenced heavily by peaks in upstream river discharge (Figure 16 a). Milwaukee, however, appears less affected by changes in upstream river discharge, with relatively stable nutrient concentrations across time. Since the Milwaukee ISCO was located at the mouth of the Milwaukee River, but between the inner and outer harbor, at least part of this stability is likely a result of Milwaukee's large harbor volume which increases τ, buffering against upstream changes in discharge.

Both time series show several sudden large declines in TP concentration, though this is more apparent at SHB. The most notable shared cut occurs August 23-25. Examination of water temperature data (Figure 18) shows a decrease in temperature starting on August 20 that reaches its minimum on at both locations on August 25, suggesting a strong upwelling event. This is confirmed by temperature string data from the Atwater 20m buoy that show a nearly isothermal upwelling event between those dates.

Upwelling appears to provide an important harbor flushing mechanism. Bringing cool nutrient poor water to the harbor and transporting relatively nutrient rich harbor water into the lake. Conversely, this may mean that upwelling also provides an important mechanism for exporting nutrients from harbors and nearshore areas to the pelagic. Note that upwelling temperatures seem more extreme in Milwaukee than in Sheboygan (Figure 18). This may be due to the orientation and size of Middle Gap in Milwaukee harbor, which has an E-W opening parallel to the direction of upwelling typical on the E. side of Lake Michigan. Sheboygan's gap faces N-S, which to an extent may shield its harbor from upwelling.
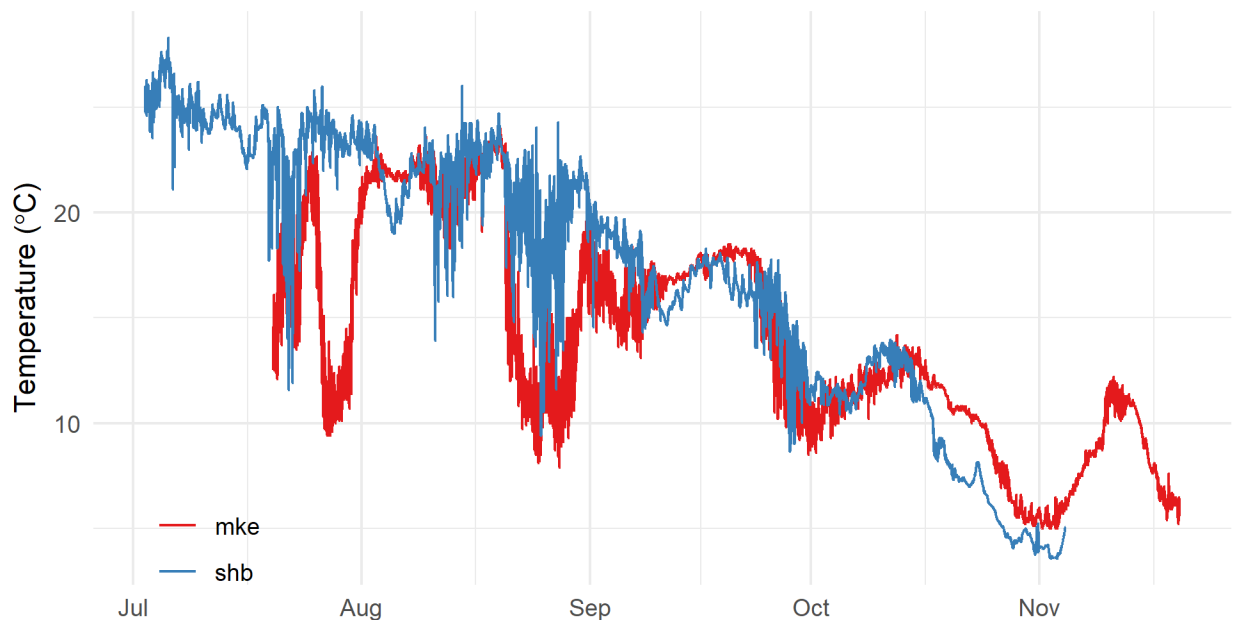
Figure 18: Temperature Data Time Series

A strong upwelling event from August 23 – 25 may have flushed nutrients from both rivers. An upwelling event in late July appears to be less synchronous. Upwelling appears to affect the rivers somewhat differently, with stronger temperature gradients apparent at Milwaukee perhaps due to channel and gap orientation.

Worth noting is the shared, though somewhat out of phase, cyclical sinusoidal temperature pattern beginning in early September. This is likely the result of a wind induced internal Kelvin wave (Beletsky et al., 1997). The wave appears to have a period slightly less than a month.

Soluble Phosphorus
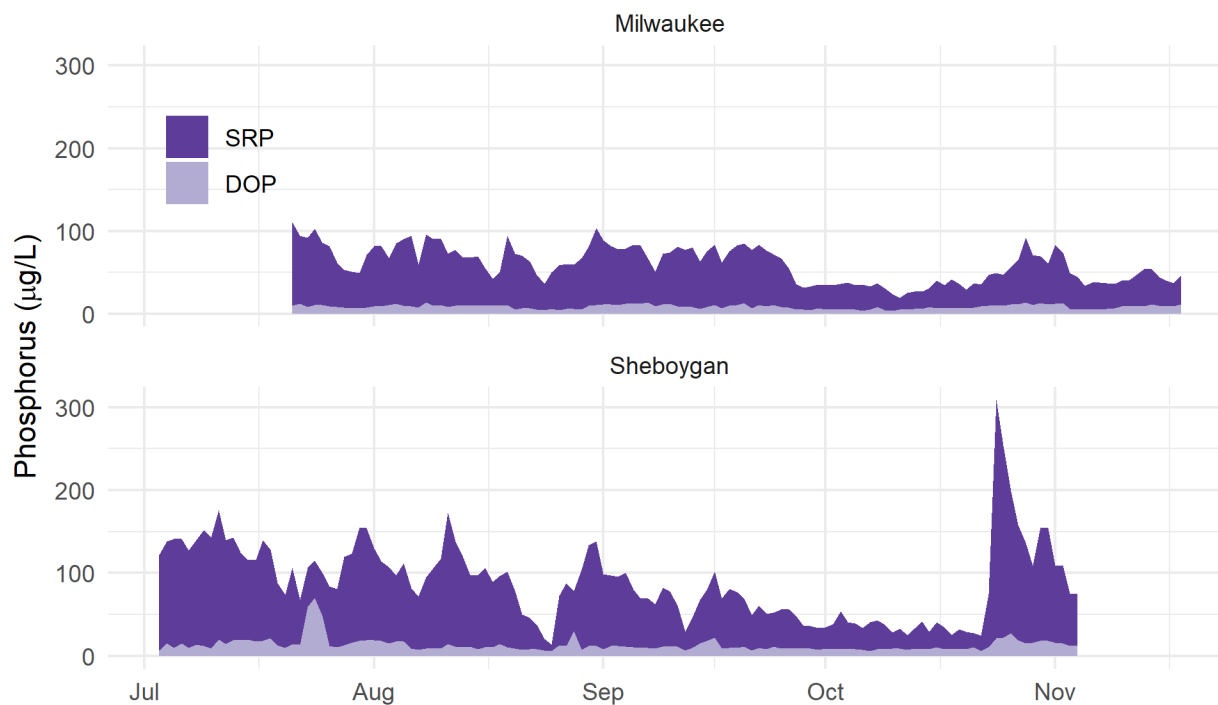
Figure 19: Soluble Pool Stacked Area Chart Time Series

Soluble forms made of the largest percentage of TP, with SRP dominating the soluble pool. Soluble forms seem to decrease moving from summer to fall, though a large precipitation event in late October increased soluble forms. This was especially true at Sheboygan (bottom row).

For both locations, soluble forms of P dominated accounting with a mean of 63% and 69% at Milwaukee and Sheboygan respectively. Within the soluble pool, SRP was the primary contributor at 79% for Milwaukee and 85% for Sheboygan. Generally, the soluble pool was moderated by the same mechanisms that regulated TP (i.e. discharge and upwelling). However, aside from an increase in the soluble pool concurrent with a large precipitation event in late October, there was a notable decreasing trend moving from summer to fall as particulate forms of P became a larger proportion of the total P pool (Figure 16b).

DOP

DOP was the smallest and most consistent contributor to total phosphorus. Thus, several deviations in DOP contribution through time merit further investigation.

Decreases in discharge result in longer residence times which allow for greater in-route processing. Thus examining low flow conditions may reveal assimilation signals typically masked by faster river flow. At Sheboygan there was a strong negative correlation of the ranked data (Spearman's = -0.52) between percentage DOP within the soluble pool and discharge. This was especially apparent on 2020-07-24, and less apparent on 2020-08-25, and 2020-09-16. During a long period of low flow conditions (i.e. 2020-09-18 through 2020-10-24), the percent contribution of DOP was also high (see Figure 17a). However, this last event is primarily a result of the decreasing proportion of SRP rather than an increase in DOP.

Guo et al., (2016) noted that SRP dominated the dissolved pool in the Milwaukee River at 73% ± 18%, but that in the lake the dominance switch to DOP at 85% ± 18%. Decreased river flow combined with lake backwater effects may produce lake-like effects within the harbor. However, it may also be due to increased biological processing of SRP within the river by periphyton, reducing SRP and increasing the DOP:SRP ratio.

Another plausible theory is that the increase of DOP during low flow river stage has less to do with the harbor, river, or lake effects, but is a reflection of increasing contributions of groundwater base flow. While groundwater has traditionally been thought to remain nutrient poor due to rapid phosphate sorption on soils, recent work has shown that a variety of DOP compounds associated with animal waste can leach through soils much more readily than the more frequently monitored orthophosphate (McDowell, Worth, & Carrick, 2021). This leaching

74

effect is more pronounced in soils that have low natural sorption capacity or have already become saturated with phosphate anions.

SRP

SRP was the largest contributor to TP at both locations. SRP is also the most reactive fraction of TP as well as the one most readily assimilated by nearshore nuisance algae like *Cladophora*. Thus, mitigating SRP contributions to TP has the greatest payoff in terms of *Cladophora* abatement. However, this reactive nature is true for SRP in-route from the watershed to the lake too, and some proportion of SRP may be assimilated prior to lake delivery. Larson et al. (2019) attempted to measure this proportion of river-mouth assimilation by calculating first order loss rates of SRP in short term incubation experiments. The results varied widely, perhaps because loss rate models were limited to 2 time points, and perhaps due to container effects. But with daily ISCO sampling, it may be possible to circumvent confounding container effects and detect loss rates within time series from the river itself.

Given that changes in water residence time can affect in-route processing, I choose to focus my analysis of SRP during times when residence time was increasing, and thus the hydrograph was falling, i.e. the base flow recession. As discussed in the introduction of this thesis, baseflow recession begins after overland flow has ceased, which can be estimated from watershed size using Equation 2. Theoretically, if no additional precipitation is added after the initial overland flow event, the recession constant should represent the first order loss in ground water discharge. This constant is unique to each watershed. Baseflow recession constants should show minimal variation and can be calculated from flow data with Equation 3 or by fitting streamflow data with an exponential decay model.

Because the hydrograph data used for the MKE ISCO in this study was a combination of 3 rivers, (i.e. the Milwaukee, Menomonee, and Kinnicknic), I was not able to retrieve a consistent baseflow recession constant. Thus, the following analysis was only conducted at Sheboygan. However, this same analysis methodology could also prove fruitful at an upstream sampling location on the Milwaukee.

First, I identified date ranges that were preceded by an overland flow event, but did not receive an additional rainfall contribution for at least 5 days. This left me with 3 recession events. For each date range, I calculated the expected number of days of overland flow with Equation 1 and removed this period from my analysis set. For each event, I calculated the baseflow recession constant using Equation 2 and found good agreement with a mean baseflow recession constant of -0.065 ± 0.0047 d^{-1} confirming that changes in flow were primarily a function of groundwater drawdown. Finally, I filtered out any remaining days with small contributions of rain to reduce noise leaving me with analysis data for July 19 – 24 (-July 21), August 12 – 23, and September 17 – 27.

With this cleaned analysis set, I first analyzed linear relationships between discharge and SRP and found that they were strongly correlated (Figure 20: A, B, and C, R^2 = 0.99, 0.72, 0.67, p < 1e-3, < 1e-3, 1e-3).
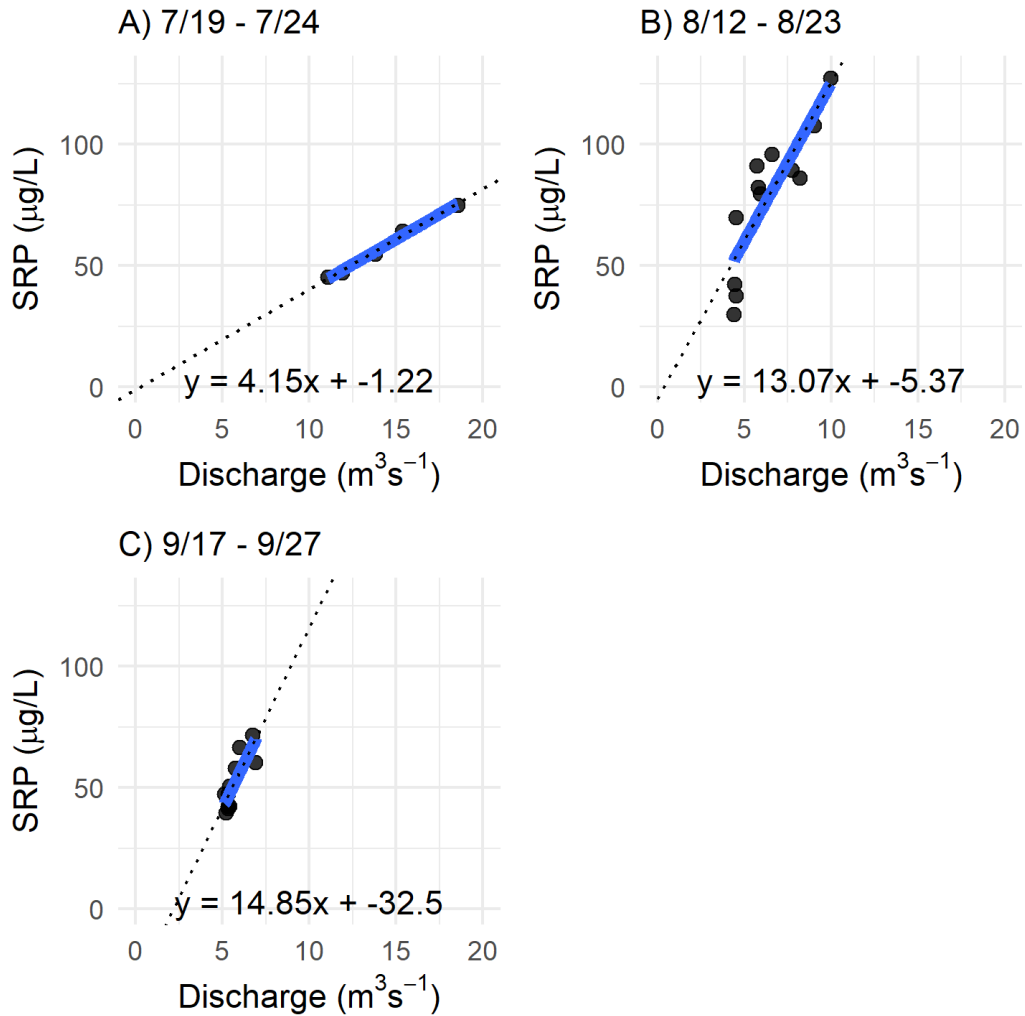
Figure 20: Linear Relationships between SRP and Discharge during Baseflow Recession.

Blue line show's fitted linear model. Dotted line shows model extrapolation to aide in comparison. Note that each plot has a the same x and y limits. A-C show different baseflow recession events, each with a similar baseflow recession constant, but a different relationship between discharge and SRP concentration. Generally slopes increase moving from summer to fall suggesting that increased discharge has a greater effect on SRP concentration in the fall than in the summer.

Since 1 µg/L = 1 mg/m^3 the slope of each line can be interpreted as the per cubic meter reduction in mgSRP for each equal drop in streamflow. This decline in SRP with discharge is likely the result of residence time. The intercepts are difficult to interpret. However slopes

show a seasonal trend, with increasing slopes from summer to fall suggesting that fall discharge

has a greater effect on SRP than does summer discharge.

This same analysis came be repeated in in exponential form by finding the decay

constant alpha for SRP through time during each baseflow recession event. Alpha, in this case,

can be interpreted as the first order loss rate of SRP through time i.e. days.
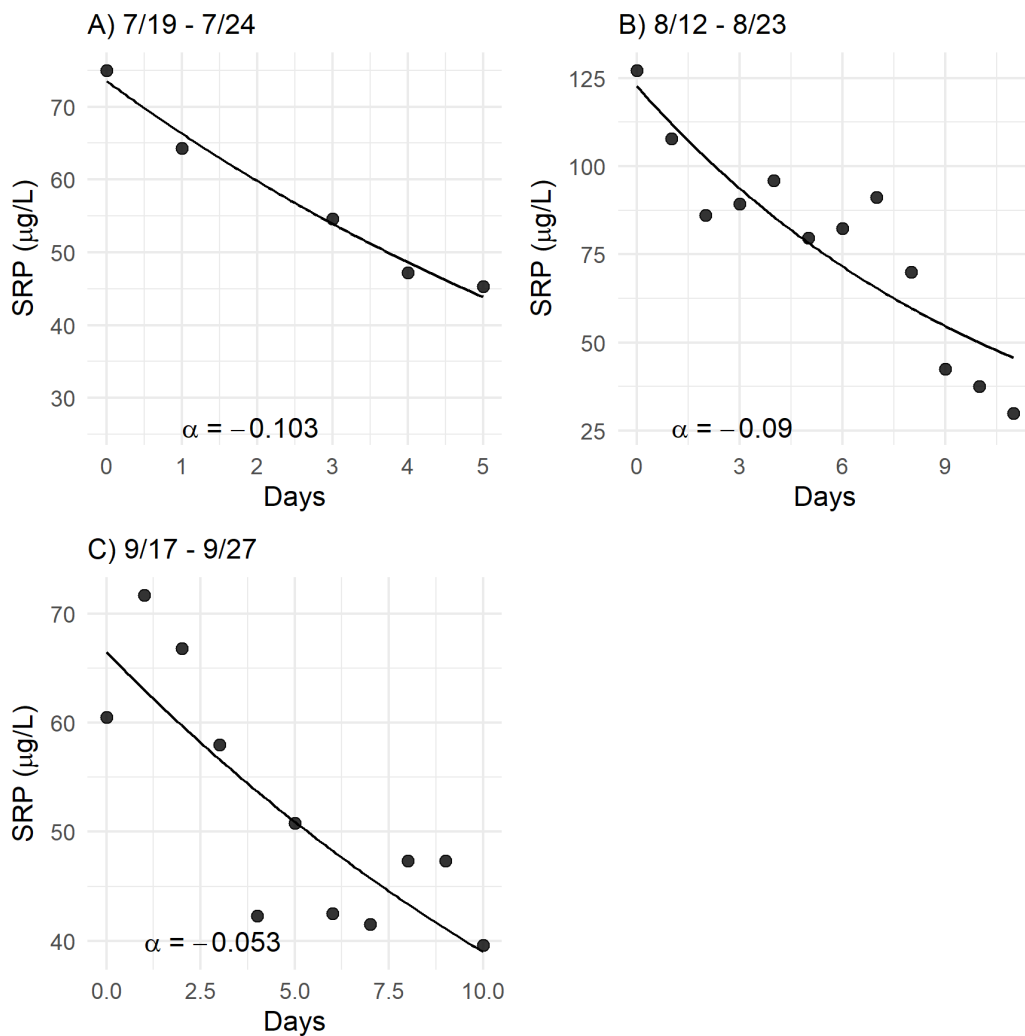
Figure 21: Exponential Decay Models of SRP Loss

Exponential decay models show a similar trend with greater assimilation (i.e. more negative loss rates) in the summer months and decreasing assimilation in the fall.

Similar to the linear model analysis, the exponential decay models show that alpha is more negative in July than it is in September. One interpretation of this result is that the river's assimilative capacity is greatest during the summer, which could be due to increased sunlight and photosynthetic activity. If this is the case, changes in stream flow do not affect the SRP reduction as greatly during the summer because the river is assimilating SRP at a greater rate. Conversely, in fall, when light diminishes and photosynthesis is reduced, stream assimilation is weak, and changes in stream flow can have a large impact on SRP delivery to the lake.

However, the change in alpha could also be interpreted as a change of SRP infiltration and/or retention within the groundwater aquifer. Reductions of SRP uptake due to the harvest of crops in the fall may allow for greater SRP infiltration into the aquifer. Excess SRP infiltration in groundwater can overwhelm soil retention capacities due to a finite number of cation binding sites (e.g. iron, aluminum, calcium, manganese, etc.). Land use and groundwater interactions such as this are still poorly understood in the Great Lakes region, but may be of critical importance (Robinson, 2015).

Knowledge of first order loss rates such as this could be incorporated into loading models improving estimates of load timing, concentration, and bioavailability. This would aide nearshore forecasts of HABs and nuisance algae. Additionally, continued monitoring of loss rates may provide insights into management strategies that could aide/repair natural P buffering mechanisms. Such process based knowledge could prove particularly useful in predicting the potential effects of climate change on river hydrology and biogeochemistry.

Particulate Phosphorus
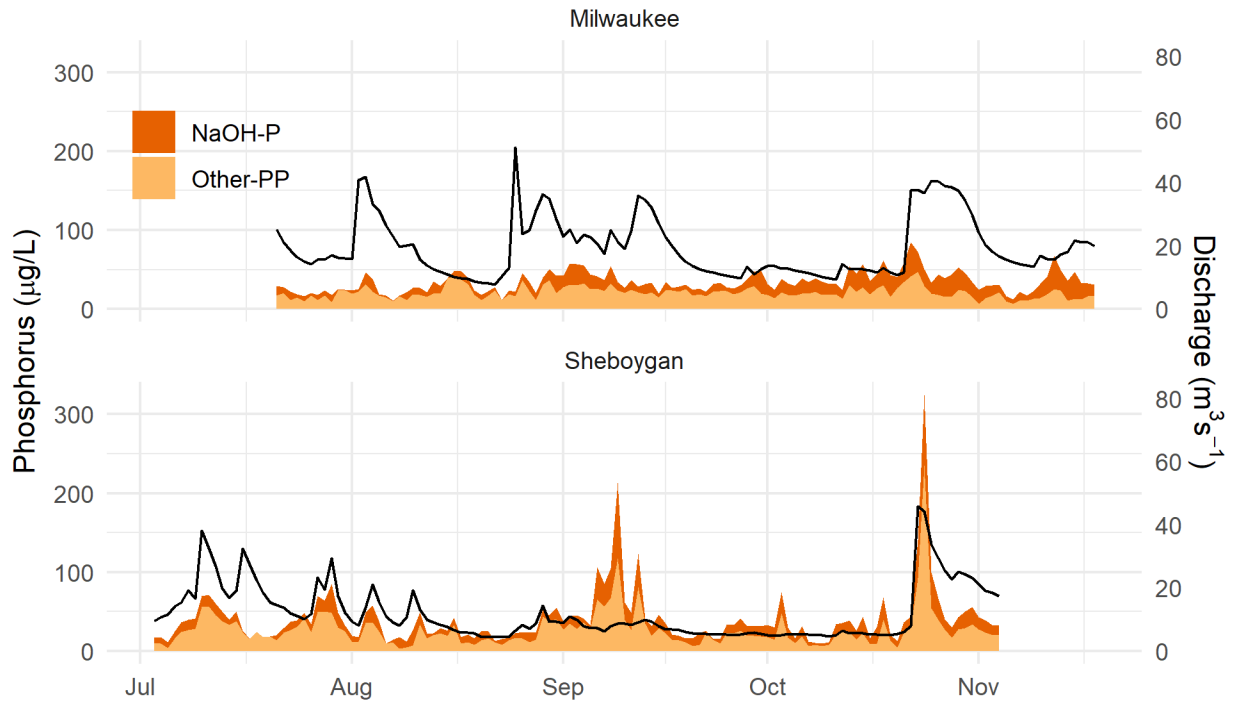
Figure 22: Particulate Phosphorus Stacked Area Chart.

Particulate phosphorus was moderately correlated with discharge at Sheboygan, but only weakly correlated at Milwaukee (r = 0.48 and r = 0.22 respectively).

Particulate phosphorus contributed less to total phosphorus that was expected with a mean percentage of 37.2 ± 13.4% at MKE and 31.5 ± 15.1% at SHB. Total PP at Sheboygan was moderately correlated with discharge (r = 0.48), while MKE was only weakly correlated (r = 0.22). Visual inspection of time series shows the greater variability in PP at Sheboygan as well as some of the correlation with discharge.

Other-PP

Within the PP pool, most of the PP was Other-PP (i.e. non-NaOH-P), which is generally considered less bioavailable than NaOH-P. For the purposes of this study, Other-PP was the fraction of least concern. It may consist of a variety of mineral compounds including apatite. Apatite is a stable primary mineral resistant to weathering. Thus fluxes from this pool to the

SRP pool are generally considered to be slow. However, some have suggested that apatite plays a large role in regulating benthic phosphorus dynamics (Brooks & Edgington, 1994).

NaOH-P

NaOH-P is the P fraction considered to be the most bioavailable to algae (DePinto et al., 1981). It is a loosely bound P fraction primarily made of adsorbed and sorbed P with soils that have high aluminum (Al) and iron (Fe) oxide content such as clay. During a study in upstate New York, Prestigiacomo et al., (2016) found that the highest proportion of NaOH-P with in PP pool was associated with a stream that also had the highest agricultural land use. However, in this study NaOH-P made up 39% of PP at Milwaukee and only 33% at Sheboygan, which is opposite of what would have been expected.

Previous studies have suggested that the fraction of NaOH-P within in the PP pool at a given tributary is relatively constant during periods of runoff. This is because NaOH-P composition is influenced largely by particle size and soil properties of the watershed influenced by geological history, mineral content (e.g. apatite), and land use (DePinto et al., 1981; Sharpley et al., 1992). However within this dataset, NaOH-P showed a strong negative correlation with minimum daily temperature at Milwaukee both as a fraction of the particulate pool and as a fraction of the TP pool (r = -0.66 and -0.69). This effect was dampened at Sheboygan (r = -0.27 and -0.42). It is difficult to interpret correlations to temperature since they are confounded with time (r = -0.85 SHB, r -0.84 MKE). Moreover, without a mechanistic explanation, this correlation offers little causal insight. However, several mechanism come to mind that could explain this pattern.

1) Microbial breakdown of PP $\rightarrow$ SRP increases with temperature.

81

2) Changes in temperature are concurrent with seasonal agricultural patterns such as crop harvest.

3) Temperature and concentration optimized phosphate buffer mechanisms (i.e. coprecipitation and sorption respectively) act to simultaneously decrease SRP while increasing PP.

Mechanism 1: Microbial Breakdown of PP → SRP

To test the first hypothesis, I went back to the incubation bottle data from the ISCO and created a linear regression model for change in NaOH-P (i.e. "Old" – "Fresh") as a function of sample collection date, while controlling for site location (Figure 23). The overall mean trend (dotted blue line) showed no effect of sample date (as a proxy for ambient air temperature) on NaOH-P
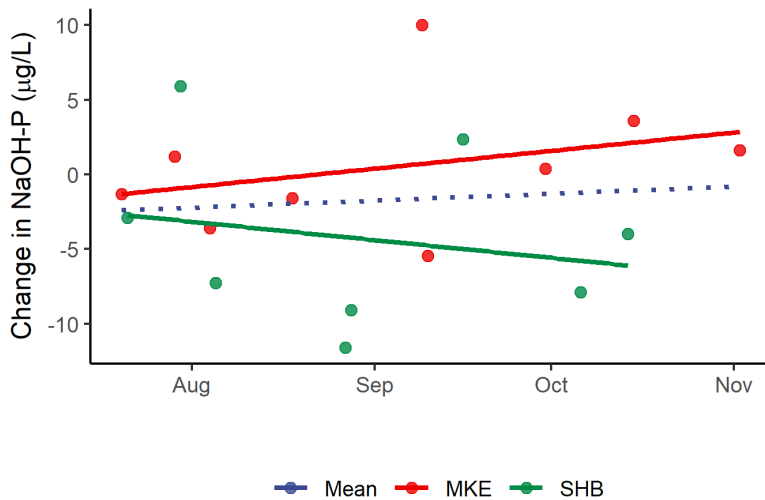
Figure 23: Change in NaOH-P within Incubation Bottles by Date.

There was no significant correlation between change in NaOH-P between the fresh and old replicates suggesting that changes were not induced by change in bottle effects, but were changes to the ambient river water concentration over time.

degradation in the incubation bottles. There was a slight increase of NaOH-P degradation at Sheboygan, and a small decrease in NaOH-P degradation at Milwaukee. However, none of these trends were statistically significant ($p > 0.09$, $R^2 = 0.21$).

Mechanism 2: Seasonal Land Use Practices

Corn for grain, primarily used as livestock feed, is the #1 crop in Wisconsin (USDA, 2006)

Typical harvest dates of corn for grain in Wisconsin are Oct 15 – Nov 15 (UW-Madison

Agronomy, 2014). Highlighting the dataset during this time period and controlling for location, provides the following visualization (Figure 24). NaOH-P as a percent of total P increased significantly (R^2 = 0.42, p < 2e-16) for both locations as did NaOH-P as a percent of PP (R^2 = 0.23, p < 3.67e-15). While this may provide some evidence for an agricultural land practice signal, it is still difficult to decouple this question from time in general. Furthermore, there seems to be no site specific signal (i.e. the slopes terms for each watershed from the regression are not statistically different from each other (%NaOH-P of TP p = 0.06; %NaOH-P of PP p = 0.95). The signal that is strongest, though not significantly so (p = 0.06), is for %NaOH-P of TP from Milwaukee. This is not what would be expected given Sheboygan's agricultural land use is greater than Milwaukee's.

It is possible that the consistent increase in PP export may be less related to corn, and more related to general seasonal patterns of vegetation P uptake and release. For example, aquatic macrophytes have maximum P uptake during the spring when they store nutrients for growth during the optimal light and temperatures of summer. However, uptake and growth decline in the early fall followed by cessation and release of detrital P in late fall/winter (Ready et al., 1999; Wilkins, 1984). This mechanism may explain both the increased SRP loss rates in the summer, and increased export of PP moving from summer to fall. However, this mechanism does not explain the increase of NaOH-P within the PP pool.
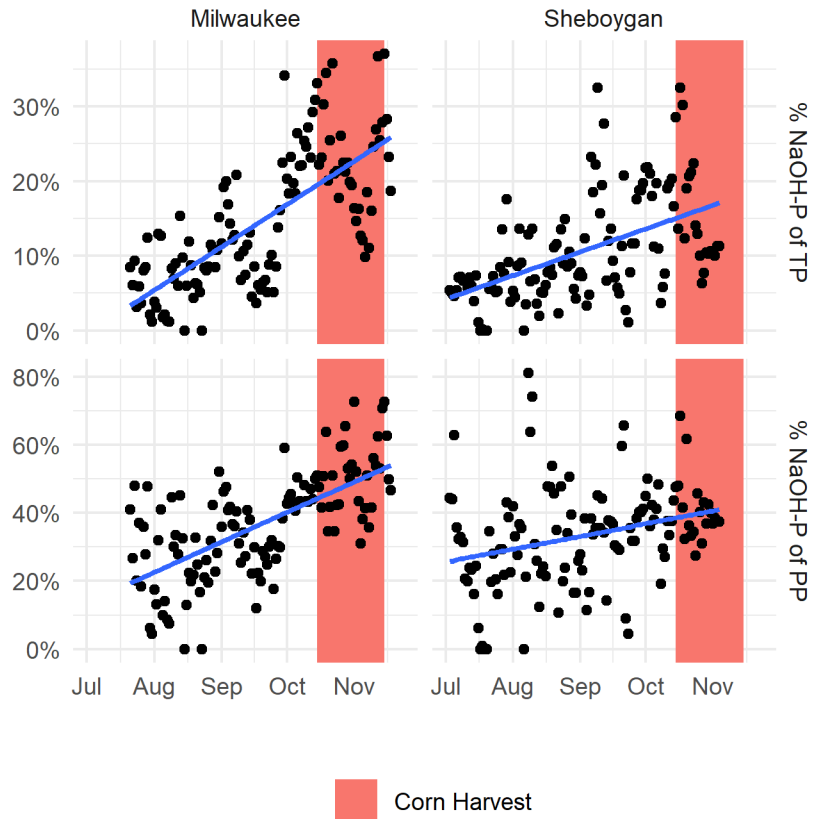
Figure 24: Linear Regressions of %NaOH-P by TP and PP.

Percentages of NaOH-P increased within both TP and PP pools moving from summer to fall. Differences between sites were not statistically significant, though Milwaukee showed a stronger signal, which was unexpected.

Mechanism 3: Interactive Phosphate Buffering Mechanism

NaOH-P is generally highest in fine-grained sediments that are rich in clay. Clays are

known to contain high Fe and Al oxide content as well as having a large surface area to volume

ratio, which increases the number of possible sorption sites for P. Sorption capacity is further

enhanced by clays complex 3-d structure full of intricate pore spaces. Thus, fine-grained

suspended clay sediments can act as an SRP buffer, by moving P from the dissolved to the

particulate pool. However, this "phosphate buffer mechanism" (Richardson, 1985), is not

unique to phosphate, but can occur with other anions that compete for charged receptor sites. The buffering mechanism takes place in two phases (Figure 25) (Froelich, 1988).

1) Anions rapidly sorb to charged receptors (minutes to hours).

2) Anions diffuse into the interior of the particle (days to years).

However, previous work has shown that buffering mechanisms can become overwhelmed, and actually decreases at phosphate concentrations > 60 µg/L due to pore space plugging (Griffin and Jurinak, 1973). Additionally, other anions (e.g. SO_4^{2-}, F^-, $B(OH)_4^-$, OH^-) can compete with phosphate for charged sites on particle surfaces. This reduces both the fast reaction phase through direct competition for surface sites, and the overall sorption capacity by changing the diffusion gradient during the second phase (Froelich, 1988). Thus, phosphate buffering should be optimized when ambient SRP concentrations are below 60 µg/L and the concentration of competing anions is reduced.
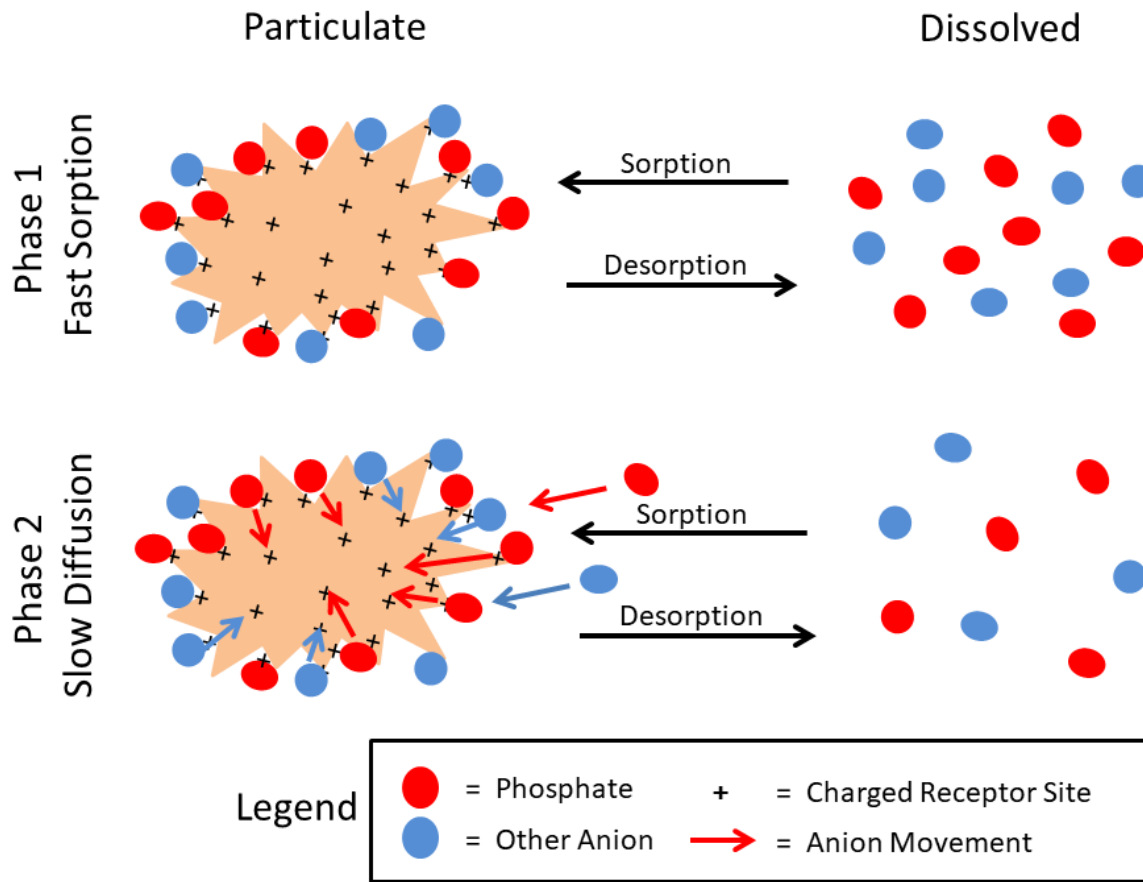
Figure 25: Two Phase Anion Sorption Diagram.

Phase 1 is rapid as anions sorb to charged sites on a particles surface. Phase 2 is slower, as anions diffuse into the particles interior, allowing for greater anion saturation.

Another phosphate buffering mechanism that exists in hard water lakes and could produce optimum conditions for sorption buffering is coprecepitation of phosphate with calcium carbonite ($CaCO_3$). Previous work has shown that this coprecipiation mechanism is also maximized when phosphorus concentrations are below 60 µg/L, but is aided further when pH is high (i.e. > 8.5) and temperature is near 10 °C (Birdsey, 1985).
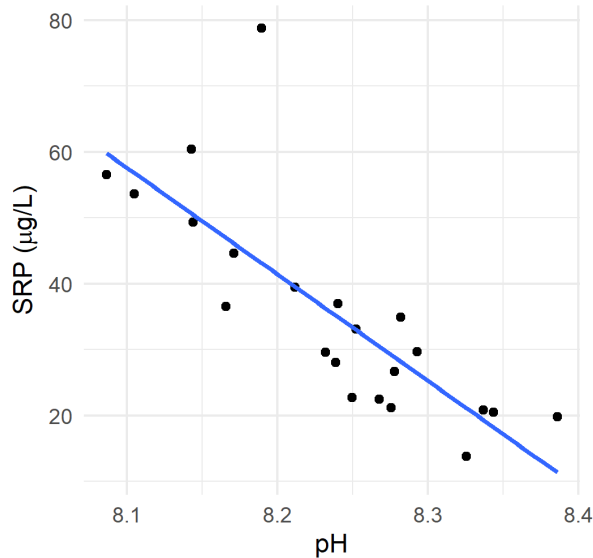
Figure 26: Linear Regression of SRP with pH.

SRP and pH showed a strong negative correlation (R^2 = 0.61) during late October when temperatures were optimum for coprecipitation of PO_4^{3-} and $CaCO_3$.
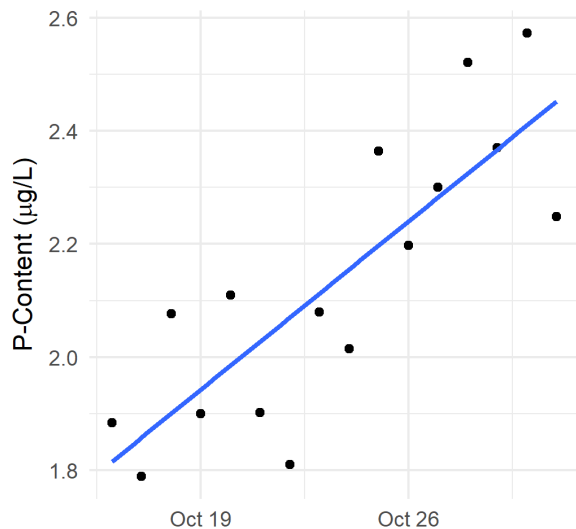
Figure 27: P-Content in Late October.

Concurrent with decreases in SRP was an increase in particle P-Content, suggesting some of the phosphate moved from the dissolved to the particulate pool.

During October, water temperatures at the MKE ISCO averaged 10 ± 2.6 °C, the optimum for coprecipitation of PO_4^{3-} and $CaCO_3$. Furthermore, pH was high and SRP was < 60 µg/L for all but one date, 2020-10-28 SRP ~80 µg/L (i.e. outlier point in Figure 26). A linear regression showed a strong negative correlation between pH and SRP concentration (R^2 = 0.61, p < 1.1e-5 Figure 27). Concurrent with decreases in SRP concentrations, was an increase in particle P-Content (i.e. µgP/mgTSS), which increased from 1.8 µg/mg to near 2.6 µg/mg in the second half of October (Figure 27).

Remarkably, during this time SRP reached its lowest value of the season at 13.8 µg/L, which was ~18 µg/L less than what was experienced in during the most extreme upwelling event of the season from August 23-26. Additionally, during this time Milwaukee experienced the 2nd largest precipitation event of the season at ~50 mm over 4 days. In spite of the heavy rain, typically associated with increases in SRP, the river mouth maintained low SRP.

For context, during the same rain event, Sheboygan experienced the largest recorded SRP measurement of the season at nearly 300 µg/L. Given that the two sites had similar temperatures during this period (see Figure 18) this difference in concentration cannot be explained by differences in upwelling.

Discussion

Coprecipitation of PO_4^{3-} and $CaCO_3$ can form hydroxyapatite, $[CA]^{10} [PO_4^{3-}]^{6} [OH^-]^2$, which also remove OH^- from the water column, reducing competition for positively charged sorption sites on particle surfaces. At times, the OH^- in hydroxyapatite is replaced by chloride (Cl^-) or floride (F^-). Regardless of the anion species, competition for positively charged surface sites is reduced when non-phosphate anions are removed from solution, allowing for greater phosphate sorption. An increased ratio of phosphate to other-anions on the particle surface may then create stronger diffusion gradient, increasing internal phosphate stores within the particles interior and ultimately removing more SRP from the water column.

If these observations and interpretations are correct, they may reveal an important 2-fold natural buffering mechanism that mitigates SRP at the Milwaukee River mouth. Initial coprecipitation of SRP with $CaCO_3$ reduces the ambient SRP concentration of the waterbody and also removes OH-, reducing anion competition for sorption site. Reduced anion concentration, both PO_4^{3-} and OH^-, may keep positively charged Fe and Al receptors on the surface of fine-grained particles from becoming overwhelmed, plugging up possible entrances to the complex 3-d internal structure of the particle. In the end the particles have a higher

overall sorption capacity and higher internal P-content as SRP is reduced twice, and the PP:SRP

increases accordingly.

Changes in Particulate to Dissolved Phosphorus Ratios

Baker et al. (2014) suggested that changes in agricultural practices, in particular the

adoption of no-till and reduced till soil conservation programs in the 1990's may have been

responsible for the increased export of SRP from the Sandusky and Maumee rivers from 1991 -

2012. This suggestion may also be true for the Milwaukee and Sheboygan watersheds (Figure

28), which show strong increases in the percentage of TP exported as SRP in the last 30-40

years. No-till soil conservation practice have been shown to reduce the amount of TSS export

from a watershed, but also may increase the saturation of phosphate in top soil, and increase

surface runoff due to soil compaction and crusting (Baker et al., 2014; Logan & Adams, 1981).

Additionally, SRP may infiltrate into groundwater in areas where soils have become P saturated

due to prolonged excess fertilizer application (Robinson, 2015).
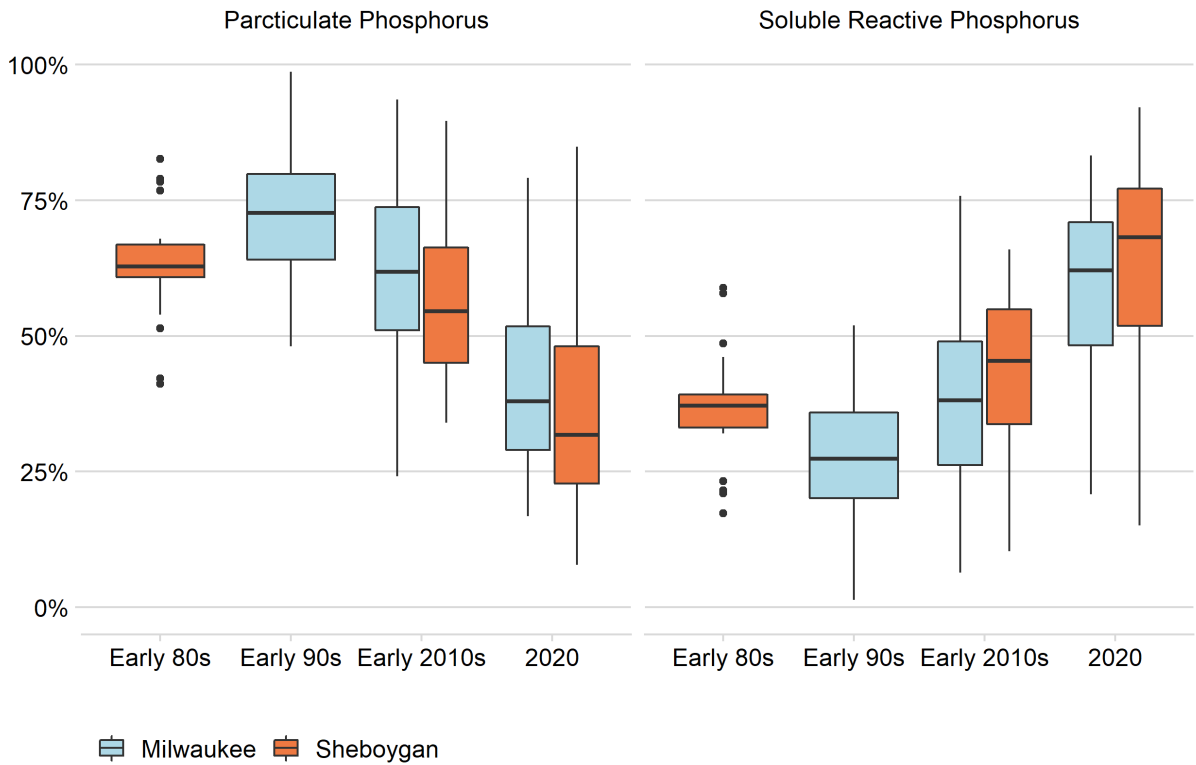
Figure 28: Change in Percent Contribution of PP and SRP over Time

Data filtered to only show months of 2020 sampling effort, July - October. Only showing %PP vs %SRP which leaves out DOP. DOP was not included in the historical USGS data and was dropped from my dataset to match the historical record.

Evidence supporting this theory was seen in elevated SRP concentrations at Sheboygan during the baseflow recession, which at times was as high as 125 µg/L. Sheboygan had mean SRP concentrations of 64 ± 23 µg/L throughout the baseflow recession periods in this study. Some of this SRP may have been assimilated by the river, with a higher assimilation rate in the summer than in the fall. However, differences in SRP concentration and loss rates may also reflect assimilation by summer crops on land and not river assimilation. Currently, a precise assimilation mechanism is not known, but future studies capable of determining this mechanism would be useful.

In general, the change in mean daily PP:TDP ratio increased with time at both locations (Figure 29). Within the PP pool it was the increasing proportion of NaOH-P that seemed to drive the increased PP:TDP ratio. Some part of this may be due to agricultural land use customs such as the harvest of corn for grain which exposes soils to erosion. Since NaOH-P is strongly associated with Fe and Al in clays that are common in agricultural land and that have high sorption capacity, we expected that Sheboygan would yield a higher proportion of NaOH-P than Milwaukee. However, the opposite was found as NaOH-P was greater at Milwaukee than it was at Sheboygan.
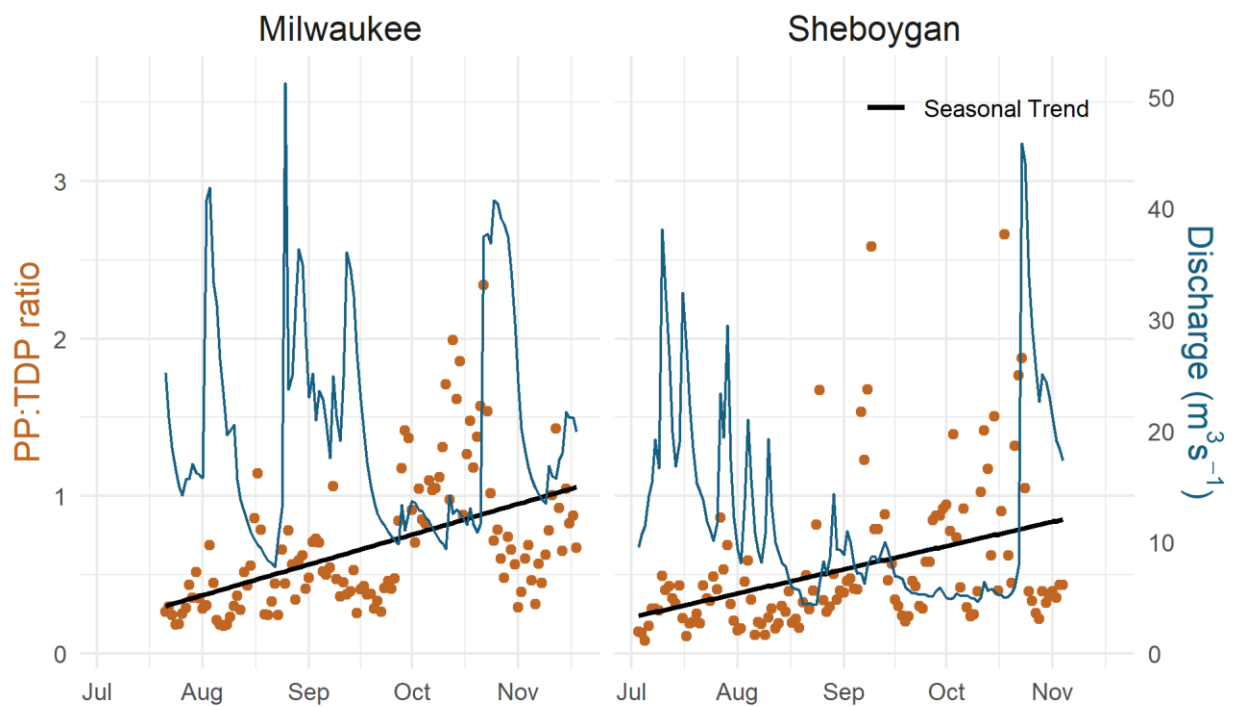
Figure 29: PP to TDP Ratio by Location.

Both locations experienced an increase in PP:TDP ratios. However, the increase at Milwaukee was greater than it was at Sheboygan. This was the opposite of our expectation. It is worth noting that some of the highest PP:TDP ratios occurred in late-September – mid-October during a period of low flow.

A possible explanation for the lower SRP and greater NaOH-P proportions at Milwaukee involves a complex 2-fold buffering mechanism in which the coprecipitation of SRP with $CaCO_3$ may reduce competition of phosphate with other anions for charged receptor sites on fine-grained particles. Additionally, reduced phosphate concentrations due to precipitation may also reduce the initial reaction rate of the P sorption buffering mechanism, keeping pore holes unplugged and increasing the overall saturation capacity of the particle.

If this NaOH-P sorption buffering mechanism exists more generally outside of instances of reduced SRP due to coprecipitation of $CaCO_3$ the above suggest that the best place to look for it is in post runoff conditions when small fine-grained particles are suspended in the water column and SRP has declined sufficiently to allow for greater P sorption capacity. Moreover, since PP forms tend to decline after quickflow, the best metric to detect this trend is not the concentration of PP in the water, but the P-content of the suspended material (i.e. µgP/mgTSS).

Horton overland flow occurs when the precipitation rate exceeds the infiltration capacity of the ground cover (Horton, 1933, 1940). Using Equation 1 from the general introduction gives an overland flow estimation of 3.35 days for Sheboygan and 3.87 days for Milwaukee. Generally, overland flow increases the mobilization and transport of particulates downstream. Particulates can be mobilized from 2 major sources, 1) the "stock" of surface particulates that have accumulated on the ground since the last rain event and 2) the riverbed itself with resuspension of bed particles due to high discharge velocities and turbulent flow. When precipitation ends, declining discharge velocity allows larger particles to settle back to

the riverbed, but fine-grained particles may remain suspended. Theoretically, this process can affect phosphorus fractionation patterns in 3 main steps.

1) Precipitation exceeds infiltration capacity and mobilizes particulate matter rapidly increasing the PP fraction.

2) Riverbed sediments are resuspended by high discharge velocities and turbulent flow adding to transport of additional PP.

3) Rain stops, discharge slows, and larger particulates settle, decreasing PP.

4) Fine-grained particles with high sorption capacity remain suspended in the water where SRP sorbs to them, increasing PP with no net effect on TP or TSS, but visible in an increase in P-Content.

5) As the hydrograph continues to fall, SRP continues to decrease due to increased residence time and biological assimilation. This slows the initial sorption reaction rate and allows for greater overall sorption capacities.

To search for this signal, I filtered the dataset to the two largest storm events of the season which began on August 2, for Milwaukee and October 22 for Sheboygan. My thought was that these larger events had the best chance of producing a signal both to greater mobilization of land surface and stream bed P stocks. I truncated the Milwaukee dataset to end on August 18 to avoid the influence of the coming upwelling event and used the remainder of the Sheboygan data time series which ended on November 4.

Figure 30 shows the predicted pattern in which the P-content of the suspended sediments is inversely related to the discharge. P-content at Milwaukee began near 2.75 ug/mg, decreased

slightly to 2 μg/mg during overland flow, but then proceeded to increase to a P-content near 5

μg/mg. Sheboygan saw a similar trend, though somewhat dampened with P-content starting

near 1.5 μg/mg and increasing with the falling hydrograph until reaching a value of ~3.3 μg/mg.

This suggests that both rivers have the capacity for an SRP sorption buffering mechanism,

though Sheboygan's mechanism appears somewhat dampened.
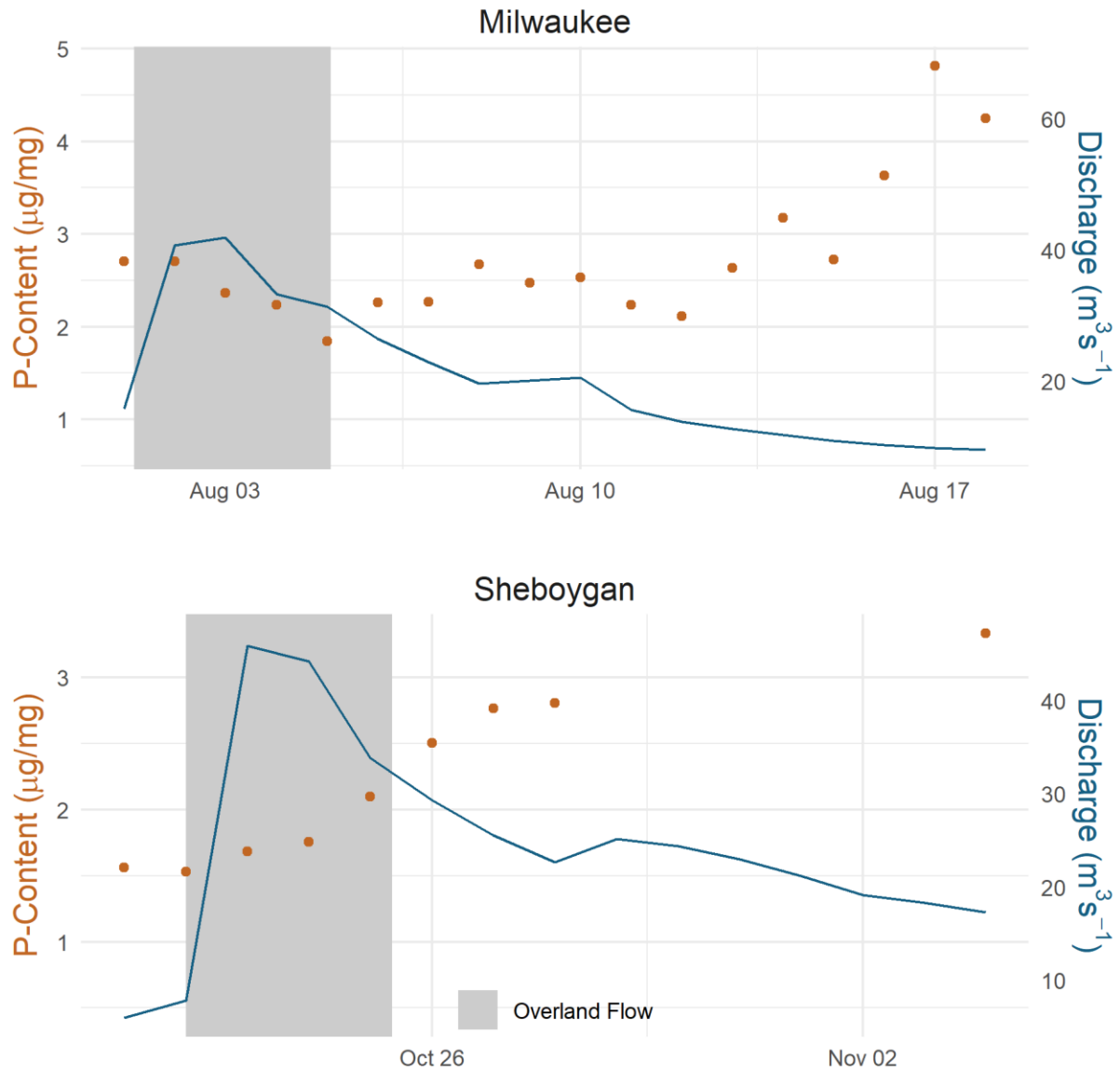
Figure 30: Increased P-Content During in Post-storm Recession.

Both Milwaukee (top row) and Sheboygan (bottom row) saw increases in P-Content during a post-storm recession. This may be due to sorption of phosphate onto fine-grained particles. Note that P-Content appears to have a higher ceiling at Milwaukee than at Sheboygan.

The gap in data points for Sheboygan was due to ISCO battery failure. The final data point was taken fresh on the final day of ISCO deployment, November 4.

Final summary of results and recommendations

The Milwaukee and Sheboygan River watersheds are very similar in all but their land use with Sheboygan having a higher percentage of agricultural land and lower percentage of urbanized land. Though one may expect the Milwaukee river to be "flashier" than the Sheboygan, due to the large amount of impervious surfaces in the basin's area, the effect of this on P loading is dampened by Milwaukee's large harbor. Milwaukee's harbor likely delays P delivery to the nearshore zone and transforms P forms through sedimentation and assimilation. Future nutrient modeling efforts should account for Milwaukee Harbor's increased residence time, settling, and assimilation effects by explicitly including it in the model. Sheboygan's harbor, on the other hand, likely has a negligible effect on the quantity and form of P delivered from the river to the lake except for when flowrates are extremely low.

On average, 69% of the load entering Milwaukee and Sheboygan's harbor was readily bioavailable (i.e. SRP + NaOH-P). Most of the bioavailable load was SRP, with higher SRP contributions during the summer months that align with the *Cladophora* growing season. Assuming that the fraction of NaOH-P within the PP pool has remained relatively constant through time, historic estimates of bioavailability would be much lower due to changes in bioavailability being driven by the PP:SRP ratio. NaOH-P made up a larger fraction of PP in the colder months, though this apparent temperature effect is difficult to untangle from the effects of time and land use practices.

The fractionation of measured P pools was very similar in the two rivers studied, though variable with time, especially at Sheboygan. Bioavailability decreased with season from summer to fall primarily due to increases in the PP:TDP ratio. The period of largest PP:TDP ratios was

concurrent with the typical harvest season of corn for grain. However, this pattern increased gradually instead of sharply, suggesting a broader seasonal pattern and moreover was stronger at Milwaukee than Sheboygan, which suggests that agriculture land use practices may not have been the primary driver because Sheboygan has greater agricultural land use.

It is possible that the elevated P-saturation of soils caused by buildup of legacy P (Robinson, 2015) and no-till soil practice (Smith et al., 2015) in agricultural landscapes has undermined an important SRP buffering mechanism. The data presented here support the theory that fine-grained particles play a key role in a complex mechanistic process involving particle P sorption that can either be induced by coprecipitation of SRP with $CaCO_3$ or a decline in ambient SRP associated with baseflow recessions. I hypothesize that this small trend may be an echo of a previously important feedback mechanism that buffered SRP dominance in the transport and fate of riverine P.

Based on historic monitoring data, the change in PP:SRP ratio is the driving force of increased bioavailability over the last 40 years. This strong change in P fractionation is not a novel observation, but a worrisome trend that has been reported for other Great Lakes tributaries (Baker et al., 2014; Kleinman et al., 2011; Sharpley, 2003). Continued analyses of other large river systems would help determine the large-scale effect of this potential shift in P fractionation.

Reduced mobilization of fine-grained particles due to no-till soil practices combined with a growing stock of legacy P in soils creates a double edged sword. Fewer fine-grained particles move to the stream from the land and those that do enter the stream do so with a reduced

sorption capacity. The end result is that SRP travels unhindered downstream with a faster delivery rate to the harbor. If it is not assimilated in the harbor, SRP enters the nearshore zone where it can be taken up by bacteria, phytoplankton, and benthic algae like *Cladophora*.

But what happens to the fine-grained particles? What is their fate in the nearshore zone? Fine-grained particles traveling down these two rivers are P-rich compared to their lake destination. Eventual discharge of particles into the low SRP lake environment may cause release of SRP as the particles reach a new equilibrium. Moreover, loosely bound SRP on fine-grained particle surfaces may be released during digestion in the mussel gut, enhancing the delivery of SRP to nuisance algae. If fine-grained particles play a key role in river phosphorus dynamics, it seems plausible that they have a similarly important role in the lake.

Chapter 4: Resuspension, Sorption, Settling, and Mussel Grazing

Section Overview

I tested the hypothesis that fine resuspended lake bottom sediments could act as a temporary sink for SRP, by investigating sorption (decreasing SRP and increasing P-Content) in treatment and control (i.e. sediment spiked and un-spiked) flasks of filtered lake water. Initially, I tested this effect with bulk bottom sediment samples, but eventually found that, most of the sorption effect was due to fine-grained particles. I then conducted additional experiments with the isolated fine-grained low density particles to determine sorption rates and maximum sorption capacity at various levels of ambient SRP.

Particle size distributions for the lake bottom sediments and an algal culture control were derived using image processing techniques. Settling rates were estimated theoretically using the particle size data and Stoke's Law and then effective settling rate was derived empirically with a laboratory experiment. Results from both methods showed that fine-grained particles can remain suspended in the water column for weeks to months until flocculation eventually causes sedimentation of particles. However, if nearshore mixing delivers particles near to the benthos, they may be intercepted by mussel filtration, increasing the effective particle settling rate.

I explored the effects invasive quagga mussels may have on resuspended lake sediments with laboratory experiments that compared mussel filtration, excretion, and egestion with various food sources. Mussels greatly increased effective particle settling rates in all tested groups and significantly altered phosphorus fractionation patterns in most groups. Interestingly, PP → SRP conversion efficiency (*f)* were not uniform among different food

sources. Combined, these findings provide a better mechanistic understanding of the alterations invasive bivalve mussels have made to nearshore phosphorus dynamics in Lake Michigan and provide a solid base for future modeling and experimental endeavors.

General Methods

I collected mussels and lake bottom sediments for laboratory experiments from the Atwater 20m Buoy site (43°6'0" N, 87°51'0" W) on the dates of 4/14/2021, 6/10/2021, and 8/3/2021 via SCUBA diving. On each occasion, 1-2 small-medium sized mussel covered rocks from the bottom of the lake were carefully lifted and placed into a (48 oz) whirlpak bag and sealed. This was repeated until about 4-5 bags were full. At the end of the dive, bags were stored on ice in a cooler on the boat and transported back to the lab for further processing. During the same excursion, 2-4 20 L carboys of lake water were also collected to provide a fluid medium for mussel cleaning and storage as well as for use in sediment sorption and mussel experiments.

Once at the lab, bags were emptied into 2 L clean plastic containers of the collected lake water. The containers were rocked, resuspending sediment off the rocks into the lake water. Rocks were then removed from the container and placed into an additional container of lake water for mussel removal and washing.

Mussels were removed from the rocks by carefully cutting their byssal threads with a razor blade. Once free of the rocks, mussels were gently rubbed clean against a scrub pad to remove sediment, biofilm, periphyton, and other debris from their shells. Then mussels were given a final rinse in distilled water before being transferred to an aquarium filled with filtered lake water and held in a fridge at 4°C prior to use in experiments. If mussels needed to be held

for more than two days before an experiment, they were fed an allotment of the microalgae

Raphidocelis subcapitata to ensure that the mussels stayed healthy throughout the duration of

the experiments. The allotment was proportioned based on mussel density within the holding

container. Since Lake Michigan mussels are estimated to filter approximately 1 L per day of lake

water with a PP concentration near $1 - 1.5$ µg/L, feed was scaled accordingly such that if the

container was well homogenized and mussels were filtering equally each mussel would receive

$1 - 1.5$ µg of PP per day. Practically, this was accomplished by creating a regression of Sonde

derived Chl *a* estimates on PP concentration to allow for faster determinations of algal PP

concentration than would have been possible from continuous monitoring of PP directly.

However, microalgae such as *Raphidocelis subcapitata* exhibit a 5 phase growth cycle consisting

of a 1) lag phase, 2) exponential phase, 3) declining relative growth phase, 4) stationary phase,

5) death/lysis phase. This growth cycle could have affected the PP:Chl *a* ratio, and thus the

slope of the regression curve and quantity of PP fed to the mussels. Future research aiming to

replicate this design or hold mussels for other experiments would benefit from first monitoring

the algae growth phase, regressing PP on Chl a during the stationary phase, and then culturing

the algae before death/lysis occurs to maintain the microalgae's stationary phase.

I noted that the mussels collected from the 20m site differed from mussels I had

previously collected at shallower depths. The 20m mussels had thinner more delicate shells

than their shallow (i.e. 6-10 m) water counterparts and also appeared to have a longer

incurrent siphon. These morphological traits have been noted for the deep water profoundal

mussel (Claxton et al., 1998), so it seems possible that these traits occur on a continuum based

on the selective advantages conferred by each morphological adaptation at specific depths.

The resuspended material from the first container was poured from the large plastic container into a clean 5 gallon bucket through a 600 μm sieve to remove macro algae, mussels, shells, and coarse sand from the solution. The bucket was covered and left to settle in a 4°C walk-in cooler. After allowing 3-5 days for particulate settling, I carefully siphoned the lake water from the top of the bucket, concentrating the settled sediments down to a volume of ~4L. The sediment lake water slurry was stored in an acid washed 4L polypropylene container and used for numerous experiments. The possibility of dissolution and thus declining PP and increasing SRP throughout sediment storage was considered, so initial concentrations of sediment PP and sediment P-Content were taken at the beginning of each experiment to account for this possibility. Changes to P-Content were small with the sediments maintaining an average concentration near 0.8 μgP/mg.

I observed that the water above the concentrated sediments was not completely clear after 3-5 days of settling and noted that small fine-grained particles may have remained suspended in the water column. Since particle sorption rates are largely dependent on surface area (Froelich, 1988), I hypothesized that these fine particulates may play a role in the sorption and transport of phosphate anions in the lake ecosystem. Thus, the siphoned water containing the fine particles was also saved in 4L acid washed polypropylene containers for use in sorption and mussel feeding experiments.

General Laboratory Processing Methods

Filtered lake water, which served as the fluid medium for these experiments, was prepared by filtering the Atwater20m lake water collected in the 20L carboys during sediment and mussel collection trips. Several additional trips had to be taken to collect more lake water.

Since it was impractical to return to Atwater20m station for each of these trips, water was instead collected from the 20m station nearest to Milwaukee Harbor's Middle Gap. All lake water was processed via vacuum filtration through 47mm diameter Whatman GF/F 0.7 μm pore size filters (Cat#: 09-874-71). Between experiments, filtered lake water was stored in a walk-in cooler at 4 °C.

All phosphorus fractions were analyzed by first converting, if necessary, the target P fraction(s) to SRP followed by reduction with the 4:1 molybdate-ascorbid acid method of Stainton et al. (1977) and measurement of absorbance at 885 nm on a spectrophotometer. The SRP detection limit for analysis on a 10 cm path length cuvette was 0.3 μg/L. TDP samples were digested by adding dilute sulfuric acid and peroxide, followed by a 2-hour photo-oxidation digestion. PP samples were first digested by high temperature combustion (i.e. 550 °C for 1 hour in a muffle furnace) followed by a 2-hour extraction in a dilute hydrochloric acid solution at 105 °C (Stainton et al. 1977). NaOH-PP was measured following the 17-hour shaker sodium hydroxide extraction method described in Baker et al. (2014). TSS was determined by filtering onto dried pre-weighed 0.6 μm pore size membrane filters (cat#: DTTP02500), redrying at 60-70°C for >12 hours and reweighing. Weights were measured on a Sartorius 3-digit microbalance with an accuracy of 0.001 mg. Weights of particulate matter on the filters recorded during the experiments ranged from 0.001 – 1+ mg with an average weight of 0.75 mg. Thus errors due to instrument accuracy were at most 1% and in general much lower than 1%.

Particle Sorption Experiments

Bulk vs Fine-Grained Sediment Sorption

Methods

I ran 5 initial sorption experiments with the bulk and fine-grained sediments collected from Atw20m station. Experiments were run on July 7 and 22, and August 12, 20, and 21, 2021. Each experiment was run in triplicate. The first experiment was exploratory in nature, and did not contain a control. After this initial exploratory experiment, each additional experiment also contained controls. Thus, experiments were conducted in batches of 6, with 3 control and 3 treatment flasks.

Running all the experiments simultaneously to avoid possible time confoundment would have been ideal, but this was not possible given space constraints in the lab and the long times associated with both experiment preparation and processing. While batch effects are possible, controls throughout the experiments showed good replication. As an additional quality control measure I calculated the mean percent error in total phosphorus mass balance within a batch of replicants using Equation 4:

$$\frac{\Sigma_i^n \frac{TP_{F_i} - TP_{I_i}}{TP_{I_i}}}{n} \times 100 \tag{4}$$

where

i = an iterator corresponding to each sample replicate

TP_{I_i} = the total phosphorus in the ith replicate at the start of the experiment

TP_{F_i} = the total phosphorus in the ith replicate at the end of the experiment

n = the number of replicates in each group

The experiments contained two treatment categories, bulk vs fine sediments, but also two levels of added phosphate within each category, an addition of 5 µg/L and an addition of

20 µg/L. Bulk sediment flasks had a final TSS between 25 – 32 mg/L to simulate a large and recent resuspension event. The starting TSS concentration in fine sediment flasks, however, was only 1.5 – 2.1 mg/L for the 8/20/21 and 8/21/21 experiments and ~3.3 mg/L for the 8/12/21 experiment which was designed to represent either a smaller resuspension event that only mobilized fine-grained particles or the time period following resuspension when larger particles had settled.

Unfortunately, sampling the lake during major resuspension events is impractical and potentially dangerous from a small vessel. Because of this, TSS concentration ranges were chosen based on a Milwaukee harbor survey conducted on 8/11/2020, following a violent storm that resuspended sediments within the harbor (to see the data and CTD casts associated with this survey visit LimnoExplorer App, choose the "Survey Explorer" tab, and select the date 8/11/2020 from the drop down tab). Other than the initial TSS concentration, handling of the bulk and fine-grained sediment treatment flasks was identical. Triplicate control containers were not spiked with sediments, but received the same phosphate spike as the treatment flasks in that batch and underwent the exact same handling and processing throughout the duration of the experiment. The experimental preparation and processing was as follows:

1. 1 L of 4°C filtered lake water was measured and added to each of the 6 flasks.
2. Either 100 or 400 µl of 50 mg/L phosphate stock was added to each flask to bring initial phosphate concentration to either 5 or 20 µg/L. This amount varied between experimental batches, but was always the same within a batch.

3. Bulk sediments spike amounts (ml) were target for a TSS concentration between 25 – 35 mg/L, while fine grain sediment spike amounts were targeted for a concentration between 1 – 3 mg/L. The required volume of the spike was calculated from previous measurements of the PP concentration within the container bottles and was typically ≤ 5 mL of concentrated bulk sediments and ≤ 100 mL of the fine sediments that had been siphoned from the top of the settling bucket.

4. The estimated volumes of Atwater 20m sediment spikes, either bulk or fine-grained, were added to the treatment containers.

5. Flasks were inverted to homogenize the sediments and then each flask was filtered through a pre-weighed 0.6 μm pore size membrane filter to attain initial measurements of TSS and PP.

6. At the same time, acid washed polypropylene containers were used to collect each flasks filtrate for SRP determination.

7. Flask openings were covered with aluminum foil to prevent dust contamination, placed in a refrigerator set at 4°C, and left overnight to incubate for 17-19 hours.

8. The next morning, steps 5-6 were repeated to acquire final measurements of TSS, PP, and SRP.

All TSS, PP, and SRP data were processed with the methods discussed earlier in the general methods section. For mass balance determinations, TP was estimated as SRP+PP. This mass balance does not account for the contribution of DOP. However, DOP should not have been a significant contributor since phosphate was added directly via the 50 mg/L stock and

prior measurements of the filtered water from the bulk and fine-grained sediments showed SRP

and DOP values below the detection limit of < 0.3 µg/L. Thus, PP concentrations should

represent added sediments + sorbed phosphate and SRP concentration stock phosphate –

sorbed phosphate.

Results

In general, mass balance accounting showed that TP was lost from the flasks during the

duration of the experiment, with an average of -0.59 µg P/L and an average percent loss of -3%.

This loss could be due to a combination of physical and/or biological effects. Physical loss could

be a result of charged particles sticking to the glass flask's walls whereas biological loss could

result from the formation of bacterial biofilm on the container walls. However, observed losses

were generally small relative to the TP pool, and the main area of interest for this experiment

was not TP gain or loss but within-bottle fractionation of P species.

Both control and treatment containers showed a general trend of increasing PP and

decreasing SRP, though SRP was often lost slightly faster than PP was gained Figure 31. I tested

the difference in percent change of phosphorus fraction for control and treatment bottles for

each experiment date/phosphorus fraction pair (i.e. SRP and PP for each date) with a null

hypothesis of no change using R's linear model function "lm" (R Core Team, 2020). Percent

change, in this case, refers to the percent change of a P species (i.e. SRP or PP) as it relates to

the TP within each flask and is thus defined as (final species – initial species)/(initial TP).

Results from these tests are presented in Table 4.

Table 4: Linear Model Results from Bulk vs Fine Sediment Sorption Experiments.

Gold highlights show significant (p < 0.05) difference in percent change of P species from the null hypothesis of no change (i.e. mean percent change = 0), red highlights show highly significant difference in percent change (p < 0.001). The fine sediment group showed much greater mean percent change in both 5 and 20 µg/L levels, though the sorption effect was most pronounced with higher initial added phosphate and higher initial mean TSS.

Fraction	Sediment Group	Experiment Date	Initial Added Phosphate (µg/L)	Mean Initial TSS (mg/L)	Group	Estimate of Mean Percent Change	Standard Error of the Mean	Test Statistic	P Value
PP	Bulk	7/8/2021	20	0.14	Control	0.041	0.016	2.587	0.061
PP	Bulk	7/8/2021	20	27	Treatment	-0.010	0.022	-0.434	0.687
PP	Bulk	7/22/2021	5	0.14	Control	0.050	0.054	0.933	0.403
PP	Bulk	7/22/2021	5	25	Treatment	0.000	0.076	-0.002	0.998
PP	Fines	8/12/2021	20	0.05	Control	0.018	0.055	0.329	0.759
PP	Fines	8/12/2021	20	3.3	Treatment	0.577	0.077	7.449	0.002
PP	Fines	8/21/2021	5	0.09	Control	0.045	0.063	0.715	0.514
PP	Fines	8/21/2021	5	1.6	Treatment	0.218	0.090	2.438	0.071
PP	Fines	8/20/2021	20	0.13	Control	0.026	0.009	2.774	0.050
PP	Fines	8/20/2021	20	2.0	Treatment	0.149	0.013	11.239	0.000
SRP	Bulk	7/8/2021	20	0.14	Control	-0.051	0.016	-3.261	0.031
SRP	Bulk	7/8/2021	20	27	Treatment	-0.046	0.022	-2.104	0.103
SRP	Bulk	7/22/2021	5	0.14	Control	-0.103	0.021	-4.804	0.009
SRP	Bulk	7/22/2021	5	25	Treatment	0.079	0.030	2.610	0.059
SRP	Fines	8/12/2021	20	0.05	Control	-0.033	0.013	-2.424	0.072
SRP	Fines	8/12/2021	20	3.3	Treatment	-0.544	0.019	-28.663	0.000
SRP	Fines	8/21/2021	5	0.09	Control	-0.033	0.109	-0.305	0.775
SRP	Fines	8/21/2021	5	1.6	Treatment	-0.339	0.154	-2.193	0.093
SRP	Fines	8/20/2021	20	0.13	Control	-0.043	0.011	-3.785	0.019
SRP	Fines	8/20/2021	20	2.0	Treatment	-0.256	0.016	-15.916	0.000

In general, the bulk sediments did not produce an effect significantly different from the null hypothesis of no change for either SRP or PP. The exception to this was for two batches, 7/8/2021 20 µg/L and 7/22/2021 5 µg/L, where change in SRP was significantly less than zero. This may represent a small sorption signal but could also be due to loss of SRP to container walls. In contrast, the fine sediments, despite representing only a fraction of the initial TSS load compared to the bulk sediments, showed significant difference from the controls with increases

in PP and decreases SRP in all but the 8/21/21 experiment conducted at 5 ug/L. A visual inspection of the 8/21/21 data revealed that the trend was still in the same direction, i.e. declining SRP and increasing PP in the treatment flasks, but that the lack of significance for this experiment can be attributed to poor replication in the SRP controls and PP treatments. This is not surprising since replicating results at very low levels of SRP and PP can be challenging as it pushes determinations closer to the SRP detection limit, near 0.3 µg/L.

PP gains and SRP losses were greatest in the flasks containing ~3.3 mg/L TSS of fine sediments Figure 32. PP increased by 57.7% and SRP decreased by 54.4% after adjusting the treatment flasks by subtracting concurrent changes in the controls (see Table 4).

It is worth noting that the initial SRP of the fine sediment flasks was substantially lower than that of the controls despite being spiked with the exact same amount of phosphate stock. This suggests that perhaps two sorption reactions were occurring simultaneously, a faster initial reaction which occurred before the initial SRP filtrate was collected (i.e. on the order of minutes), followed by a slower secondary reaction that took place during the overnight incubation (i.e. on the order of hours).

The P-Content of all fine sediments roughly doubled during the duration of the experiment while the bulk sediment P-Content remained fairly stable (Figure 33). However, the P-content of the fine sediments did not exceed 6 µg/mg. To determine whether this threshold signified a maximum sorption capacity for these fine-grained particles, I designed a follow-up experiment to determine maximum sorption by exposing fine sediments to a range of SRP concentrations and measuring the changes of SRP and PP through time.

Figure 31: Bulk vs Fine-Grained Sediment Sorption.

Orange colors show PP, while purple colors show SRP. Lighter shades are measurements from the beginning of the experiment i.e. "initial" and darker shades are measurements at the end of the experiment i.e. "final". Phosphorus concentrations, top row, refer to either PP, or SRP, and thus are labelled as "P". Percent change refers to percent change of total phosphorus and is thus defined as (final species – initial species)/(initial TP). Bulk sediments, left column, did not produce significant changes in either SRP or PP for either phosphate level i.e. 5 or 20 μg/L. However, fine sediments, column 2, showed significant decrease in SRP and significant increase in PP at the 20 μg/L phosphate spike level.
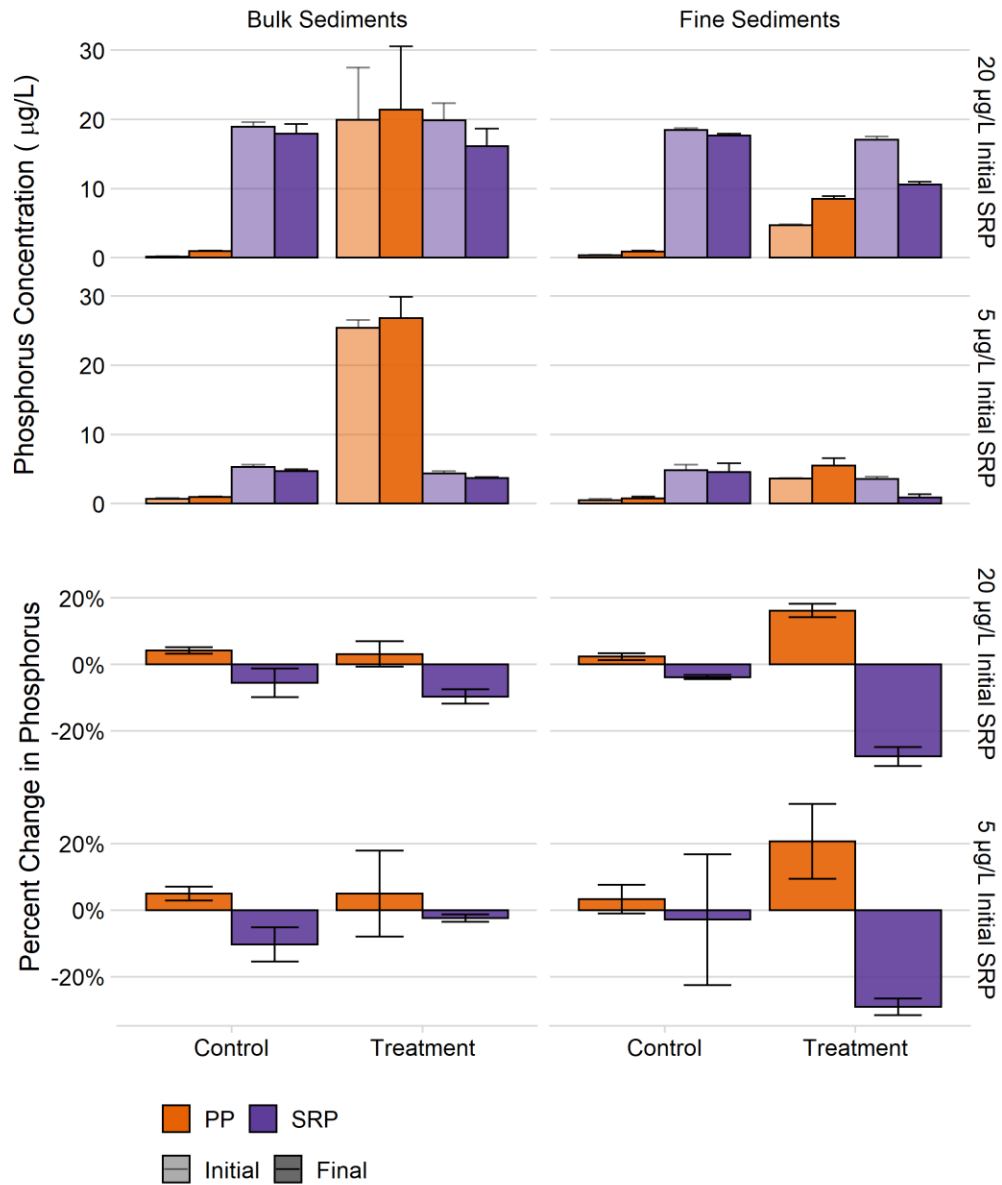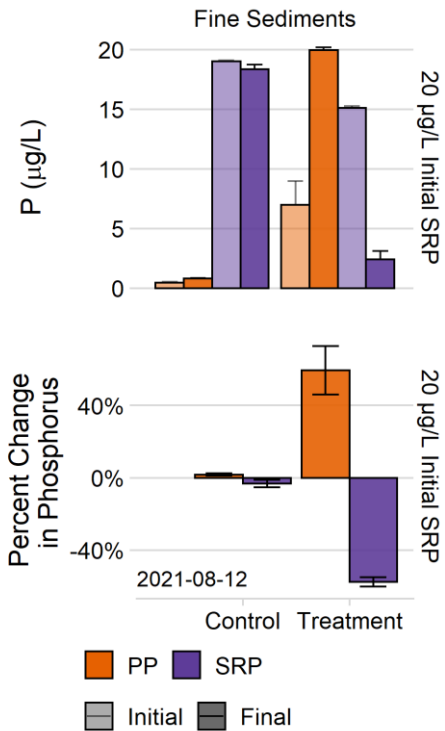
Figure 32: Fine Sediment Sorption Experiment 8/12/2021.

Orange colors show PP, while purple colors show SRP. Lighter shades are measurements from the beginning of the experiment i.e. "initial" and darker shades are measurements at the end of the experiment i.e. "final". Phosphorus concentrations, top row, refer to either PP, or SRP, and thus are labelled as "P". Percent change refers to percent change of total phosphorus and is thus defined as (final species – initial species)/(initial TP).

With a higher initial TSS concentration near 3.3 ug/L, this experiment showed clear and significant declines in SRP and increases in PP due to phosphate sorption (i.e. $p \ll 0.001$, and $p < 0.002$ respectively). Changes to the controls during this experiment were small and not statistically significant.
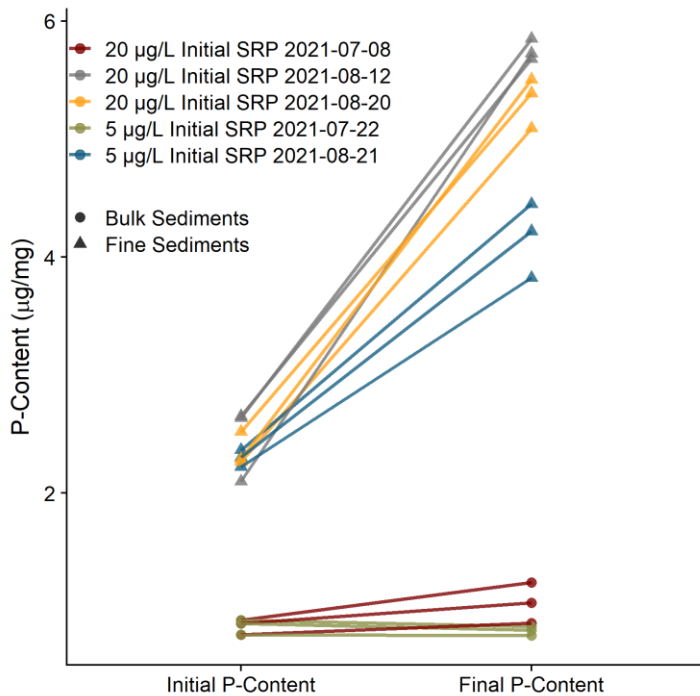
Figure 33: Increasing P-Content in Bulk vs Fine Sediment Sorption Experiments.

Bulk sediments are shown with triangles and fine sediments are shown with circles. Experiment date is shown with color (see legend on left of figure). Points on left are the initial P-Content and and the right are the final P-content. Each line is drawn between the initial and final P-Content of a replicate flask.

P-Content in the fine sediment group increased for all replicates during the experiment. Bulk sediments had slight increases in P-Content in the 20 ug/L flask, but increases were much smaller than in the fine-sediment group.

111

Fine-Grained Sediment Sorption Capacity and Kinetics

Methods

To test the sorption capacity of fine-grained lake sediments I prepared 9 aliquots with a

volume of 1 L of 0.7 μm GF/F filtered 4°C lake water in 1-liter acid washed Erlenmeyer flasks. To

each flask I added an initial SRP spike ranging from 0-30 μg of added P stock. Then, I added 100

mL of additional lake water that contained the fine-grained particulates of interest. This

resulted in a series of flasks with close to the same fine sediment load, but initial SRP

concentrations ranging from 0 – 27.27 μg/L. After the sediment slurry was added, I

homogenized the flasks by covering and shaking them, then immediately filtered 50 mL of

water through a pre-weighed 0.6 μm membrane filter.

Filtrate was collected from each flask to measure the initial SRP concentration, while the

pre-weighed filters were used for TSS, PP, and P-content analysis. I repeated this

homogenization and filtration routine four times over 6 days to produce a time series analysis

of sediment P-content (Figure 35). The 1-liter Erlenmeyer flasks were individually capped with

aluminum foil to protect from dust contamination and stored in a refrigerator at 4°C between

each filtration event.

Results

Replication among flasks was reasonably good with an initial TSS concentration between

2.74 – 3.2 mg/L and a mean concentration of 2.95 mg/L. Initial P-content of the sediment was

also consistent, with a range of 1.24 – 1.78 μgP/mg and a mean of 1.5 μgP/mg. Initial SRP

concentrations were much lower than would have been expected if sediments were not

reacting rapidly with SRP (Figure 34 A). As before, I used mass balance estimates as a quality control metric. Since TDP was not measured in the experiment, TP represents SRP + PP.

Generally, mass balance metrics were reasonable but again showed loss of TP over time. Initial samples had a mass balance error ranging from 0 – -13% representing up to a 13% loss of TP from the expected TP given the sediment and phosphate spikes. TP Losses were greatest on day 6 of the experiment with greater mass balance errors ranging from -32 – -56 % (Figure 34 B).
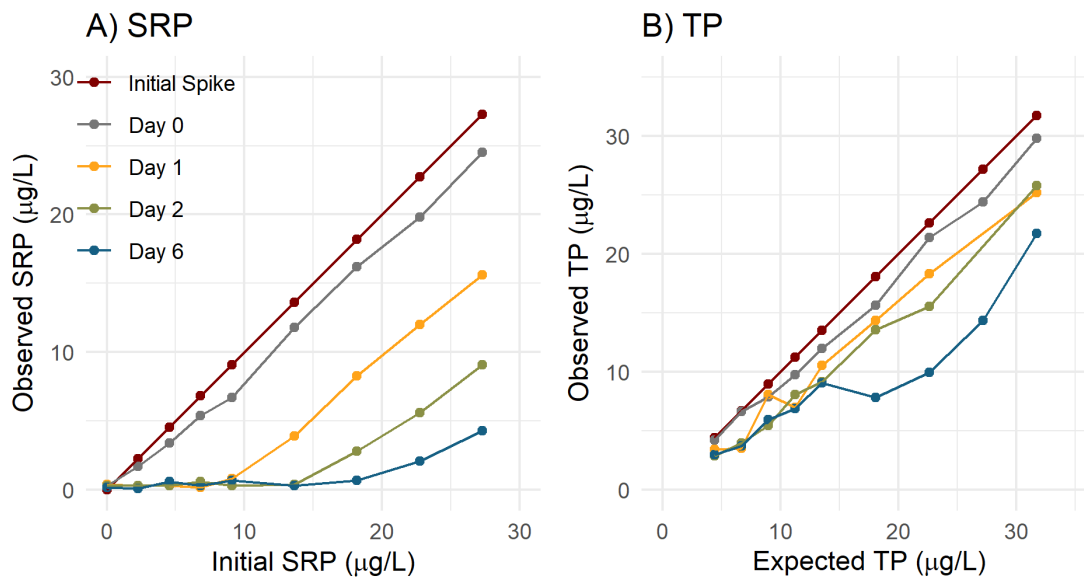
Figure 34: Fine-Grained Particle Experiments: Declining SRP and TP.

SRP and TP both declined during the experiment; however SRP declined faster due to sorption on sediments and thus movement from the SRP to PP fraction. TP declines, i.e. declining mass balance, may indicate loss of P due to sticking or uptake bacterial biofilm. TP losses were greatest by day 6. Initial measurements of SRP again showed lower than expected values considering the amount of phosphate added which may show an initial fast reaction of phosphate sorption to sediment surfaces.

The fine-grained sediments quickly sorbed P, evidenced by rapid initial gains in P-content

(Figure 35). However, by day 6 of the experiment P-Content had plateaued suggesting that the

continued loss of SRP in the flasks with > 18 µg/L initial SRP spikes may have been due to

biofilm uptake on container walls.

I fit the sediment P content vs time data with the following non-linear equation:

$$c = \frac{c_{max}[t]}{c_m + [t]}$$
(6)

where c = the fine-grained sediment P-Content at time t

c_{max} = the maximum saturation point (µg/mg)

c_m = the half-saturation point (µg/mg)

t = time (hours)

The c_{max} and c_m parameters where estimated from the data using a Gauss-Newton

algorithm from R's "nls" function in the "stats" package (R Core Team, 2020). Since parameters

were estimated for each bottle, with concentrations of SRP ranging from 0 – 27.27 µg/L, it was

possible to fit these parameters with a linear model based on the initial SRP concentration of

each flask (Figure 35 B and C). Both the maximum saturation (Figure 35 B) and half-saturation

(Figure 35 C) data fit the linear models well with Adjusted R-squared values of 0.98 and 0.97

and P-values of 9.08e-08 and 7.12e-07 respectively.

Figure 35: Sediment Saturation Curves and Parameter Linear Model Estimation.
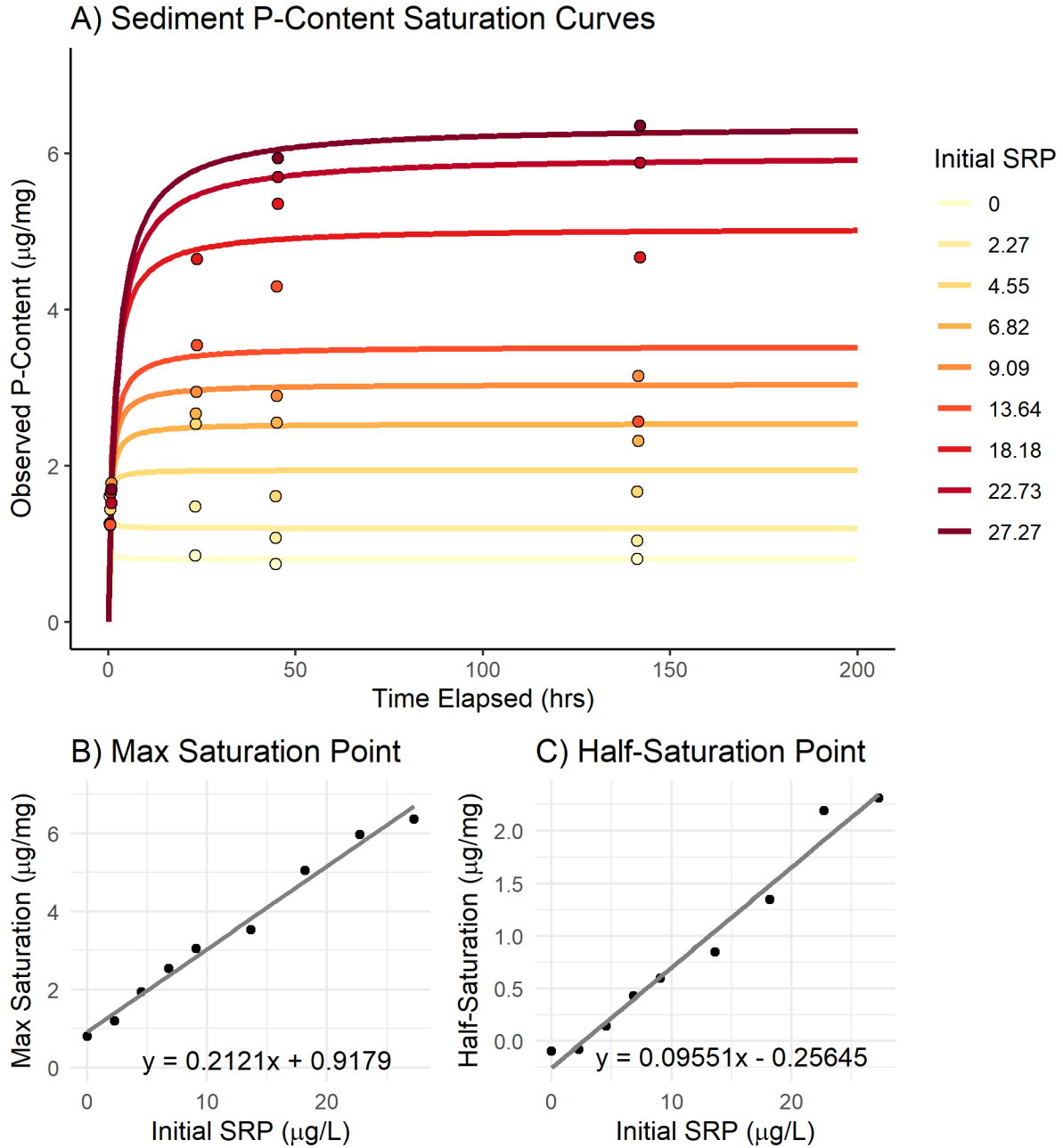
A) Sediment sorption curves fit to the data using Equation 5. Sediment sorption capacity as measured by P-Content increased with increasing levels of initial SRP. B) The maximum saturation was achieved at the highest initial SRP concentration. C) The reaction speed, as quantified by half-saturation point also increased with increasing levels of initial SRP.

Discussion

The information gained from these experiments allows for prediction of fine-grained sediment P-Content, and thus sorption based on ambient SRP concentrations and time. Since the initial reaction rate is fast (i.e. on the order of hours) relative to resuspension and sinking time scales, the time component of these reactions can likely be ignored. This information can be incorporated into nearshore phosphorus model to help understand how resuspension of reactive fine-grained sediments may alter the transport and fate of phosphorus.

The knowledge of fine-grained sediment sorption rates and maximum sorption capacity led to several important follow up questions:

1) How long do fine-grained particles stay suspended in the water column following a disturbance event (i.e. settling rates). What is the particle size distribution of these sediments?

2) What do mussels do with this resuspended material? Do they filter it, increasing effective particle settling rates? If fine-grained particles are consumed and digested by mussels, is sorbed P on the particle surface re-released into the water column?

Settling Rate Experiments

Particle Size Distribution

Methods

Particle size distributions were estimated from 2048 x 1536 pixel images of sediment taken on an EVOS™ XL Core Imaging System. I used an inverted bight-field microscope with a 20x air objective. Images were processed using ImageJ software (Schneider et al.,2012) following a cell counting procedure developed for Microalgae cultures (Esra Dökümcüoğlu & Yılmaz, 2020). As a quality assurance measure as well as means of comparison, images of the

microalgae *Raphidocelis subcapitata*, whose size is well documented, were also taken and run through the same image processing procedure.

Extracting discrete counts from an image is easiest when the image is relatively uncluttered, allowing for separation of particles and/or algae from one another. If an image is too densely populated with sample, separation is difficult and particle size may become biased high due to unintended aggregation of adjacent pixels. To avoid this bias, we aimed to keep our total pixel area covered by sample lower that 20 %. However, it can also be problematic to have too few particles in an image, especially if samples are heterogeneous, so we aimed to have a minimum of 2 % pixel area coverage.

We pipetted 3 drops of sediment slurry or algae culture into 3 wells each to produce triplicate samples from each sample group. Our groups were 1) Lake Bottom Sediments, 2) Lake Bottom Sediments after allowing for 2 hours of natural settling, and 3) Algae culture *Raphidocelis subcapitata.* After pipetting, the well plate was rocked to aid with homogenous particle spread across the bottom of the well plate. The surface and bottom of the well plate tray was cleaned with 70 % isopropanol alcohol, after which particulates were allowed to settle for ~5 minutes prior to image collection.

Briefly, the image processing protocol of Esra Dökümcüoğlu & Yılmaz (2020) involves converting a standard image to 8-bit (i.e. grayscale) subtracting out excess background variation with a smoothing algorithm, manually adjusting an intensity threshold to minimize left-over background noise, and then delineating and quantifying the area of pixel aggregates.

Particle area was converted from pixels to microns by a microscope magnification-specific conversion factor. For ease of comparison, pixel area values were standardized into equivalent spherical diameters (ESD) using Equation 6:

$$2 \times \sqrt{(A/\pi)} \tag{6}$$

where

A = the area of the particle in microns.

Results

After trying multiple sediment-slurry and algae culture dilution factors we were able to meet our target of 2 – 20% pixel coverage in the sediment and algae culture images with good replication between results (Table 5).

Table 5: Particle Image Analysis - Mean Pixel Coverage by Sample Group.

Sample Group	Mean Pixel Coverage	Standard Deviation
Lake Sediment	14.1%	±2.2%
2hr Lake Sediment	6.9%	±1.2%
Algae	2.1%	±0.1%

Images of the lake bottom sediment at various stages of settling show a heterogeneous mixture of particle shapes and sizes (Figure 36 A-C) whereas the algae culture appears more uniform in both shape and size (Figure 36 D). Larger particles are visible in the initial lake sediment sample (A), but have mostly disappeared after 2 hours of settling (B). When particles were left undisturbed for long periods of time (i.e. several weeks to months) they began to flocculate (C).
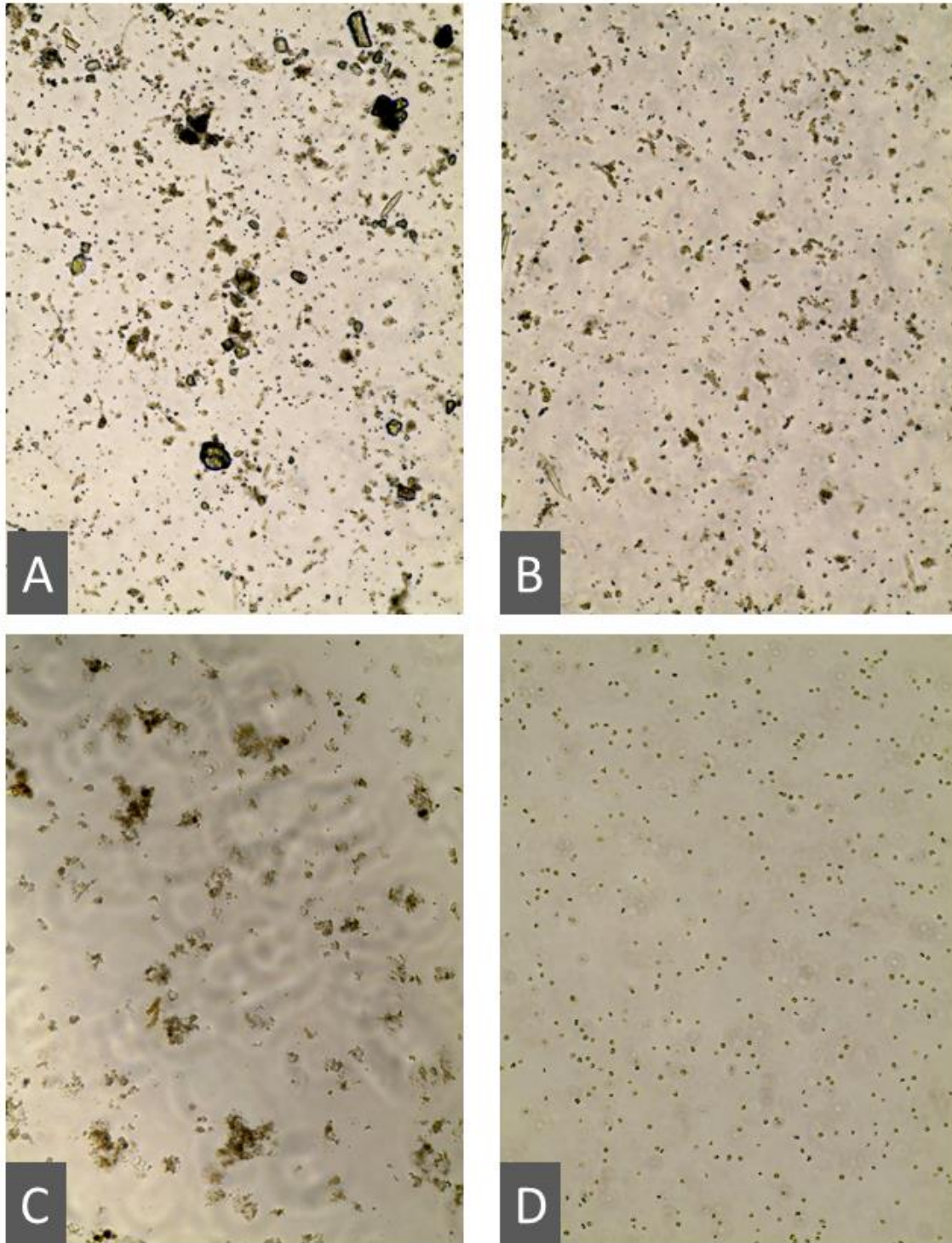
Figure 36: Images of Lake Sediments and Algae Culture.

A) Bulk lake sediments after being homogenized and subsampled. B) Lake sediments after 2 hours of settling. C) Fine-grained lake sediment flocs after > 1 month of settling. D) Algae culture *Raphidocelis subcapitata.*

Particle sizes were determined by converting pixels to microns based on a microscope/magnification specific conversion factor that had been determined in previous work by the microscopes primary user (Eric Ostovich, Personal Communication). Particle size histograms derived from the analysis followed a roughly log-normal distribution (Figure 37 A).

Raphidocelis subcapitata have a sickle shape cell that often curves in to form a hollow circle shape with mean cell lengths ranging from 8-14 um and widths between 2-3 μm. (AlgaeBase, 2020). I multiplied length x width to estimate cell areas between 16-42 μm^2 and from that calculated that ESD should fall between the bounds of 4.5-7.3 μm. The calculated average ESD from the image processing procedure fell within these bounds at 6.93 ±1.49 μm, providing confidence in the procedure and results.

Replication was first assessed as good based on visual comparison of the histograms and sina distributions (Figure 37) and then determined more formally in a nested linear model analysis in which replicate was not a significant predictor of particle ESD (P >= 0.05). The one exception of this pattern was replicate C from the algae group which was significantly smaller than replicates A and B from the same group (F = -2.36, p = 0.02).

Lake bottom sediments ranged from ESD of 1.63 – 102 μm with a mean ESD of 7.15 μm in the original sample and a mean of 6.87 μm after 2 hours of settling. This mean diameter is very similar to the algae species *R. subcapitata* used as a reference in this particle size analysis. This same culture of *R. subcapitata* was used again later in the mussel filtering and feeding experiments discussed later in this chapter. It is worth noting that the ~1 – 100 μm size range

includes sizes of other common lake phytoplankton species from small picoplankton to large diatom species as well freshwater bacteria.

Small-particle deposits rest as a fine skin of easily resuspended material in the nearshore benthos. Within this matrix likely resides a mixture of biotic and abiotic waste from autochthonous cell debris of lake phytoplankton and bacteria to allochthonous clays and detritus exported from nearby tributaries. Data presented above indicate that this material can serve as a phosphate sink in laboratory experiments, but that leads to several key follow up questions:

1) When and by what hydrodynamic mechanisms do resuspension events occur?

   a. Is resuspension seasonal, episodic, or both?

2) How long do resuspended particles stay suspended in the nearshore?

   a. Can particles be exported from the nearshore to the pelagic or do they resettle in the nearshore?

3) What do mussels do to these particles?

   a. Do they filter and digest them or reject the particles as pseudofeces?

   b. Is the sorbed PP easily desorbed by mussel filtration/digestion and released as SRP where it can be assimilated by nuisance algae?

   c. Do mussels garner any nutritional value from particles?

These questions have major implications for nearshore and whole-lake biogeochemistry.

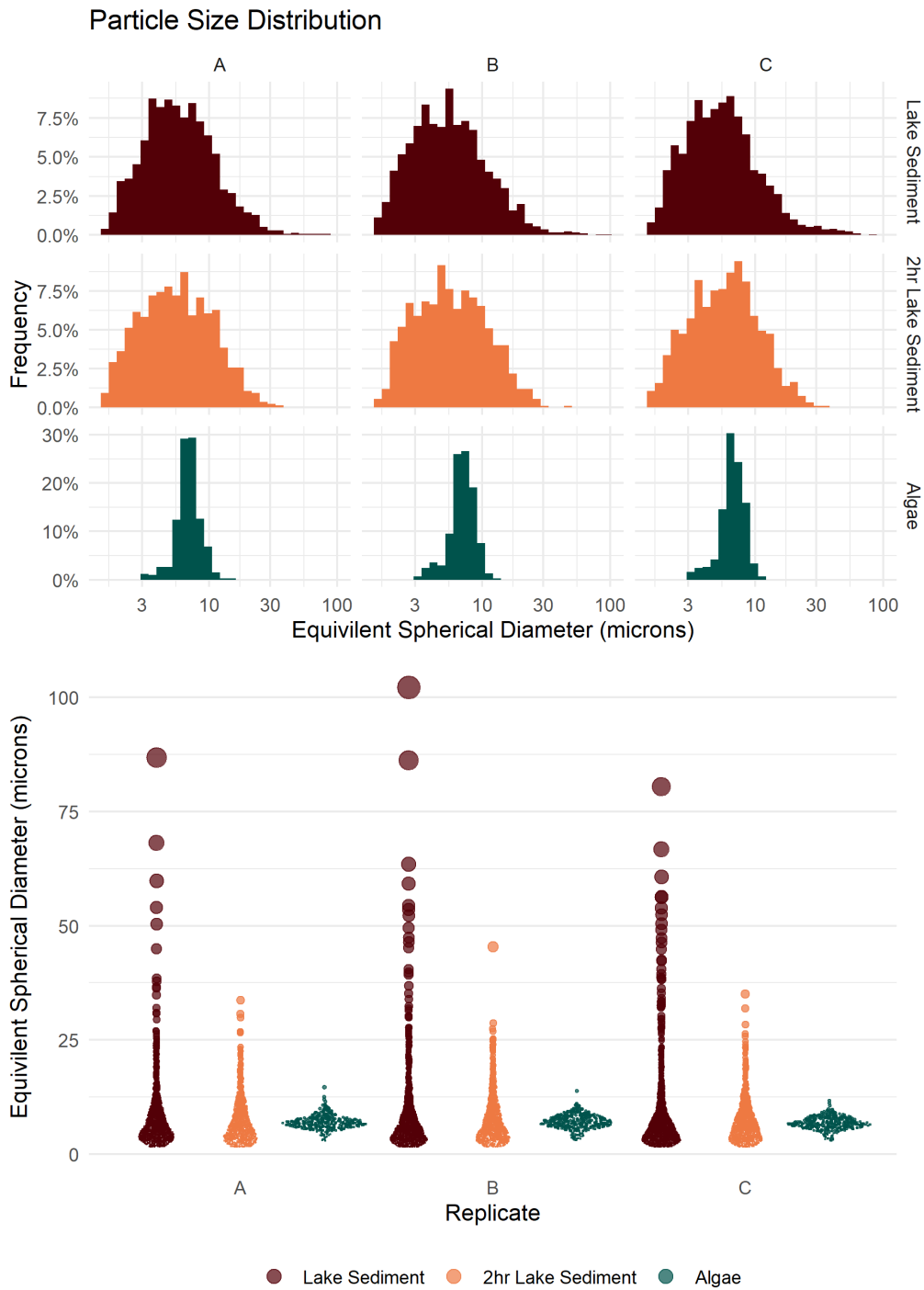Figure 37: Particle Size Distribution Histograms and Sina plots.

Lake sediments followed a roughly log-normal distribution while the algae culture followed a normal distribution. Replicates were good in all groups. Note the loss of large particles between the initial sampling of the lake sediments and the sample taken at 2 hours. Virtually all particles > 35 microns settled within the first two hours.

Estimating Settling Rates from Particle Size with Stoke's Law

Methods

Stoke's law states that when the gravitational force and buoyant force of a settling

spherical particle are at steady state (i.e. not changing with time), the settling velocity v can be

calculated with the following equation:

$$v = \frac{2}{9}\frac{(\rho_p - \rho_f)}{\mu}gR^2 \qquad\qquad (7)$$

where

g is the gravitational field strength (cm/s^2)

R is the radius of the spherical particle (cm)

ρ_p is the mass density of the particle (g/cm^3)

ρ_f is the mass density of the fluid (g/cm^3)

μ is the dynamic viscosity (g/(cm*s)).

The equation above, combined with the particle size distribution data and estimates of

particle density, can be used to estimate settling rates. Based on material density values for

sand, clay, and silt on engineer's toolbox, I estimated that particle density for the fine-grained

lake sediments was between 1.1 and 1.5 g/cm^3. Density was likely higher for large particles that

consisted fine sand, but I was less interested in the sinking rates of large, dense particles since

they had shown to be minor players in the sorption experiments.

Results

The mean equivalent spherical diameter across all groups was ~7 microns. Plugging a

radius of 3.5 microns into the above equation along with constants associated with water at a

room temperature (i.e. ρ_f = 0.9982 g/cm^3, g = 980.665 cm/s^2, μ = 1.002e-2) we can estimate an

average settling rate somewhere between 1-5 cm/hr depending on particle density (Figure 38).

However, we can also see that for larger particles in our distribution, sinking rates are much

higher with the largest particles sinking at ~200-1000 cm/hr. The smallest detectable particles

from the distribution, near 2 microns, settle at a rate of ~1.9 – 9.3 cm/day.
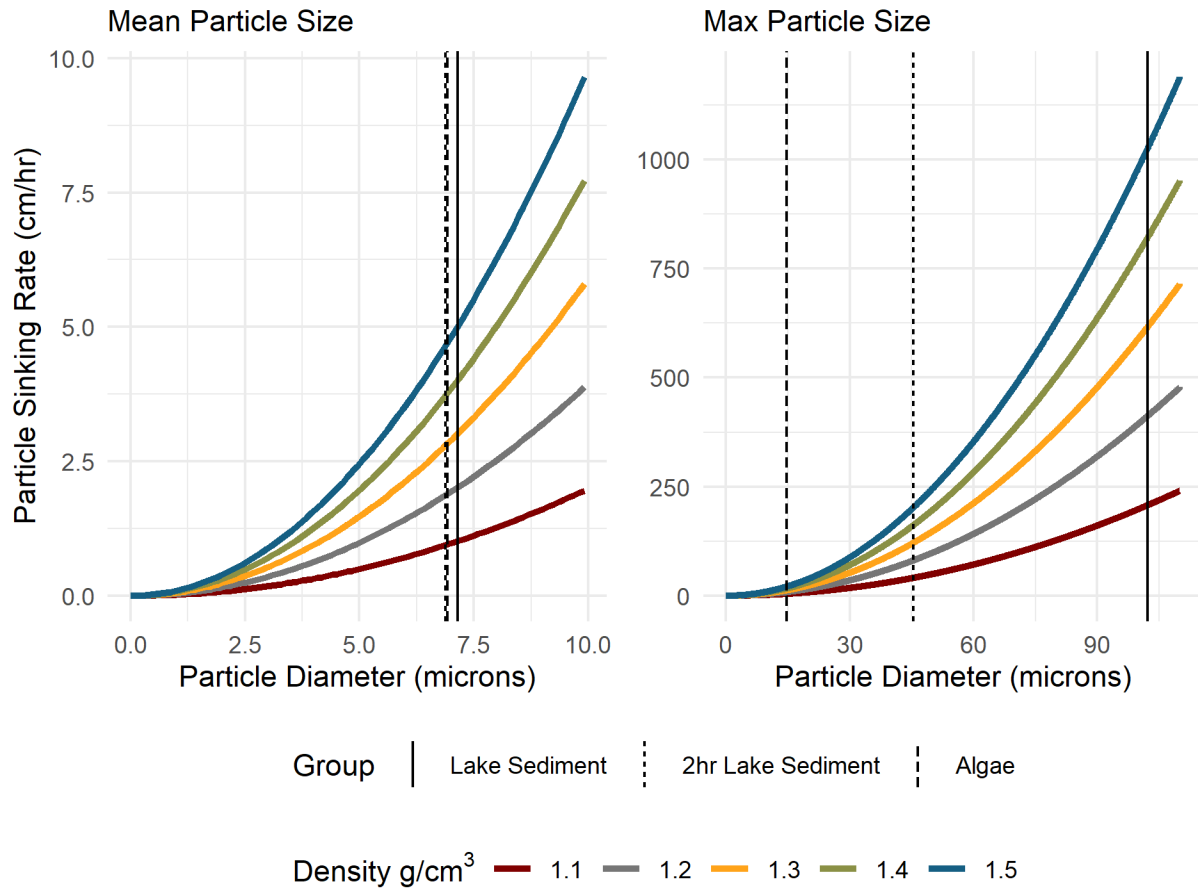
Figure 38: Particle Sinking Rate Estimates Derived with Stokes Law.

With a mean particle size of 7 microns, particles likely settle at a rate of 1-5 cm/hr depending on particle density. Larger particles settle approximately two orders of magnitude faster (i.e. 200 – 1000 cm/hr). This combined with their lack of reactivity with SRP as shown in the previous section provides more evidence that large particles likely play a smaller role in altering lake water biogeochemistry compared to fine-grained sediments.

Effective Settling Rates from Laboratory Experiments

In addition to estimating settling rate from particle size distributions using Stokes' Law, I also conducted a laboratory settling rate experiment.

Methods

A rectangular settling column (Figure 39 A) was constructed from an acrylic sheet using Weld-On SciGrip 4 and 16 to glue the four walls and bottom together into a column. It had an internal area of 23 cm X 15 cm with a total height of 120 cm. A small hole was drilled into the side of one wall near the bottom of the column and a release valve was glued in to allow for draining between experiments. The column was fastened to a fitted acrylic base with set screws to help stabilize the column during the experiment. The column was filled and leak-tested for 48 hours before being drained, cleaned, and prepared for use in the settling rate experiment.

A transmissometer (Figure 39 B) was built using a red (652 nm) laser pointer as the collimated light source and a LI-COR PAR logger (LI-192) as a detector. The light source and light detector were fastened to a C-clamp which was custom built to fit the external dimensions of the settling column. Both light source and detector were fitted onto the clamp such that the light passed directly through the center of the column to minimize potential edge effects. The C-clamp also had a level installed to ensure that all measurements were taken uniformly level.

The column was filled with particle free distilled water leaving 15 cm of head-space at the top to accommodate the addition of sediment slurry and provide space to measure blanks (Figure 39 A). We marked 5 cm intervals from the surface of the water column to the bottom, for a total column depth of 105 cm. Thus with an internal area of 23 x 15 cm and depth of 105 cm the settling column had a volume of ~36.2 liters.
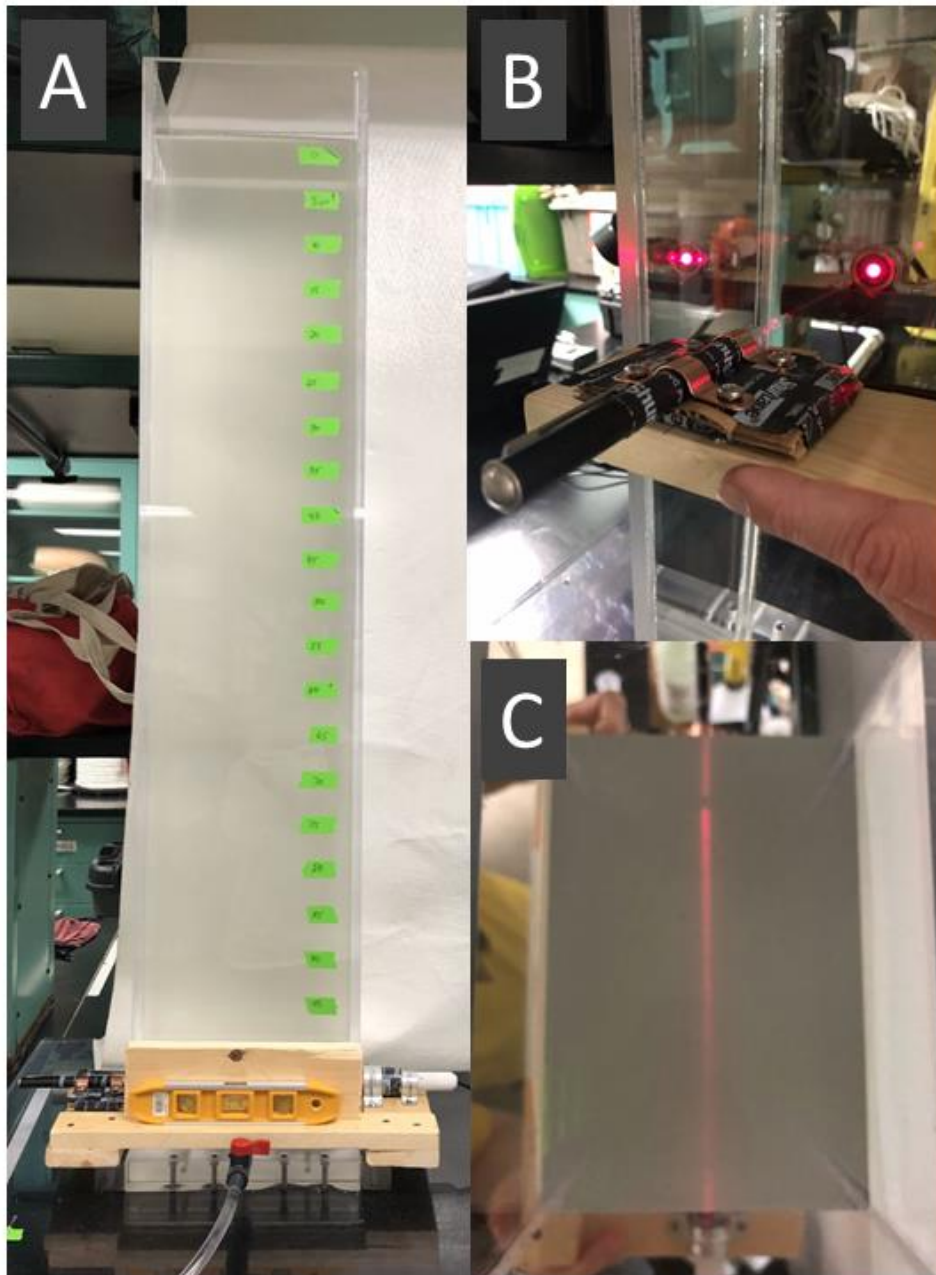
Figure 39: Settling Column and Transmissometer.

A) Full view of settling column. Green tape shows 5 cm intervals used as a guide during column profiles. The Wooden C-clamp, laser pointer, and PAR logger are visible at the bottom of the image. A level, bottom of image, was used to help ensure consistent measurements. B) Transmissometer constructed from a 652 nm laser pointer and PAR logger mounted to wooden C-clamp. C) Top view down into the column after the addition of sample has given the column a "milky" appearance.

One technician was in charge of reading from the PAR monitor and entering data into a spreadsheet template while the other technician moved and held the transmissometer stable at each height, 0 – 105 cm. Prior to adding the sediment slurry and beginning the experiment, several blank measurements were made. We took an "air blank", by holding the transmissometer away from the column so that the laser only passed through air to the PAR detector. This helped us detect if the laser alignment had become un-centered, or if laser battery needed to be changed. A "column blank" was measured through the head-space at top of the settling column where no water was present, providing an adjustment for light attenuation due to the acrylic walls. There was no difference between this column blank and a sample blank taken through the lower part of the column filled with distilled water, indicating that the water was particle free prior to sediment addition. Finally, a "blank profile" was taken in which we measured PAR values at each 5 cm interval throughout the column to ensure that the acrylic material had a uniform effect across the entire depth range and that there was no interference from scratches or watermarks. Initially this helped us determine that movement during the sampling process was causing the laser to drift off-center. Once the laser and PAR logger were better secured, the mean PAR reading was 139 ± 1.03 μmol m^{-2} s^{-1}. Thus, variance due to differences in the column walls was < 1%. Each day, before taking experiment profiles, we took "air" and "column" blanks with the goal of keeping measurements as consistent as possible and making adjustments to the DIY transmissometer as needed.

The experiment was started by carefully adding 150 mL of homogenous Atwater 20m bottom sediment slurry to the top of the settling column. The slurry was added slowly and smoothly near the surface of the water in an attempt to avoid creating turbulence within the

settling column. We then measured PAR at each column depth, 0 – 105 cm while tracking the time at which each measurement was made. Initially, profiles were measured frequently to capture the rapid change in water transparency at the start of the experiment. Out of a total of 25 profiles, 15 were taken within the first 24 hours. Changes in water transparency slowed drastically after day 1 and the final profile was taken on day 10 of the experiment.

We developed a calibration curve to convert measured PAR values first to absorbance and then to suspended sediment concentration (μg/L). The curve was designed to cover the full range of PAR values encountered during our experiment, from ~0.2 – 160 μmol m^{-2} s^{-1}. Each standard for the curve was created by spiking a small amount (0 – 40 mL) of Atwater20m sediment slurry into 2 liters of particle free distilled water. The 2 liters were homogenized via shaking and a small subsample (10 – 100 mL) was taken and filtered onto a pre-weighed membrane filter. Meanwhile, the remainder of the standard was added to the cleaned and empty column where its PAR value was measured with the same transmissometer used during the settling experiment. Membrane filters were re-weighed after 24 hours in a drying over to produce TSS values which were fit with a linear model against the calculated absorbance data which was produced by the equation $A = 2 - log_{10}(\%T)$ where A = absorbance, and $\%T$ = percent transmittance which is calculated as $\%T = 100\frac{I}{I_0}$ where I = the PAR value of the standard and I_0 = the PAR value of the blank standard. This was the same equation that was used to convert PAR to TSS for the sampling days, where I_0 was the measured column blank for each sampling profile.

Results

Initial changes in the column's transparency were readily visible. We noted that several larger particles sank to bottom of the column before we could complete our first profile (i.e. < 5 minutes). There was also a strong top to bottom gradient in the first profile (Figure 40, profile on far-right hand side), however this gradient quickly diminished within the first 6 profiles (i.e. 30 minutes) until there was no distinction between the top and bottom of the settling column.
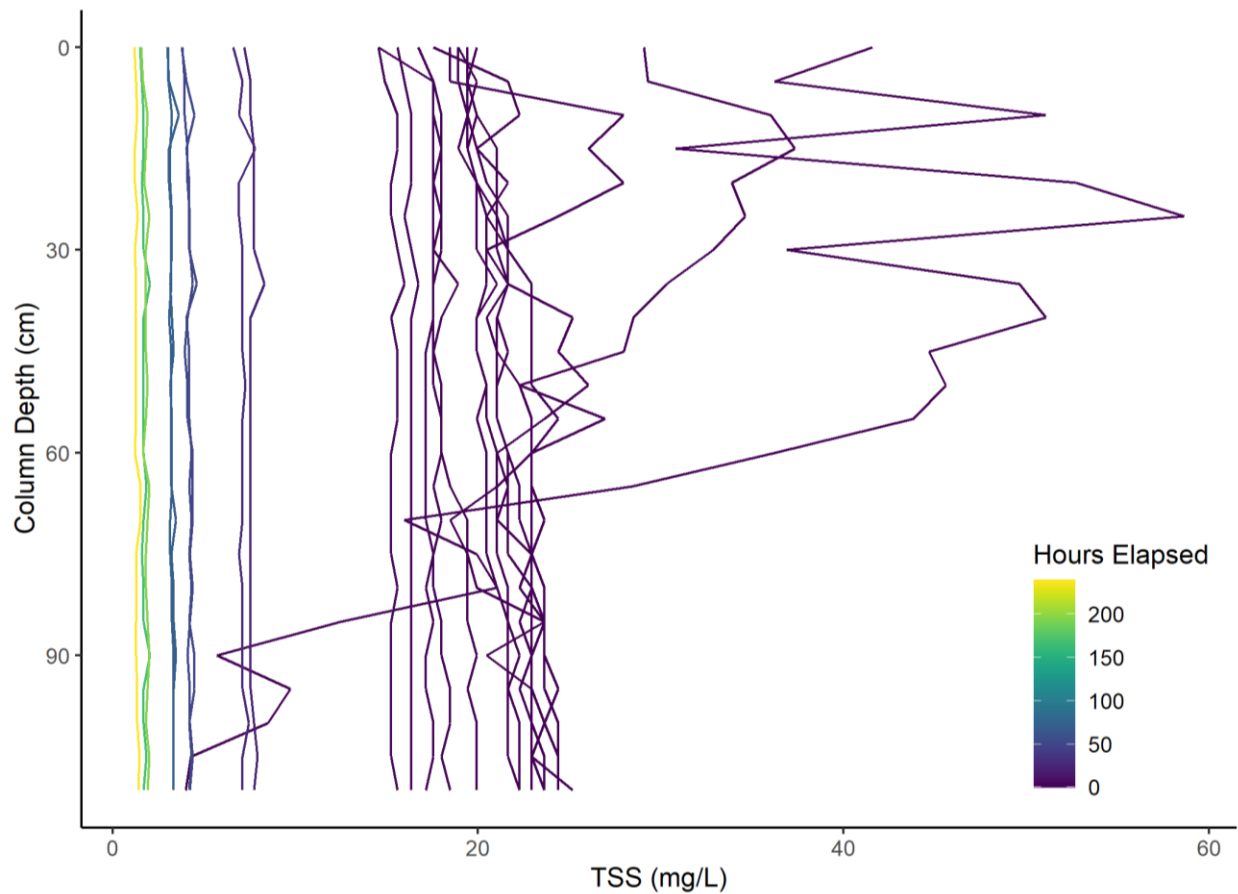
Figure 40: TSS Profiles from Laboratory Settling Rate Experiment.

While there was some distinction between the top and the bottom of the column initially, the column quickly became mixed with virtually no difference between top and bottom of the column by the 6th profile. 15 of the 25 profiles occurred within the first 24 hours and thus are difficult to distinguish, but generally increased time led to decreased TSS and thus the profiles are organized from right to left with the initial column profiles falling on the right side of the figure.

After 30 minutes there was no visual distinction between the top and bottom of the
column so we shifted our analysis from one of column concentration by depth and time, to
changes in the column concentration over time alone. Additionally, by day 10, changes in the
total depth-averaged concentration appeared to cease, or became too small to detect with our
transmissometer and the experiment was ended.
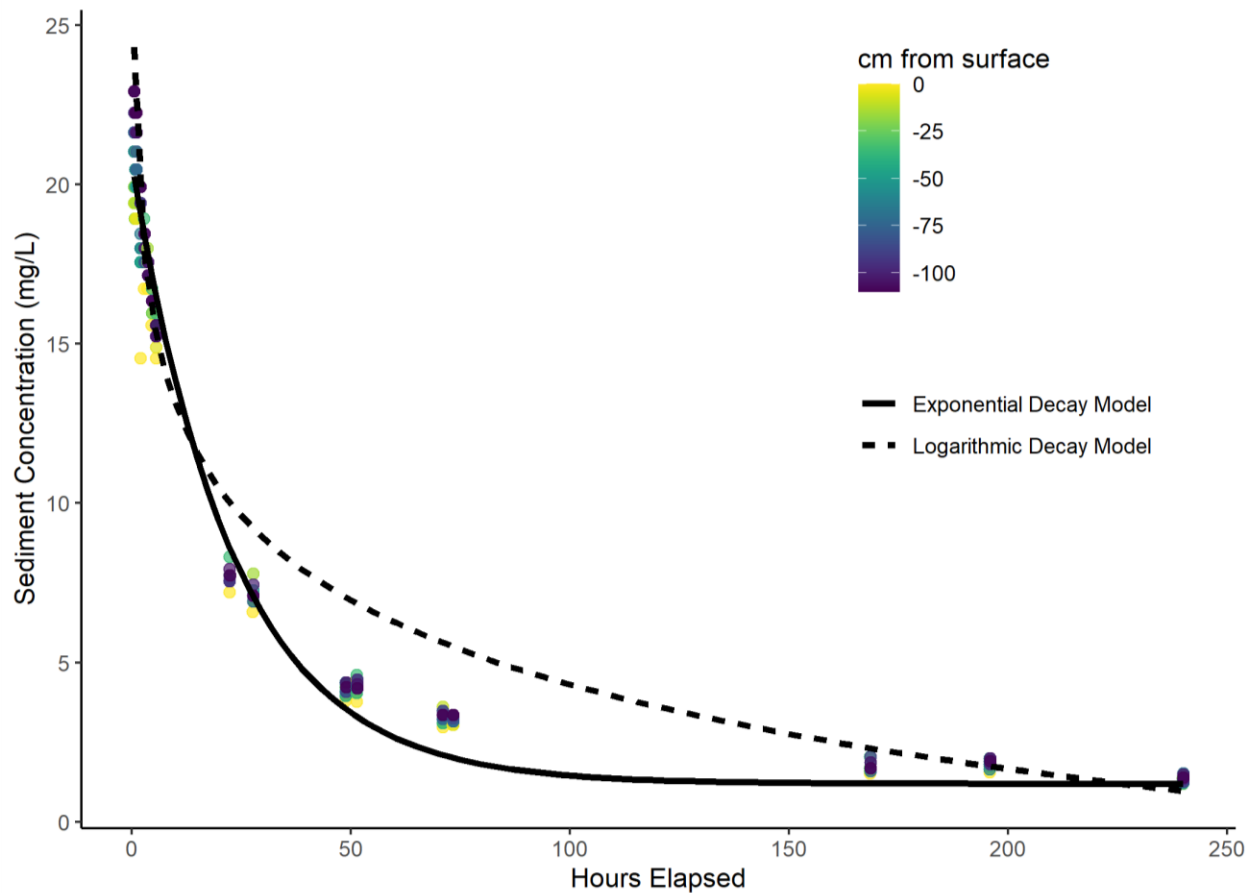
Figure 41: Exponential and Logarithmic Decay Models of TSS Loss Rates.

Note that data points, small circles, overlap considerably, showing that depth in the column was no longer an
important factor after the first 30 minutes of the experiment. The logarithmic model, dashed line, fit the data
initially, but over predicted values after the first 12 hours. The exponential decay model, solid line, generally under
predicted values, but had an overall better fit to the data and produced a decay constant of -0.043 hr^{-1}.

After filtering the data to remove the first 30 minutes of the experiment, where depth gradients were still apparent, I fit the concentration vs time data with both exponential and logarithmic decay models using R's nls package (R Core Team, 2020). Both equations were adjusted to meet the final depth-averaged concentration of the settling column at the end of the experiment. The logarithmic model fit the data better toward the beginning of the experiment, but then over predicted concentrations after the first 12 hours (Figure 41). Conversely, the exponential model generally under-predicted concentration, but gave an overall better fit to the data than the logarithmic model. The exponential model yielded a gross TSS loss rate of -4.3% per hour. This loss rate can be multiplied by the column height, i.e. 105 cm, to come up with an effective settling rate of -4.46 cm hr^{-1} (~1.1 m d^{-1}), which is similar to literature *in situ* measurements of settling velocities for particles 1 – 64 microns (Burns & Rosa, 1980). Moreover, this experimental estimate is very similar to the estimate derived analytically in this study using Stokes Law for settling of a particle with a diameter of 7 μm, the mean particle size derived from image analysis, and a density between 1.4-1.5 g/cm^3 at room temperature conditions (as was used in this experiment).

Convective mixing of small particles within the column likely explains the vertically homogeneous concentrations observed in the latter part of the experiment. This mixing likely came from two sources, 1) small changes in the room temperature that warmed the edges of the column faster than the column center, and 2) evaporative losses from the surface of the column causing cooling, sinking, and the development of thermal cells. While a repeat of this experiment could make an attempt to correct for these issues, the observation that small, fine-

grained particles appear to disappear at the same rate from all depths suggests that these

particles can remain suspended within the lake by even small mixing forces.

Discussion of Resuspension, Sorption, and Settling

If a large resuspension event occurs in the nearshore, thoroughly mixing the water

column from 0-10 meters, how long will it take for particles to settle? With the settling rates

calculated from Stoke's Law, we can estimate that most particles with a diameter of 50-100+

μm will settle within the first few hours. Slightly smaller less dense particles will settle within a

day. However, average sized particles observed in this study with a diameter near 7 microns

may take a week to over a month to settle. The smallest particles in the sample have the

potential to stay suspended for hundreds of days, but may be subject to other settling forces

such as flocculation.

These approximate calculations provide more evidence that small reactive particles

could provide an important transport mechanism for phosphorus in the Lake Michigan

nearshore zone. We have already seen that fine-grained particles have high sorption capacities

and are able to reach a P-Content ≥ 6 μg/L. Additionally, particles with low sinking rates are

more susceptible to hydrodynamic forces, and may have a greater likelihood of being

transported from the nearshore to the offshore than particles that quickly fall out of

suspension. Thus, high P-content combined with a low settling rate leaves the potential for

transport of P from the nearshore to the low P pelagic zone.

But where do currents near Atwater 20m generally go? While this question is best

answered from a calibrated hydrodynamic model, we can make some initial guesses based off

ADCP data. Looking at the current speed data from the Atwater20m buoy (GLOS buoy 45013);

132

we can grossly estimate mass transport by creating a progressive vector from the velocity north

and velocity east components of the data. Figure 42 shows a brief analysis of the ADCP data at

both the surface (i.e. 2m) and bottom (i.e. 20m) depths.
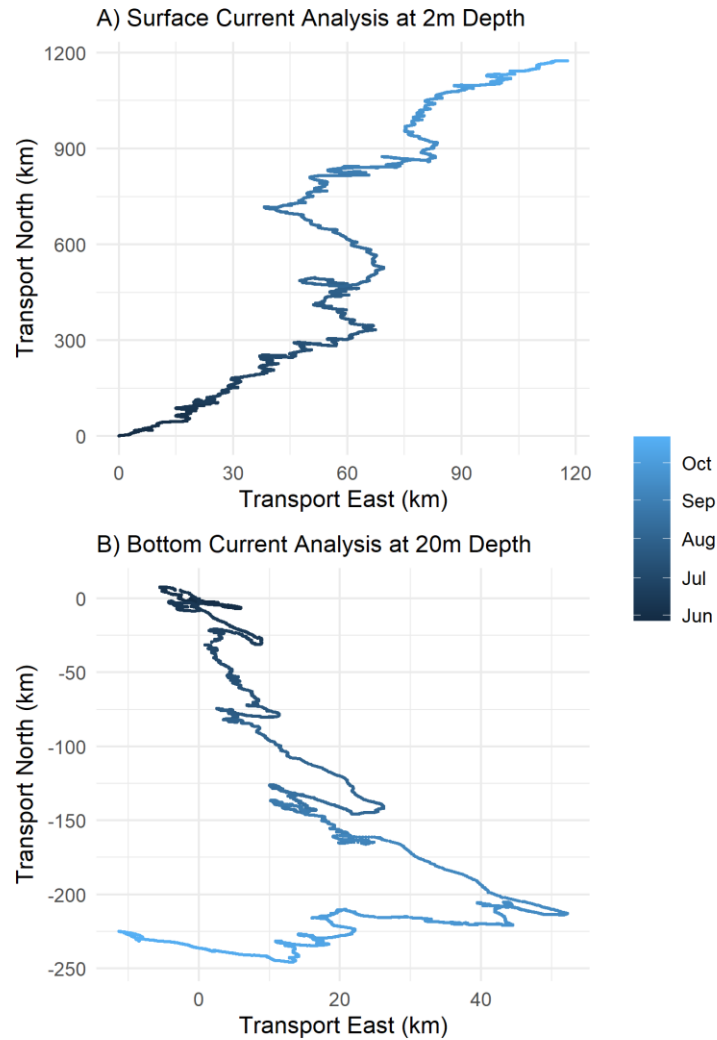
Figure 42: Progressive Vectors of Potential Particle Transport.

A) Primary currents at the surface. B) Primary currents at bottom. Note that scales are not equal distance, but have been stretched in the E-W direction to help visualize some of the E-W current velocity patterns. For both surface and bottom currents, most transport is in the N-S direction, though surface currents primarily travel N and bottom currents primarily travel S. E-W transport is roughly 1/10 of transport for surface currents, but closer to 1/4 of transport for bottom currents. Both surface and bottom currents show nearshore-offshore currents heading primarily E, though this trend is reversed for the bottom currents in October as transport moves primarily W.

Values to create Figure 42 were calculated from ADCP current data by taking the cumulative sum of each velocity component after multiplying current velocity by the sampling interval to acquire distance measurements. Distances are shown in Km to ease of interpretation, however estimates are likely overestimates since they are derived from water velocity only and do not include particle drag and other transport corrections. However, this analysis is still useful for determining the general direction of transport from the Atwater20m buoy and relative magnitude between longshore vs offshore transport. During the 2020 season, it seems that most of the surface currents moved in the NE direction, though movement north was an order of magnitude greater than movement eastward (see the x and y axis scales of Figure 42 A). Conversely, currents on the bottom primarily moved S, with some horizontal currents traveling E at the beginning of the season, but shifting to a primarily W trajectory in October (Figure 42 B). In this case, however, relative transport in the N-S direction was only ~4.16 x greater than it was in the E-W direction. So both surface and bottom currents show the possibility for nearshore-offshore transport. Such currents, and thus transport mechanisms, are much weaker than dominant longshore currents.

The next question that arises is what evidence do we have that P-rich fine-grained particles exist in the nearshore water column? The data in hand do not provide a direct answer to this question. Perhaps this question could be estimated with a more thorough analysis of the organic/inorganic composition of particulates from different particulate sources such as river seston, resuspended lake bottom sediments, and water column seston. This comparison of percent organic vs inorganic could readily be obtained by filtering particulate material onto a pre-weighed filter, drying, reweighing, ashing the filter (to remove the organic fraction), and

then reweighing the filter again to estimate the weight of the inorganic proportion. From this, a Bayesian mixing model could be employed to help estimate how much of the suspended material in a nearshore water column sample is from each of the particulate sources. However, in lieu of this, there are several *in situ* measurements of P-Content that show P-Content in the nearshore waters of Milwaukee to be very similar to the P-Content of the resuspended fine-grained sediments.

A survey of the nearshore zone conducted on 10/8/2021 took TSS and PP samples from Green Can Reef to Whitefish bay in what appeared to be "baseline" conditions. TSS had a mean of 0.54 ± 0.14 mg/L. PP had a mean of 1.25 ±0.47 µg/L. This makes for a mean P-Content 2.28 ±0.44 µg/mg, a value very similar to the initial P-Content of the fine-grained sediments used in the sorption experiment (Figure 33). Additionally, Chl a was low during this survey at with a mean < 0.4 µg/L.

This same survey, from Green Can Reef to Whitefish Bay, had also been conducted on 8/20/20, however this survey was in the wake of a large wind event which induced nearshore resuspension and instigated a large E-W seiche on 8/11/20. This initial resuspension event was followed by a smaller wind event and subsequent E-W seiche on 8/18/20 which may have maintained higher TSS concentrations in the water column. Although mean TSS concentrations were only slightly higher than in the October survey at 0.93 ± 0.55 mg/L, the PP concentration was much higher with a mean of 5.13 ± 4.41 µg/L. This yielded P-Content with a mean of 5.28 ± 3.23 µg/mg, similar to the P-Content values seen at the end of the fine-grained sediment sorption experiments (Figure 33).

While these observations may be coincidence, they may also provide preliminary evidence of fine-grained particle resuspension and SRP sorption within Lake Michigan's nearshore zone that could be important for nearshore-offshore transport. However, based on the analytically derived sinking rate and observations from the settling column experiment, it seems that at a certain particle size/density combinations, it may not be particle sinking that dictates effective settling rates. Instead, the vertical mixing rate may become the dominant force in the z (i.e. depth) direction. Using the disequilibrium between reactive/conservative daughter/parent radionuclide pairs Waples et al., (2017) estimated nuclide-derived POC and PP fluxes at ~15 and ~30 times greater than those measured in offshore sediment traps (Eadie et al., 1984), suggesting that particle delivery to the nearshore benthos is dominated by vertical convective mixing and bottom scavenging rather than passive settling. This may be important to mussels/fine-grained sediment interactions because vertical mixing may act as a conveyor belt, delivering the resuspended fine-grained particles back to mussel beds where they can be recaptured by mussel filtration. But this leads to more questions:

1) Do mussels filter resuspended sediments or reject/ignore them?

2) If sediments are filtered, are filtration rates similar to rates associated with phytoplankton filtration or do mussels modify filtration based on the "food" type?

3) Beyond initial filtering, which would increase effective settling rates, are fine-grained and bulk resuspended sediments actually digested/processed by mussels?

4) If digested, is sorbed SRP on the particle surfaces re-released into the water column?

Mussel Grazing Experiments

The primary goal of the mussel grazing and filtration experiments was to separate the relative effects of particulate settling and mussel filtration on removal of particles from the water. Since the lake bottom sediments are a heterogeneous mixture of particle sizes, bulk settling rates are difficult to estimate analytically with Stoke's law. Additionally, assumptions related to Stoke's Law may be violated in the lake environment and there is uncertainty related the particle densities. Thus, I took an experimental approach and measured bulk settling in control (i.e. mussel free) tanks and bulk settling + mussel filtration in treatment (i.e. mussel occupied) tanks. Comparison of the difference between control and treatment tanks allowed me to derive an estimate of mussel clearance rates for resuspended sediment.

Methods

Mussels from the Atwater 20m site were collected and cleaned as described in the general methods. Of the cleaned mussels, I selected 96 healthy, defect-free mussels with lengths between 15 and 25 mm for use in the grazing experiments. All 96 mussels were placed in a clean 8 L aquarium filled with 7 L of 4°C filtered lake water. A control aquarium with no mussels was also filled to the 7 L mark. Both tanks were carefully placed inside a fridge and aerated evenly throughout the duration of the experiments with an EcoPlus8 air pump. Sondes were placed inside each aquarium and programed to record data every 30 seconds with an instrument wipe before each sample. Variables recorded included turbidity, temperature, conductivity, dissolved oxygen, and Chl a. Mussels were given ~1-2 hours to acclimate to the tank/aerator and initiate normal grazing behavior before the experiment was started.

At the start of the experiment, the 4 L container of Atwater 20m bottom sediment sludge (preparation described in the general methods) was homogenized by rapid shaking. I then pipetted 25 mL of the sediment slurry into each tank (i.e control and treatment). Once the tanks appeared to be well mixed, usually after a few minutes, I took initial samples from each tank and filtered them for SRP and PP analysis. Aquaria were left in the fridge overnight for mussels to filter undisturbed for 17.5 – 21.5 hours.

The next morning, a final sample was taken from near the top of the water column of each tank and filtered for SRP and PP analysis. Then mussels were carefully removed from the treatment tank before mixing both tanks with a gloved hand and taking a final "well mixed" sample.

Data was downloaded from each Sonde and processed with a custom written R script that merged the two data sources and adjusted the turbidity measurements of the treatment Sonde by subtracting the change in turbidity of the control Sonde. This data was further standardized to have a minimum turbidity of 0.01 FNU for each experiment to avoid log(0) errors and bias associated with decay constants that do not converge to zero. Finally, the turbidity data was fitted to an exponential decay model using R package nls so decay constants and clearance rates could be estimated for each experiment.

To determine changes in the concentration of PP over time, turbidity was used as a proxy for PP. Prior to the grazing experiment, I created a calibration curve to convert the Sonde's turbidity readings (FNU) to PP. I accomplished this by adding spikes of Atwater 20m sediment to 2 L of distilled water, homogenizing the container with shaking, and inserting the

Sonde to record the average turbidity of the container over the course of a minute. After the turbidity measurements were completed, the container was homogenized with shaking again before being filtered for PP analysis. This process was repeated for a total of 10 standards. The calibration curve was designed to include all expected turbidity values throughout the duration of the experiment from 0 – 40 FNU.

Results

The data obtained for the calibration curve fit a linear model well (R^2 = 0.9877) and yielded the equation $PP = 1.3 \times FNU + 0.6$, which was used to convert turbidity data from each experiment into measurements of PP. Converted FNU → PP data taken by the Sondes during the experiment were compared to the measured data derived from standard chemical extraction and showed good agreement (Figure 43 A).

At the end of each experiment I noted a visible difference between the control and treatment tanks, with water in the tanks containing mussels appearing much clearer than the tank without mussels. This difference was also apparent in both the derived PP from turbidity and chemical data (Figure 43 B). On general, both tanks started with a mean PP concentration near 24 ug/L. Even after ~17 hours, small particulates in the control tank had not fully settled leaving the final PP of the controls near 6.5 µg/L whereas the final PP in the treatment tank was < 0.5 µg/L.

Figure 43: Comparison of Sonde and Chemically Derived Estimates of PP.

A) A linear regression between PP measurements of the Sonde vs PP measurements from directly measured PP via typical chemical extraction. Shapes show final vs initial values, and colors show experiment ID A-D. B) Simplified bar plots showing the mean ± SD PP for all four experiments with chemically vs Sonde derived measurements.
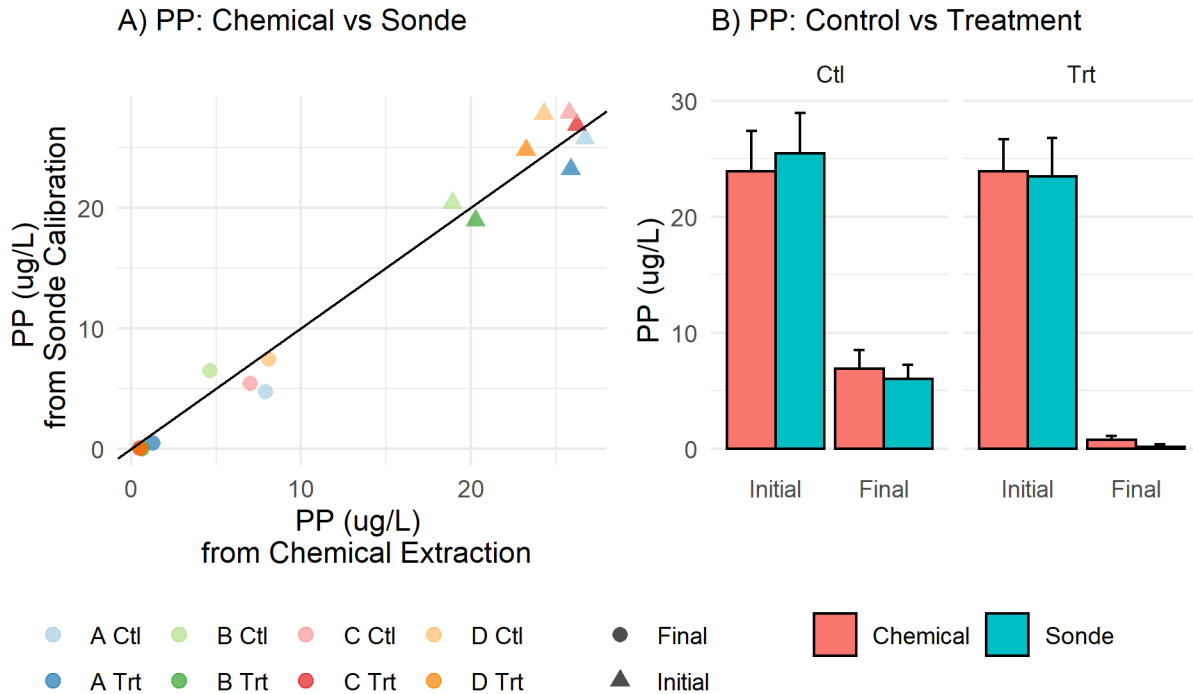
However, it is possible and common to estimate clearance rates from PP or Chl *a* data alone.

This is frequently done (Ackerman, 1999; Berg, Fisher, & Landrum, 1996; Diggins, 2001; Horgan & Mills, 1997; Naddafi & Rudstam, 2013; Tang, et al., 2014; Vanderploeg et al., 2001; Vanderploeg et al., 2010) with the following equation:

$$CR = [(lnC_0 - lnC_t) - (lnC'_0 - lnC'_t)] \times \frac{V}{t}/n \qquad (8)$$

where

C_0 = the initial concentration of the treatment tank (μg/L)

C_t = the conentration of the treatment tank at time t (μg/L)

C'_0 = the initial concentration of the control tank (µg/L)

C'_t = the concentration of the control tank at time t (µg/L)

V = volume of water in the tanks (liters)

T = time (hours)

n = number of mussels in the treatment tank

CR = the mussel specific clearance rate (L/mussel/hr)

The above equation uses two time points, the start and end of the experiment, and fits an exponential decay model between these two points. In other words, the equation transforms the data by taking the natural log, and draws a straight line between those two points. The slope of that line is the decay constant.

The CR is simply a standardized decay constant that accounts for the specific experimental set up (i.e. volume of the container, length of the experiment, and number of mussels used in the experiment, and natural settling in the control tank). The implicit assumptions of the CR model are that 1) The reduction of concentration over time is due only to gravitational settling (hence the control tank) and mussel filtering when mussels are present. 2) The pumping rate of the mussel is constant. 3) The suspended material remains homogenous throughout the experiment (hence the aeration). 4) The data measured with chemical extraction are both accurate (i.e. true) and precise (i.e. replicable). 5) That the function is asymptotically approaching zero. These last two assumptions are important because small errors can make a big difference in calculated CR. With only two points, a small error, especially if the error occurs to a number close to zero, can have a large effect on the calculation. For

example, the calculation of log(0.5) - log(0.1) is the same as log(5) - log(1) (i.e. ~1.6), thus

chemical uncertainty as small as < 1 µg/L could have a large impact on the CR derivation when

experiments are allowed to a point that PP in the tank's water column is low. Additionally, if the

the function is not approaching zero, but some other positive steady state value, estimates of

the decay constant will be biased low.

With these assumptions in mind, I used the chemically extracted PP data to estimate a

mean CR of 8.86 ± 1.53 mL per mussel per hour. However, these values were roughly 1/5 of

what I expected based on published estimates (Ackerman, 1999; Berg, Fisher, & Landrum, 1996;

Diggins, 2001; Horgan & Mills, 1997; Naddafi & Rudstam, 2013; Tang, et al., 2014; Vanderploeg

et al., 2001; Vanderploeg et al., 2010). I concluded that these erroneous estimates were likely

due to the small errors associated with final PP concentrations < 1 µg/L and non-zero steady

state PP concentrations. Therefore, I decided to use the full sonde time-series data to derive

CR more robustly from turbidity (Figure 44).

Figure 44: Derivation of Mussel CR from Turbidity Data.

A) The raw turbidity data merged from both Sondes, i.e. Ctl and Trt, shows that particles were cleared by mussels at a faster rate than from settling alone. B) Processed turbidity data is normalized by subtracting the change in the Ctl tank (i.e. natural settling) from the Trt tank (i.e. mussel filtration). The processed turbidity data is further standardized to converge to a steady state near 0 to meet the assumptions of an exponential decay model.
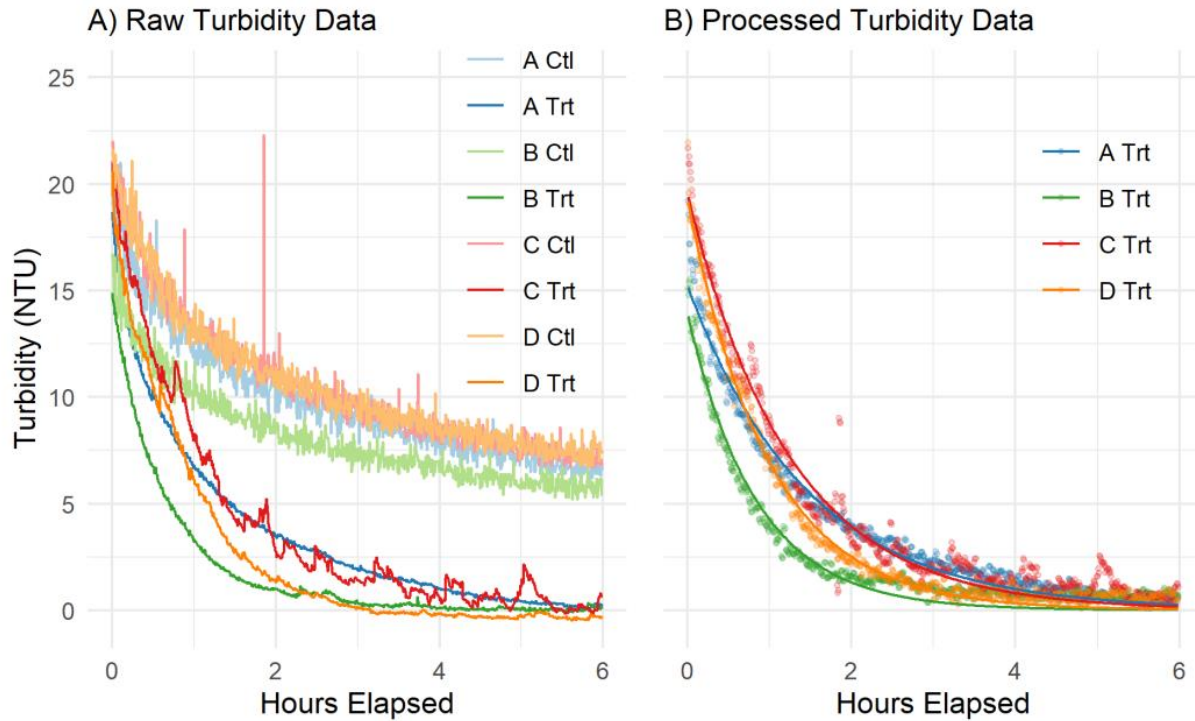
Clearance rates (CR) were calculated from the time series data by using the equation:

$$CR = \frac{-\alpha \times V}{n}$$ (9)

where

α = the decay constant calculated from adjusted turbidity data using an exponential decay model (hrs^{-1}).

V = the volume of water in the aquarium (L),

n = the number of mussels in the treatment tank.

This gave a mean CR of 67 ± 1.6 mL per mussel hr^{-1} or ~1.6 liters per mussel per day. For comparison, a previous experiment that used similar methods, but fed the mussels a phytoplankton culture at various temperatures produced a linear model that would have predicted a CR of 40 mL per mussel hr^{-1} at a temperature near 4°C. Thus, mussels appear to filter resuspended lake sediments just as quickly, if not faster than they would filter a more favorable food source such as cultured phytoplankton.

Mussel Excretion and Egestion Experiments

The primary goal of the excretion and egestion experiments was to determine whether different food sources that mussels can be expected to be exposed to in the Lake Michigan nearshore zone might result in different phosphorus excretion and egestion rates. The food sources used in these experiments can be broadly categorized as 1) none/control (e.g. particle free lake water), 2) biological (e.g. phytoplankton), 3) other (e.g. lake sediments and river seston). Additionally, I hoped that by investigating the P-content of the egested mussel waste, I would be able to estimate the proportion of nutrients mussels converted from PP → SRP from each food source during the digestion process.

This logic assumes that the reduction of P in the P-Content of the egested material is primarily due to PP digested by the mussel that will eventually either be egested as SRP through the anus with feces, or taken further for intracellular digestion, metabolized, and excreted as SRP. This assumption is most valid under 2 conditions.

1) Assimilation of PP into stored biomass is a small fraction of PP ingested or that the mobilization of stored biomass for metabolism and/or storage of PP in biomass are balanced (i.e. the mussel is not growing or shrinking)

2) The contribution of pseudofeces to the final filtered PP is small compared to the contribution of egested material out the anus.

Methods

Due to space and time constraints, these experiments were run in batches of 6 at a time with 3 treatment and 3 control replicates. Prior to the experiment, 30 healthy, defect-free mussels were selected from the cleaned mussels as described in the general methods section. All mussels for these experiments came from the 8/3/2021 collection date at the Atwater 20m site. The selected mussels were left overnight in an aerated chamber of filtered lake water to allow them time to evacuate their gut contents prior to each experiment.

From the group of 30 mussels, I placed 5 mussels into each of the 6 acid washed containers filled with 3.5 L of filtered lake water. Mussels were given approximately 1.5 hours to acclimate and begin normal filtration patterns prior to starting the experiment. Each container was gently aerated to facilitate homogeneity throughout the feeding portion of the experiment.

Once all the mussels appeared to be actively filtering, I spiked each container with one of the following "food" sources.

1) Filtered Lake Water (None/Control)

2) Homogenous Atwater 20m Bottom Sediments (Other)

145

3) Algae Culture (Biological)

4) Milwaukee River Water (Other)

5) Fine-grained Atwater 20m Bottom Sediments (after they had been allowed to become P-saturated) (Other)

I let the feeding chambers mix for ~ 1 minute before taking 50 mL subsamples which were immediately filtered onto pre-weighed membrane filters for TSS, PP, and P-content analysis. I also collected the filtrate to monitor the SRP in the feeding chamber. These samples were analyzed with the methods described in the general methods section.

The amount of food spike added to each container was based of initial TSS targets similar to what was used in the settling rate and sorption experiments. For the bulk lake sediments this was a target between 25 – 35 mg/L. For the fine-grained particles, the target was 1.5 mg/L. The algae culture was also added with a target TSS of 1.5 mg/L to see how fine-grained sediment and pure phytoplankton digestion compared at the similar TSS levels. The Milwaukee River water was added with a target between 2 – 7 mg/L, which represented the range of values that we had sampled during Milwaukee River plume events within the Milwaukee Harbor and Nearshore zones. Theoretically, the controls (i.e. filtered lake water) should have had an initial TSS of 0 mg/L. However, this was not the case (see Figure 45) and controls had a TSS of 0.15 and 0.025 mg/L (SRP spiked and unspiked respectively).
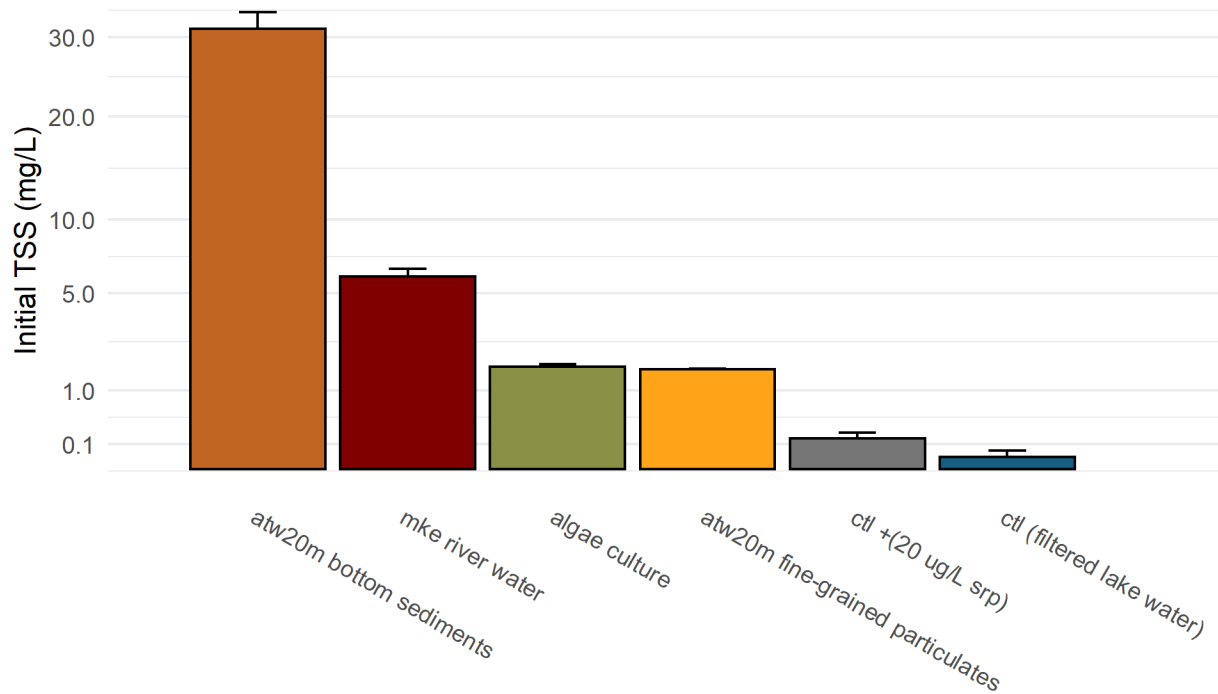
Figure 45: Initial TSS of Mussel Feeding Experiments.

Note the square root transformation on the Y axis. From left to right, TSS was near 31 mg/L for the bulk bottom sediments meant to represent a recent resuspension event. Milwaukee River water TSS was 6 mg/L, similar to values seen in the nearshore during a river plume event. Algae culture and fine-grained sediments were near 1.7 and 1.6 mg/L respectively, close to levels seen during baseline surveys. Controls had TSS values 0.15 and 0.025 mg/L.

Mussels were left in these large feeding chambers to filter the particulates for 3-4 hours. Assuming constant filtration and a short gut residence time, as evidenced by production of feces shortly after initial feeding (Lei et al., 1996), this should have been enough time for the mussel gut to be saturated with the feeding material. When the feeding time was complete, mussels were transferred to smaller acid washed excretion/egestion chambers of filtered lake water with a known SRP concentration (usually between 0.3 – 0.7 µg/L). Mussels were left in these chambers in the fridge at 4°C for 1.33 – 2.5 hours to excrete and egest gut material.

After this incubation time, mussels were removed from their chambers. The small chambers were well mixed with a gloved finger to ensure egested material was not stuck to the bottom of the container and the entire volume of the chamber was filtered onto a membrane filter for TSS, PP, and P-Content analysis. The filtrate was collected for SRP analysis. Mussels used in the experiment were dissected, removing soft tissue, and freeze dried in pre-weighed weigh boats before reweighing to attain a dry mass for each replicate. This experiment was repeated on 6 different dates with various treatment options.

After investigating the excretion results from the first few batches of experiments, I became concerned that results were being influenced by the initial SRP in the feeding tanks. For example, the Milwaukee River, algae culture, and fine-grained sediment feeding groups showed higher excretion rates, but also were fed in chambers with a higher initial SRP concentration. When a filtering mussel is disturbed, it ceases filtration, and closes its shell. Therefore, a mussel likely retains a certain, albeit small, volume of water within itself when moved from the feeding chamber to an excretion and egestion chamber. Because of this, measurements of SRP in the small, low-SRP (i.e. < 100 mL and < 0.6 µg/L) excretion/egestion chambers could be influenced by the release of this stored internal volume into the container, causing over estimates of SRP excretion for groups that were fed in high-SRP tanks. To test this, I created a new treatment group of filtered lake water with an additional spike of PO_4^{3-} to bring the feeding tank's initial SRP concentration to ~20 µg/L. Since no particulates were added to this group, increases in SRP excretion within this group could be attributed to the addition of the PO_4^{3-}, and not release of SRP from digestion of particulates.

Results

It was easy to identify filters by their feeding source by coloration and feeding vs

egestion filters could be determined by the size and distribution of particles on the filter, with

larger more heterogeneously distributed particles on the egestion filters (Figure 46). This

observation suggests a more thorough particle size analysis of pre and post mussel filtration

particles may be informative. Quantifying whether or not mussels generally increase particle

size and density of filtered material may help verify this part of the nearshore phosphorus shunt

hypothesis which suggested that an increase in size of filtered particulates would result in

greater longshore and downgradient transport of enlarged particulates along with greater PP

burial in sediments and loss of PP at the lake outflow. Combined, these processes would act to

reduce the amount of P returned to the pelagic water column, driving a divide between

nearshore and offshore and decoupling external loading rates from mean yearly pelagic water

column concentrations (Hecky et al., 2004).

Figure 46: Image of Mussel Feeding and Egestion PP Filters.

Filters taken from the feeding tanks (far left), filters taken from the egestion/excretion chambers (middle), and filters from the egestion/excretion chambers of the paired control group (right). Filters post egestion appear darker with more heterogeneous distribution of particles compared to the feeding filters. Small particles are also visible on the control egestion filters, which was unexpected.
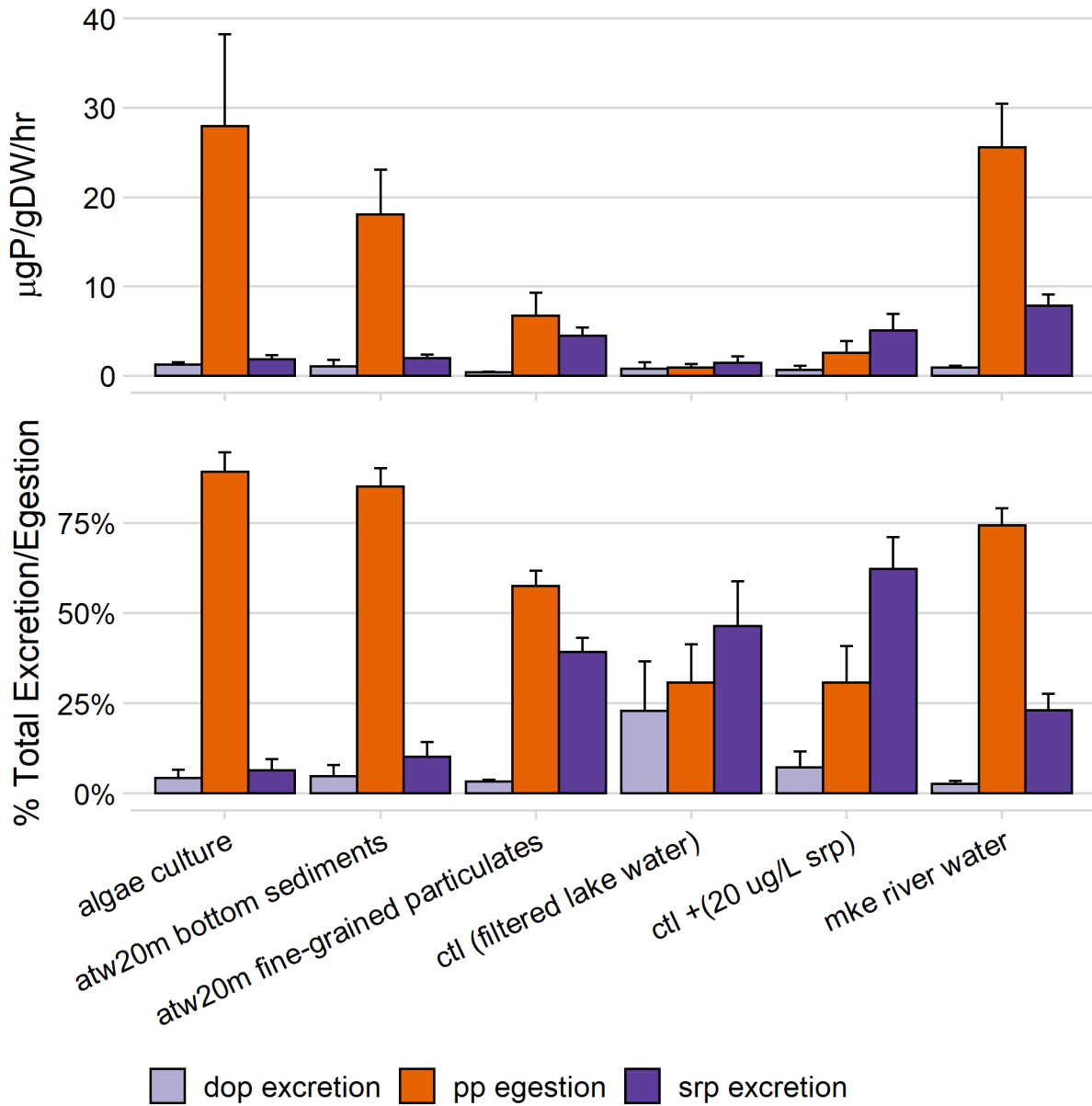
Figure 47: Excretion and Egestion by Food Source.

A high proportion of the food source was egested as PP from the algae culture, bulk bottom sediments, fine-grained particulates, and mke river water. Interestingly, the fine-grained particles and algae culture seemed to have been processed differently despite having similar initial TSS concentrations with the fine-grained sediments producing much more SRP excretion than the algae culture.

I compared SRP and DOP excretion as well as PP egestion between treatment groups. Comparisons were made based on rates normalized to mussel soft tissue dry mass (i.e. µgP/gDW/hr) as well as the percentage each fraction contributed to the sum of total excretion and egestion, which for simplicity I will refer to as "waste" (Figure 47). Rates and fractionation varied greatly between the 6 treatment groups. Mean SRP excretion ranged from ~1.8 – 7.8 µgP/gDW/hr, whereas mean PP egestion rates ranged from 0.9 – 28 µgP/gDW/hr. DOP was the smallest waste contributor in each treatment group. Particulate waste was the largest contribution in the algae culture, homogenous bottom sediments, MKE river, and fine-grained sediment groups whereas SRP excretion was the primary waste in both control groups. The high proportion of PP egestion is somewhat novel, though it should not be surprising. A previous study estimated PP egestion to be ~40% of mussel waste generation (Mosley & Bootsma, 2015). This estimate is slightly higher than the value I measured in both controls (i.e. ~30%) but lower than each other treatment group. The ~40% estimate came from measurements made immediately after removing mussels from their pelagic lake bottom habitat which had low ambient PP and SRP concentrations (i.e. near 1.5 and 0.5 µg/L respectively).

If we imagine a model of the mussel gut as a 1-D advection dispersion column with transport, retardation, and transformation of PP → SRP during the digestion process, this result is not particularly surprising. Increasing initial SRP, TSS, and PP (i.e. the inputs) at the inflow of the column (i.e. the mussel's incurrent siphon) would naturally, given enough time to move through the column, have an effect on the outflow (i.e. mussel excretion and egestion at the excurrent siphon). This is, in fact, what was seen as SRP excretion, PP egestion, and TSS production were primarily determined by the initial SRP, PP and TSS concentrations of the

152

feeding chambers (Figure 48). While few studies have measured such high egestion rates, this may be because few studies have conducted experiments on quagga mussels with the high levels of initial TSS and PP used in this study. Part of this may be due to sampling bias since *in situ* surveys of mussel excretion and egestion are likely to occur during relatively calm conditions.
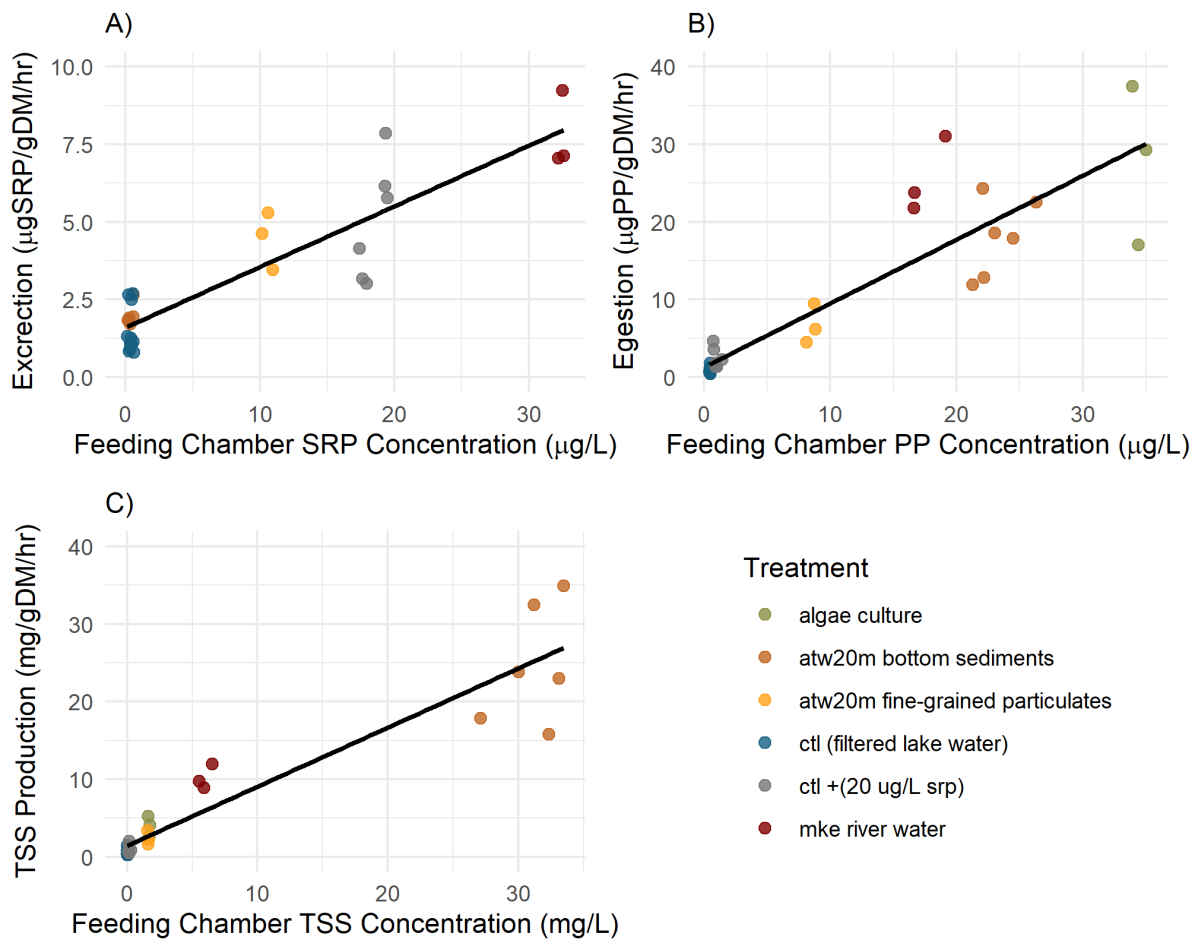
Figure 48: Egestion and Excretion Rates as Determined by Feeding Chamber Conditions.

Linear models showing effect of initial concentration in the feeding chamber on the perceived waste production rates. A) = SRP, B) = PP, C) = TSS. Unsurprisingly, the primary determinant for what comes "out" of the mussel is what originally went "into" the mussel. *In situ* measurements have not previously captured such high TSS or PP egestion rates. But *in situ* experiments are also generally limited to calmer weather that does not include major river plume or resuspension events.

A simple and direct method that may circumvent some of the complications typically associated with measuring processes related to mussel filtration and digestion is to investigate the change in P-content between fed and egested material. This change in P-Content can be used to estimate the proportion of PP that was or will eventually be converted to SRP, which is a desirable modeling parameter sometimes referred to as *f*. This method is not a perfect solution for determining food source effects when initial concentrations of PP vary as a mussel may still pass more material more quickly in a high PP concentration environment while holding material longer for a fuller digestion when in a low PP environment. However, it could provide another useful tool for measuring and quantifying activities related to the mussel digestion process. An analysis of this type follows below.

There were large differences in initial P-Content between the different food sources with the initial P-Content of the algae culture highest near 22 µg/L and the Atwater 20m bottom sediments lowest < 1 µg/L (A). Despite these large initial differences, 29 out of 33 replicates showed a decline in P-content of biodeposits compared to food source (Figure 49 B). The 4 replicates that did not conform to this pattern all came from the Atwater 20m bottom sediments group.

Interestingly, measureable and repeatable differences also occurred in both control groups, which was not expected. We expected that the controls would have both TSS and PP near zero. However this was not the case, and moreover, the controls seemed to produce a predictable reduction in P-Content similar to what was seen in the other food source categories.

This observation may represent the P-content of bacteria that passed through the 0.7 µm pore size glass fiber filter but was captured on the 0.6 µm pore size membrane filter. Previous studies have shown that although often considered "sterile" technique, microfiltration can allow passage and even shape selection of slender spirillum-shaped strains of bacteria. Once in the filtrate and free of other competitors these bacteria can experience greater than average growth rates (Wang, et al., 2007). If this reduction in P-Content does represent mussel filtration of micro-filterable bacteria it shows that mussels were able to capture and strip P from these bacteria. Another possibility is that Lake Michigan water contains small micro-filterable particles between the 0.6 and 0.7 µm range. A study from the late 1980s showed that small micro filterable (i.e. 0.45-0.7 µm) mineral crystals made up a substantial fraction of suspended particles in Lake St. Clair (Hawley & Zyren, 1990). Perhaps similarly fine mineral crystals made it through the initial 0.7 µm filtration of Lake Michigan water to be captured and chemically altered by mussel filtration. Alternatively, it may show that dust or other particle contamination entered the filtered lake water either during storage or experimentation in which case mussels were able to strip P from this unknown contaminant. Regardless of the contaminate source, the consistent and predictable reduction in P-Content suggests that mussels altered the composition of very fine-grained particles within the control groups.
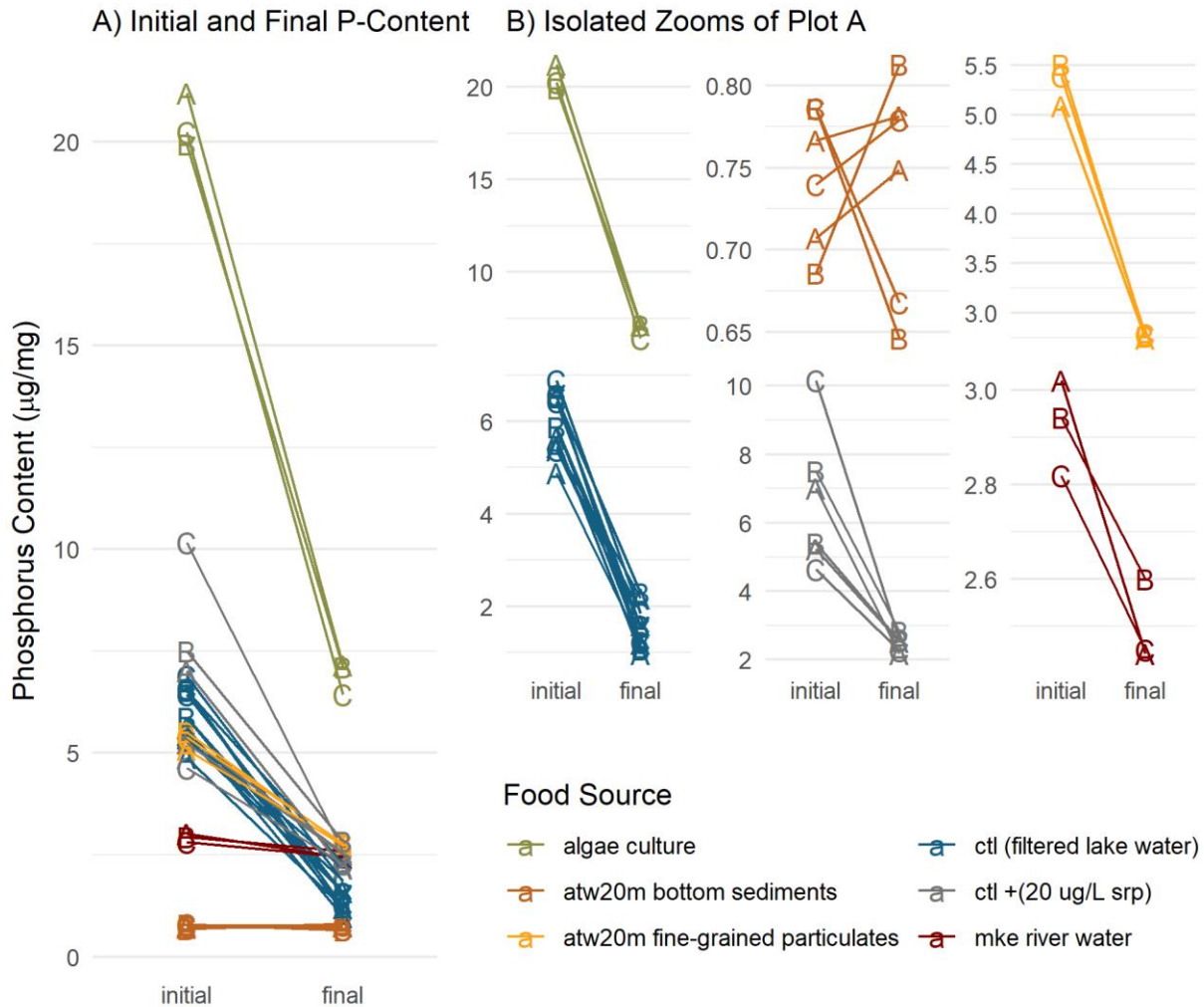
Figure 49: Initial and Final P-Content by Various Mussel Food Sources.

A) Full view of change in P-Content, initial on the left, final on the right, for all food sources. B) A zoomed in view of each food source to see P-Content change closer up.

P-Content decline monotonically in all but the Atwater 20m bottom sediments group. Interestingly, the final P-Content for most food sources fell in the range of 1.5 – 3 µg/mg. Exceptions to this trend were the algae culture, which had a very high initial P-Content, and the bottom sediments, which had a very low initial P-content. A-C labels represent replicates. Thus groups that were run in more than one batch have multiple A, B, and C's, but each line represents a unique replicate.

In terms of percent change in P-content, I first analyzed the data by the broad food

categories defined at the beginning of this section (i.e. none, biological, other). The initial

expectation prior to seeing the data was that the change in the "none" category would be near zero. However, Figure 49 shows that this was not the case, again possibly due to either biologic or other particle contamination. Instead, I hoped this comparison would shed light on the contamination source. For example, if the contamination was biological, I would expect that its mean percent change would fall within the range of the biological group. It was also possible that there would be no differences between broad categories, which would indicate that mussels process each food source uniformly, regardless of food source "quality".

The biological and none (i.e. control) categories did not differ significantly (p = 0.765) with a mean percent change in P-content of -66.3 ± 1.92% and -69.2 ± 10.5% respectively
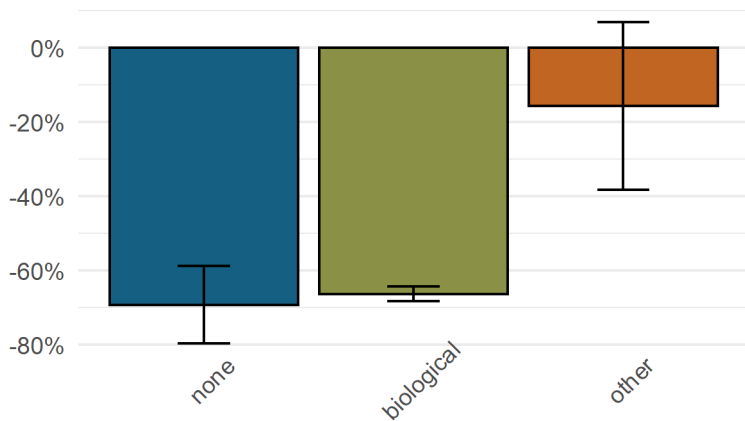
Figure 50: Comparison of Percent Change in P-Content by Broad Food Categories.

Change in particle P-Content of feeding and egested material showed that there were no significant differences (p = 0.765) detected between the "none" group (i.e. controls) and biological) group (i.e. algae culture). The other group, which consisted of river seston and lake sediments (bulk and fine-grained) had a significantly lower reduction in P-Content (p = 2.61e-5). This may suggest that the mystery contaminant was of biological origin, however further tests would be needed to confirm this.

(Figure 50). On the other hand the other category was significantly lower at -15.8 ± 22.6% (p = 2.61e-5). This initial analysis provided some evidence that the contamination in the "none" (i.e. control) group was biological. However, further testing would be required to confirm this. Moreover, the large variation in the "other"

category suggested that further partitioning of variance may reveal interesting effects.

To investigate this large variance in the "other" category, I reanalyzed the data, grouping this time at the "pp food source" level. The unspiked ctl group saw the largest change in percent P-content overall at -74% while the 20 µg/L spiked ctl was reduced by 60%. Atwater 20m bottom sediments were effectively unchanged by mussel filtration. The algae culture, which should represent an ideal food source, lost 66% of its P-content during mussel digestion. The fine-grained particulates and MKE river water saw reductions of 48% and 15% respectively (Figure 51).
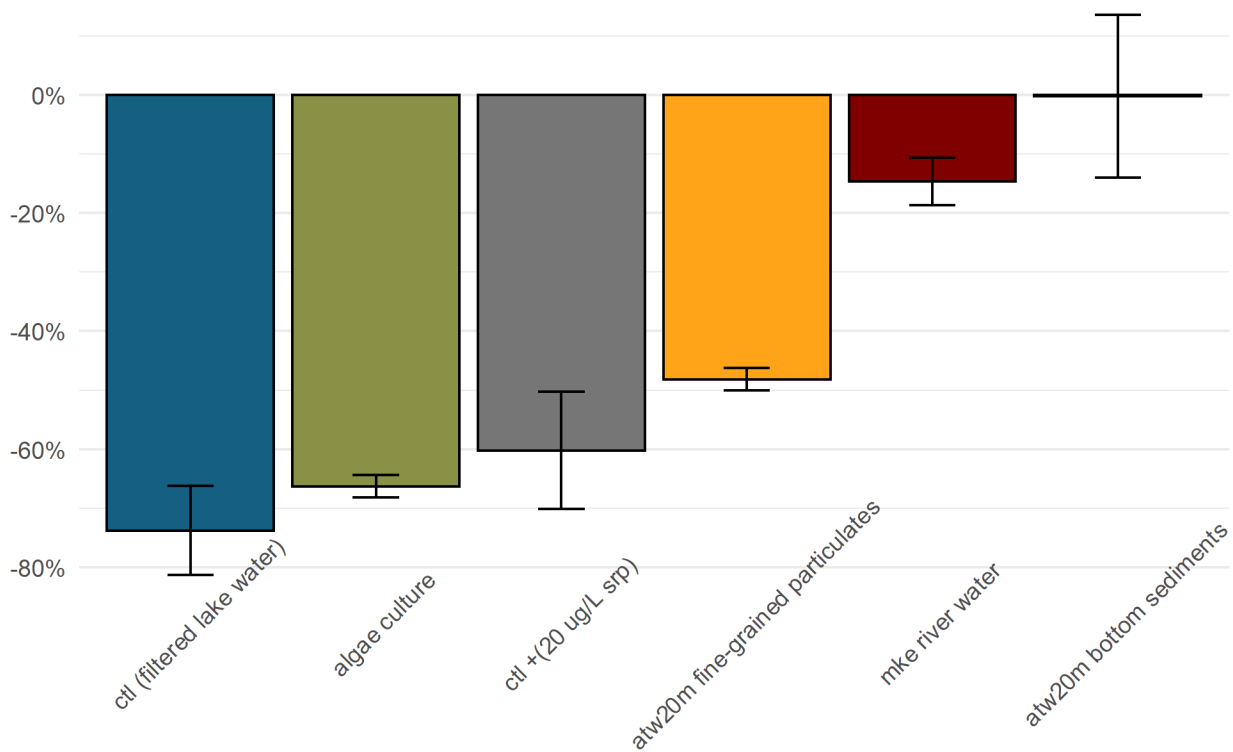
Figure 51: Percent Change in P-Content by All Food Sources.

Change in P-Content between the feeding and egested material. The unspiked ctl group saw the largest change in percent P-content at -74% while the 20 μg/L spiked ctl was reduced by 60%. Atwater 20m bottom sediments were effectively unchanged by mussel filtration. The algae culture, which should represent an ideal food source, lost 66% of its P-content during mussel digestion. The fine-grained particulates and MKE river water saw reductions of 48% and 15% respectively.

Discussion of Mussel Filtration and Feeding Experiments

Previous work has suggested zebra mussel filtration, ingestion, and assimilation decline dramatically when exposed to large quantities of inorganic sediments (Madon et al., 1998), with declines in particle clearance rates at inorganic sediment levels as low as 1 mg/L and copious production of pseudofeces at inorganic sediment levels of 100 mg/L. However, such a reduction in particle clearance rates was not witnessed for the quagga mussels in this study, which rapidly cleared the bulk lake bottom sediments with a mean CR of 67 ± 1.6 mL mussel^{-1} hr^{-1} even at initial TSS concentrations as high as 25 mg/L. Moreover, even if much of the filtered inorganic material is egested as pseudo-feces, the act of filtration still has important implications for the nearshore light regime since filtering increases the effective settling rate, clearing the water column more quickly. Additionally, other experiments on zebra mussels have shown that mussel particle clearance rates do not decline until TSS concentrations are greater than 27 mg/L (Lei et al., 1996), which is slightly higher than concentrations used in this study, but lower than the TSS concentrations associated with plume and resuspension events that were measured in this study.

Based on the work of Maden et al., (1998), Fillingham (2015) designed his mussel grazing model such when benthic shear stress was large enough to induce sediment resuspension, mussel grazing went to zero. This works suggests that such parameterization is

incorrect and that mussels can and do filter resuspended lake sediments. This is an important

finding since mussel filtration can clear the water column faster than the passive settling rate,

which was estimated here to be quite slow at ~4-5 cm d^{-1} for the average particle sizes near 7

µm. Additionally, filtration of fine-grained sediments with sorbed P on particle surfaces may

release SRP in the benthos where it can be assimilated by nearshore nuisance algae.

Moreover, filtration and retention of P-rich fine-grained sediments in the nearshore may

be a major contributor to the nearshore shunt hypothesis (R. E. Hecky et al., 2004). In lieu of

mussel filtration, P-rich fine-grained sediments could either be initially transported from

nearshore to pelagic during a river plume/mixing event, or after settling in the nearshore,

resuspended and transported to the pelagic at a later time. While particles likely travelled

predominately in the longshore direction, maintaining some residence in the nearshore, ADCP

currents show that cross-margin transport does occur and as such a proportion of small fine-

grained particles would likely move from nearshore to the pelagic.

Sediment trap studies in the 1980s, pre-dreissenid invasion, showed that the magnitude

of internal nutrient recycling due to resuspension of fine-grained NaOH-extractable P was as

large as yearly nutrient loading from all of the southern tributaries combined (Eadie et al.,

1984). Resuspension has been attributed to enhancing recycling within the microbial loop (Ji et

al., 2002) and nutrient rich sediments also played a critical role in maintaining a healthy

population of benthic pelagic detritivores (Evans et al., 1990). Shunting of P-rich river-borne

particles in the nearshore zone limits P export from the nearshore to the pelagic. While its

initial effects were likely masked at the beginning of the dreissenid invasion due to a large store

of legacy P in profundal sediments, this shunt mechanism may now partially attribute to the hyper-oligotrophic conditions experienced in the Lake Michigan's pelagic zone.

In addition, it appears that a large proportion of PP from fine-grained particulates, ~45%, is released quickly as SRP during digestion. Excluding the controls, this was the highest percentage of SRP released among all of the food types. Additionally, it should be noted that post-digestion fine-grained particles returned to a P-Content very similar to the initial P-Content of particles used in the sorption experiment, near 2.7 µg/mg. Thus, it is possible that loosely and recently sorbed P on the fine-grained sediments is re-released to the water column during mussel digestion.

Release of P from sediments, whether aided by mussel digestion or other factors, is a complicated process that depends on the type of P within the sediments. Release may come from sorbed P associated with organic matter (OM) ternary complexes such as OM-Fe(III)-PO4 or OM-Al(III)-PO4. Such loosely sorbed P on the surface of particles may become dislodged during digestion. Other sediments, especially those within areas influenced by sewage inputs, have Fe-bound P which is redox-sensitive (Boström, 1984). P can also be released through chemical equilibrium dynamics and dissolution. A potential contributor to this type of P release is hydroxyapatite, which has been hypothesized to play a key role in maintaining Lake Michigan's consistent SRP concentrations (Brooks & Edgington, 1994). Future work would benefit from a more specific characterization of the composition of lake sediments and identifying potential sorption/redox/dissolution release mechanisms and how they may

interact with mussel digestion. Some of this work has been started in Lake Erie (Yuan et al., 2020), but characterization throughout all the basins could prove insightful.

The incubation time for the excretion and egestion experiments varied from 1.33 – 2.4 hours with most experiments falling in the 1.5-2 hour range. This was due to long filtration times associated with 0.6 μm membrane filters. And while I standardized results to account for both time and mussel mass, it is likely that excretion and egestion rates are not constant, but vary with time following a feeding event. Thus, differences in incubation times may alter rate calculations. This same observation is true for excretion and egestion results compared between studies more generally and may contribute to the variance of the rates in published literature. However, mussel excretion and egestion are not typically modeled as constant rates, but variable with changes in ambient PP, and filtration rates (J. Li et al., 2020; Rowe et al., 2015; Rowe et al., 2017; Shen, 2016; Shen et al., 2020; Zhou et al., 2021). So, measuring the rate is not as important as estimating the proportion of filtered PP that is allocated to egestion, excretion, and assimilation, which can be thought of as a digestion efficiency.

The results from this experiment offer some preliminary evidence that the "quality" of the food source, as determined by food source's P-content, can affect the efficiency with which mussels remove P during digestion. Such digestion efficiency ultimately affects the proportion of PP that is converted into SRP by mussel digestion and metabolism. This PP → SRP conversion efficiency (*f*), sometimes called mussel recycling efficiency or absorption efficiency, is an important modeling parameter that, as a proportion, is constrained to fall between values of 0 – 1. Studies have used *f* values as low as 0.29 (Zhou et al., 2021) or as high as 0.8 (Shen, 2016),

with model results and interpretations varying accordingly. Sensitivity analysis have shown that model results are highly sensitive to f with major implications in terms of lake management strategies (Zhou et al., 2021). However, to date, this parameter has largely been implemented as a constant chosen largely at the discretion of the modeler (J. Li et al., 2020; Rowe et al., 2015; Rowe et al., 2017; Shen, 2016; Shen et al., 2020; Zhou et al., 2021). The work here provides a simple and novel method for estimating f with data that suggest the practice of using a single value of f for all PP sources is inadvisable.

If the change in P-content is interpreted as a proxy for f, the ~66% estimate for the algae culture is similar to estimates of f for zebra mussels fed algae cultures of *Chlamydomonas reinhardtii* and *Pandorina morum*, which were 80.5% (Berg et al., 1996). In the lake, mussels are likely exposed to a wide range of particles that possess an equally wide range of P-Contents. Particles include numerous types of phytoplankton and bacteria that are likely to have high relative P-Content, but also other particles such as river seston and resuspended lake bottom sediments that may have lower initial P-Content. Thus, it is interesting that within the "other" category fine-grained particulates had both the highest initial P-Content (i.e. > 5 µg/mg) and were by far the most transformed particulate with an f near 50%. Is it possible that bacteria colonize fine-grained particulates and provide a relatively constant food source for mussels during resuspension events?

Continued work that investigates the P-Content, and more generally nutrient stoichiometry, of various nearshore materials, may prove fruitful since ecological theory suggests that differences in food supply nutrient stoichiometry should influence nutrient

excretion, egestion, and assimilation rates (Elser & Hassett, 1994; Bootsma & Liao, 2013). Figure 52 shows the P-Content of various nearshore materials measured during the course of this study including particulates egested by mussels. The data for mussel tissue P-Content was not measured in this study, but taken from the appendix of Li et al., (2020). Knowledge of mussel tissue and food source P-Content as well as the factors that determine timing of PP food source delivery to mussel beds (e.g. river plumes, resuspension events, vertical nearshore mixing, upwelling, etc.) may help predict and modulate f values used in models, providing a better picture of what mussels "do" with different particulate materials and how mussel food processing affects nearshore phosphorus dynamics.
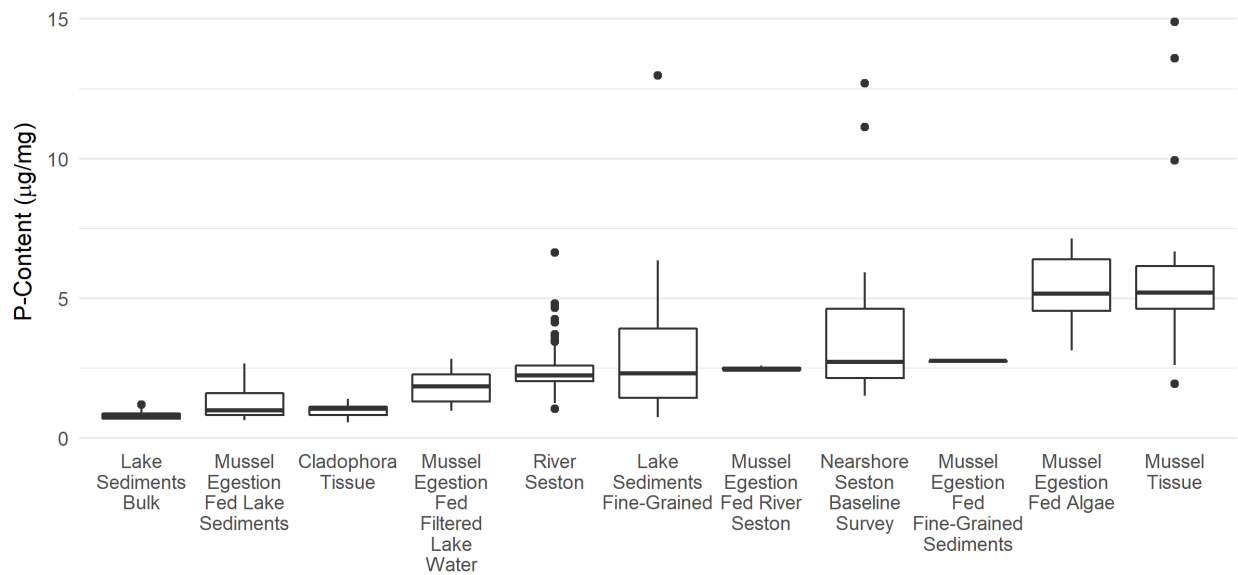
Figure 52: P-Content of Various Nearshore Materials.

Bulk lake sediments have a very low relative P-Content (~0.8 µg/mg) compared to other nearshore materials whereas mussels have a high median tissue P-Content value (~6 µg/mg). Worth noting is the similarity in the P-Content of mussel tissue and the egested waste after mussels were fed algae culture (two furthest right columns). Additionally note that mussel egestion fed fine-grained sediments and nearshore seston baseline survey have very similar median values. Additionally, *Cladophora* tissue has a low median P-Content that is only slightly higher than the median P-Content of bulk lake sediments.

Chapter 5: Conclusion

Cultural eutrophication has become the dominant water quality impairment in freshwater systems throughout the world. While other nutrients, such as carbon and nitrogen, can contribute to eutrophication, phosphorus is the nutrient traditionally considered to limit growth in freshwater systems (Schindler, 1971) and thus phosphorus management has been an important management tool both historically and presently (Schindler, 2006). Though at times it has been criticized as a reductionist approach to water quality management, phosphorus abatement has a long list of successful case studies (Schindler et al., 2016). However, despite these successes, the problem of eutrophication persists. Even after decades of work, there is still much uncertainty on the interactive effects nutrient loading can have on ecosystem structure and function (V. H. Smith & Schindler, 2009). Of particular concern is when eutrophication causes dramatic and sometimes catastrophic shifts, moving an ecosystem to an alternate stable state (Scheffer et al., 2001). Such catastrophic shifts seem most frequent within ecosystems that lack resiliency. Lack of ecosystem resiliency can also leave a system vulnerable to exotic invaders, some of which further exacerbate eutrophication issues (Gallardo et al., 2016). Organisms able to alter habitat and other abiotic factors through ecosystem engineering (Jones et al., 1994) create complex interactions destabilizing or moving a system to an alternate stable state (Emery-Butcher et al., 2020).

This thesis has examined the transport and fate of phosphorus in Lake Michigan's nearshore zone. The study was motivated by a resurgence of eutrophication issues in the nearshore zone (Auer et al., 2010), that has been paradoxically paired with issues of declining productivity in the pelagic zone (Hecky & DePinto, 2020). The very existence of this novel

165

dilemma provides evidence that Lake Michigan has experienced a phosphorus recycling paradigm shift in which external loading has been decoupled from yearly average offshore P concentrations and that Lake Michigan may be entering a new stable state. However, it is difficult to know if this regime shift is due to external (i.e. loading) or internal (i.e. nutrient cycling) mechanisms. Moreover, the answers are not mutually exclusive, and the two may be working in concert to shift the nutrient paradigm. Whatever the case, it seems clear that traditional TP management efforts are no longer working as originally intended (Chapra & Dolan, 2012), and will likely prove ineffective in reversing this state change (Scheffer et al., 2001). This underscores the need for a better mechanistic understanding of current phosphorus dynamics. The work within this thesis has attempted to aide in this understanding. The three broad questions related to the phosphorus dynamics addressed were:

1). How much (and what forms) are going into the lake?

2) Where does it go?

3) What happens to it?

Summary of Findings

Chapter two revisited Great Lakes eutrophication problems of the past and investigated the methods and models developed to combat it. It also provided some details on the development of modern modeling tools, with examples of how current models have been applied to eutrophication issues in the 21st century. Several concerns were raised over the growing complexity of models and the lack of transparency in current modeling practice.

Next, the proportional mass flux algorithm was introduced as a simple, but effective way to conduct mass balance modeling. Moreover, all the model parameters are stored efficiently and intuitively in a matrix, allowing for "clear box" modeling principles. A simple model of a River → Harbor → Nearshore → Pelagic system was constructed and used to explore several scenarios within the model system. Results revealed that not all changes to the system affected steady state nutrient fate. However, changes in flux to benthic stocks, which had long residence times, had disproportionally large effects, dramatically shifting steady state nutrient fate. Informed by both current literature review and exploratory modeling the research area was narrowed to the following:

1) Changes to and comparisons between phosphorus loading from agricultural and urban landscapes

2) Sediment phosphorus interactions

3) Mussel phosphorus interactions

Chapter 3 compared and contrasted loading from an agricultural (i.e. Sheboygan) and urban (i.e. Milwaukee) watershed. Initial results seemed to suggest that the watersheds were very similar, with similar total load and similar fractionation patterns within the load. However, when controlling for watershed size, it was Sheboygan (the agricultural landscape) that had a higher median annual TP yields (i.e. kg/km^2/yr: SHB = 31.4, MKE = 21.7).

The effect of discharge on SRP was examined for Sheboygan River during 3 major baseflow recessions with the hypothesis that increased river residence time (i.e. reduced flow) would decrease SRP. This was found to be true, and though a precise loss mechanism is not

known, the effect of discharge appeared to be seasonal. First order loss rates of SRP were calculated for each recession and revealing similar patterns with greater loss rates during the summer, and decreased loss rates in the fall. This may imply that river assimilation of SRP is light/temperature dependent, but may also suggest that it is a reduction of SRP input due to cover crop assimilation that creates a higher summer SRP loss rate in the summer. Regardless, increased river residence time in the summer, which coincides with the *Cladophora* growing season, can help reduce the export of SRP which is readily assimilated by *Cladophora*.

Comparisons between historic USGS and current P fractionation patterns revealed a large shift from particulate to soluble dominance. This patterns seems to be the driving force behind the increase in bioavailability that has been noted in other Great Lakes watersheds and may be due to land use practices such as no-till soil conservation (Baker et al., 2014). However, this trend was notable at both Sheboygan and Milwaukee, which seems to suggest that changes in agricultural land use alone cannot explain overall changes in the PP:SRP ratio. At a smaller scale, seasonal changes in the PP:SRP ratio, with increasing PP moving from summer to fall, seemed to coincide somewhat with mid-west land use practices such as the harvest of corn for grain. However, the trend was more gradual that would have been expected and it was Milwaukee that saw both greater and more sudden increases in the PP:SRP ratio in mid-October.

At Milwaukee, it was increases in NaOH-P that drove overall increases within the PP pool. NaOH-P is typically associated with fine-grained clay soils, rich in Fe and Al oxides that have high P sorption capacity and thus can act as a phosphate buffer mechanism (Richardson,

1985). A similar phosphate buffering mechanism is the coprecipitation of phosphate with calcium carbonate, which has been shown to be important in some hard water lakes (Birdsey, 1985). Optimal temperature, pH, and ambient SRP concentrations for coprecipitation may have let these two buffering mechanisms work in concert at Milwaukee in late October, maintaining SRP concentrations between 14 – 60 µg/L during a large precipitation event that drove Sheboygan SRP concentrations near 300 µg/L. Interestingly, phosphate sorption and buffering experiments conducted at the Yangze Estuary (M. Li et al., 2013) found that P interactions between water and fine-grained sediment could be induced by the precipitation of dicalcium phosphate ($CaHPO_4$) leading to Zero Equilibrium Phosphate Concentrations (EPC_0) between 14 and 60 µg/L, exactly what was seen at the Milwaukee River mouth.

Both the Milwaukee and Sheboygan Rivers showed a capacity for phosphate buffering in post-runoff recession conditions. This was evidenced by an increase in particle P-Content concurrent with the falling hydrograph. However, it was the Milwaukee River that showed overall higher P-Content, and thus sorption/buffering capacity i.e. (MKE ~1.5-5 µg/mg, SHB ~1.5-3 µg/mg). Further experimentation to determine if/which precipitate interaction occurs at the Milwaukee River and what has dampened phosphate buffering at the Sheboygan River could provide insight into nature based solutions that, if repaired or optimized, could help reduce phosphate export.

The aim of chapter 4 was to quantify processes related to and interactions between phosphorus, sediment, and quagga mussels. The primary tool was laboratory experiments. Initial experiments identified that "bulk" (i.e. non-size fractionated) lake sediments had little to

no effect on initial SRP concentrations when resuspended in bottle experiments. However, small fine-grained sediments with the same treatment showed high sorption capacity, reducing the initial SRP of the bottle accordingly.

This initial finding was extended into a fine-grained sediment sorption experiment that tracked declines in SRP and increases in sediment P-Content through time across a range of initial SRP concentrations. All sediments started with an initial P-Content near 1.2 µg/L. Sediments exposed to an initial SRP concentration near 27 ug/L (i.e. the max) sorbed phosphate and reached final P-Content near 6 µg/L, whereas sediments put into a container with an initial SRP near 0.5 µg/L (i.e. the min) desorbed SRP, and ended with a final P-Content near 0.8 µg/L, very similar to the mean measured P-Content of the bulk lake sediments. Moreover, the sorption reaction rate was fast, suggesting that reactive fine-grained sediments could quickly reduce SRP concentrations in the water column if resuspended. Additionally, settling rate experiments and calculations both estimated mean particle settling rates near 4-5 cm hr^{-1}, showing that fine-grained particles had the potential to stay suspended for weeks to months and may be important in exporting nutrients from nearshore to offshore.

However, mussel grazing experiments showed that mussels quickly reduced water turbidity, increasing the effective settling rates of both biotic and abiotic particles indiscriminately. Moreover, mussel feeding experiments showed that particle P-Content was reduced by 15 – 75% during digestion depending on food source type. Given the above average excretion rates of the fine-grained sediments group, this may indicate that sorbed P is re-released from particles during the digestion process. Additionally, it suggests that the current

modeling practice of a single value for the PP $\rightarrow$ SRP conversion efficiency is inadvisable since a range of conversion efficiencies are possible depending on food source.

Final Thoughts

So what is the take-away? What has caused Lake Michigan's nutrient paradigm shift, driving a divide between the nearshore and pelagic zones and decoupling the lakes eutrophication status from previous external TP loading models? Is the source external, or internal? It appears to be a bit of both. However, based on the data collected during this study and the results from exploratory modeling in chapter 2, it seems that external loads largely act to intensify BUIs in localized nearshore areas without necessarily affecting long-term nutrient fate. However, there is an exception to this. The increase of load bioavailability over time, in particular the large increase of SRP loading from rivers, has the potential to reduce nearshore to offshore P delivery seasonally if SRP is assimilated and stored in nearshore benthic nuisance algae. This seasonal effect may be further enhanced if sloughed nuisance algae is not transported and/or recycled in the pelagic but is more likely to stay in the nearshore zone.

But what allowed for greater benthic algae biomass in the first place? Increased water clarity due to dreissenid mussel filtration (Kuczynski et al., 2016). Thus mussels can indirectly reduce SRP export by creating a more favorable light environment for nearshore benthic nuisance algae while also directly reducing the export of river-borne PP through filtration, assimilation, excretion, and retention of PP in biodeposits. This 3-fold change in nearshore nutrient processing pathways is what has created a fundamental shift in Lake Michigan's P cycling structure and instigated the nutrient paradigm shift.

Much of this thesis has discussed the transport and fate of P-rich fine-grained particles. The question becomes, what would have happened to these particles pre-dreissenid? After potentially buffering SRP delivery to the lake through sorption dynamics in the river, fine-grained sediments may have acted as nutrient shuttles, carrying nutrients past potential biological assimilators in the nearshore zone, while simultaneously limiting benthic nuisance algae by attenuating the nearshore light environment. After a short residence in the nearshore (Hecky et al., 2004), fine-grained particles may have been exported to the low SRP pelagic zone where they may have released SRP through desorption/dissolution reactions. Dissolved phosphorus forms could have been recycled in the pelagic through the microbial loop (Azam et al,. 1983) while the remaining particulate phosphorus may have eventually settle into profundal sediments. During the winter isothermal period or early spring storms, profundal sediments can be resuspended (Eadie et al., 2008; Ji et al., 2002), loading the lake with weakly bound, nutrient rich particles at a magnitude equivalent to yearly tributary loading (Eadie et al., 1984). Additionally, fine-grained sediments may have provided an important food source for benthic detritivores such a *Pontoporeia hoyi* whose diet consisted of 99% silt and sediment (Evans et al., 1990).

What happens to P-rich fine-grained sediments presently? For starters, it seems that sediment export may be reduced due to no-till soil conservation practices (Baker et al., 2014). Sediments that do make it into the stream are potentially starting at a higher P-Content due to buildup of legacy P that can enrich groundwater (Robinson, 2015), potentially reducing their phosphate buffering capacity. However, as seen in this study, some fine-grained particles still play a role in buffering phosphate through sorption dynamics, though it seems that this

mechanism is somewhat impaired at the Sheboygan River. Upon export from the river to the lake, fine-grained particle fate changes drastically. Instead of being exported to the pelagic, particles entering the nearshore that are mixed to the benthos can be captured by mussel filtration. Mussel filtration reduces nearshore turbidity, and allows for greater colonization and faster growth rates of benthic nuisance algae (Bootsma, 2009), which in turn can assimilate the elevated SRP concentrations loaded from the river. During low pH, anoxic digestion, loosely sorbed P on the particle surface as including P bound to Fe oxides can be released as SRP, further promoting benthic nuisance algae. Egested particles have a reduced P-content, which may be further diminished by microbial colonization and eventually released as SRP (MacLellan-Hurd, 2020). If resuspended, particles may rapidly sorb SRP excreted by mussels in the benthic boundary layer, potentially limiting the export of SRP from nearshore to offshore during resuspension events. However, due to settling or vertical mixing, fine-grained particles may be returned to mussel beds and with a yo-yo like effect be recaptured by mussel filtration restarting the cycle.

Some have suggested that in order to combat offshore declines in productivity we may be able to increase non-point source loading in hopes of "making up" for the declines in offshore PP (Zhou et al., 2021). However, this view ignores the consequences of dreissenid ecosystem engineers laid out in the nearshore phosphorus shunt theory (Hecky et al., 2004), which predicts that such a strategy would only further exacerbate nearshore eutrophication issues due to mussel redirection of allochthonous nutrients to the nearshore benthos. Research within this thesis appears to confirm the shunt theory, and suggests that nearshore phosphorus management decisions may require a more nuanced approach. Such nuance may come from

gaining a deeper mechanistic understanding of nearshore phosphorus dynamics, some of which

I hope I have provided within this thesis.

References

Ackerman, J. D. (1999). Effect of velocity on the filter feeding of dreissenid mussels (*Dreissena polymorpha* and *Dreissena bugensis*): implications for trophic dynamics. *Canadian Journal of Fisheries and Aquatic Sciences*, *56*(9), 1551–1561. https://doi.org/10.1139/cjfas-56-9-1551

Alexander, R. B., Ludtke, A. S., Fitzgerald, K. K., & Schertz, T. L. (1996). *Data from selected U.S. Geological Survey National Stream Water-Quality Monitoring Networks (WQN)*. Reston, Virginia.

Arhonditsis, G. B., & Brett, M. T. (2004). Evaluation of the current state of mechanistic aquatic biogeochemical modeling. *Marine Ecology Progress Series*, *271*, 13–26. https://doi.org/10.1021/es061030q

Arhonditsis, G. B., Neumann, A., Shimoda, Y., Kim, D. K., Dong, F., Onandia, G., … Cheng, V. (2019). Castles built on sand or predictive limnology in action? Part B: Designing the next monitoring-modelling-assessment cycle of adaptive management in Lake Erie. *Ecological Informatics*, *53*(July), 100969. https://doi.org/10.1016/j.ecoinf.2019.05.015

Auer, M. T., Tomlinson, L. M., Higgins, S. N., Malkin, S. Y., Howell, E. T., & Bootsma, H. A. (2010a). Great Lakes Cladophora in the 21st century: Same algae-different ecosystem. *Journal of Great Lakes Research*, *36*(2), 248–255. https://doi.org/10.1016/j.jglr.2010.03.001

Auer, M. T., Tomlinson, L. M., Higgins, S. N., Malkin, S. Y., Howell, E. T., & Bootsma, H. A. (2010b). Great Lakes Cladophora in the 21st century: Same algae-different ecosystem. *Journal of Great Lakes Research*, *36*(2), 248–255. https://doi.org/10.1016/j.jglr.2010.03.001

Azam, F.; Fenchel, T.; Field, J. G.; Gray, J. S.; Meyer-Reil, L. A.; Thingstad, F. (1983). The Ecological Role of Water-Column Microbes in the Sea*. *Marine Ecology*, *10*, 257–263. https://doi.org/10.1021/acs.joc.6b00938

Baker, D. B., Confesor, R., Ewing, D. E., Johnson, L. T., Kramer, J. W., & Merryfield, B. J. (2014). Phosphorus loading to Lake Erie from the Maumee, Sandusky and Cuyahoga rivers: The importance of bioavailability. *Journal of Great Lakes Research*, *40*(3), 502–517. https://doi.org/10.1016/j.jglr.2014.05.001

Bannerman, R., Konrad, J. G., & Becker, D. (1979). *The IJC Menomonee River Watershed Study. Effects of Tributary Inputs On Lake Michigan During High Flows*. Retrieved from https://nepis.epa.gov/Exe/ZyPDF.cgi/20007A2T.PDF?Dockey=20007A2T.PDF

Bay, G., & Michigan, L. (2020). *DEVELOPMENT OF A HYDRODYNAMIC AND SEDIMENT TRANSPORT MODEL FOR GREEN BAY , LAKE MICHIGAN*. (May).

Beale, E. M. L. (1980). The blackett memorial lecture 1980. operational research and computers: A personal view. *Journal of the Operational Research Society*, *31*(9), 761–767.

https://doi.org/10.1057/jors.1980.143

Beletsky, D., O'Connor, W. P., Schwab, D. J., & Dietrich, D. E. (1997). Numerical simulation of internal Kelvin waves and coastal upwelling fronts. *Journal of Physical Oceanography*, *27*(7), 1197–1215. https://doi.org/10.1175/1520-0485(1997)027<1197:NSOIKW>2.0.CO;2

Berg, D. J., Fisher, S. W., & Landrum, P. F. (1996). Clearance and processing of algal particles by zebra mussels (Dreissena polymorpha). *Journal of Great Lakes Research*, *22*(3), 779–788. https://doi.org/10.1016/S0380-1330(96)70996-6

Bieiman, V. J., & Dolan, D. M. (1986). Modeling of phytoplankton in saginaw bay: II. post-audit phase. *Journal of Environmental Engineering (United States)*, *112*(2), 415–429. https://doi.org/10.1061/(ASCE)0733-9372(1986)112:2(415)

Biffi, F. (1963). Determinazione del fattore tempo come caratteristica del potere di autodepurazione del Lago d'Orta in relazione ad un inquinamento costante. *Science Letters*, *121*, 131–136.

Birdsey, P. (1985). *Coprecipitation of Phosphorus with Calcium Carbonate in Bear Lake, Utah - Idaho* (Utah State University). Retrieved from https://digitalcommons.usu.edu/etd/4401

Bivand, R., Keitt, T., & Rowlingson, B. (2021). *rgdal: Bindings for the "Geospatial" Data Abstraction Library*. Retrieved from https://cran.r-project.org/package=rgdal

Blumberg, A. F.; Mellor, G. L. (1987). A DESCRIPTION OF A THREE-DIMENSIONAL COASTAL OCEAN CIRCULATION MODEL. *Coastal and Estuarine Sciences*, *4*, 1–16.

Bootsma, H.A., Young, E. B., & Berges, J. . (2005). Temporal and spatial patterns of Cladophora biomass and nutrient stoichiometry in Lake Michigan. *Cladophora Research and Management in the Great Lakes*, 81–88. Retrieved from http://www.seagrant.wisc.edu/home/Portals/0/Files/Water Quality/Dec_05_Cladophora_Research_Workshop_Proceedings_2.pdf

Bootsma, Harvey A., & Liao, Q. (2013). Nutrient cycling by dreissenid mussels: Controlling factors and ecosystem response. In T. F. Nalepa & D. Schloesser (Eds.), *Quagga and Zebra Mussels: Biology, Impacts, and Control, Second Edition* (Second, pp. 555–574). https://doi.org/10.1201/b15437

Bootsma, Harvey A., Rowe, M. D., Brooks, C. N., & Vanderploeg, H. A. (2015). Commentary: The need for model development related to Cladophora and nutrient management in Lake Michigan. *Journal of Great Lakes Research*, *41*, 7–15. https://doi.org/10.1016/j.jglr.2015.03.023

Bootsma, Harvey A. (2009). *Causes , Consequences and Management of Nuisance Cladophora*. Retrieved from https://nepis.epa.gov/Exe/ZyPDF.cgi/P1006SLF.PDF?Dockey=P1006SLF.PDF

Bootsma, Harvey A, Waples, J. T., & Liao, Q. (2012). *Identifying major phosphorus pathways in the Lake Michigan nearshore zone*. Retrieved from

https://www.mmsd.com/application/files/9114/8192/3793/Major20Phosphorus20Pathwa ys20112.pdf

Boström, B. (1984). Potential Mobility of Phosphorus in Different Types of Lake Sediment. *Internationale Revue Der Gesamten Hydrobiologie Und Hydrographie*, *69*(4), 457–474. https://doi.org/https://doi.org/10.1002/iroh.19840690402

Boxall, A. B. A., Rudd, M. A., Brooks, B. W., Caldwell, D. J., Choi, K., Hickmann, S., … Van Der Kraak, G. (2012). Pharmaceuticals and personal care products in the environment: What are the big questions? *Environmental Health Perspectives*, *120*(9), 1221–1229. https://doi.org/10.1289/ehp.1104477

Bravo, H. R., Bootsma, H. A., & Khazaei, B. (2019a). Modeling the Transport and Fate of Phosphorus from a Point Source in the Lake Michigan Nearshore Zone. *Journal of Great Lakes Research*, *6865*(1). https://doi.org/10.1016/j.jglr.2019.09.007

Bravo, H. R., Bootsma, H., & Khazaei, B. (2019b). Fate of phosphorus from a point source in the Lake Michigan nearshore zone. *Journal of Great Lakes Research*, *45*(6), 1182–1196. https://doi.org/10.1016/j.jglr.2019.09.007

Brooks, A. S., & Edgington, D. N. (1994). Biogeochemical control of phosphorus cycling and primary production in Lake Michigan. *Limnology and Oceanography*, *39*(4), 961–968. https://doi.org/10.4319/lo.1994.39.4.0961

Bruce, J. P., & Higgins, P. M. (1978). Great Lakes Water Quality Agreement. *Eighth International Conference on Water Pollution Research*, 13–31. https://doi.org/10.1016/b978-0-08-020902-9.50006-7

Bunnell, D. B., Barbiero, R. P., Ludsin, S. A., Madenjian, C. P., Warren, G. J., Dolan, D. M., … Weidel, B. C. (2014). Changing ecosystem dynamics in the Laurentian Great Lakes: Bottom-up and top-down regulation. *BioScience*, *64*(1), 26–39. https://doi.org/10.1093/biosci/bit001

Burns, N. M., & Rosa, F. (1980). In situ measurement of the settling velocity of organic carbon particles and 10 species of phytoplankton. *Limnology and Oceanography*, *25*(5), 855–864. https://doi.org/10.4319/lo.1980.25.5.0855

Bzdusek, P. A., Lu, J., & Christensen, E. R. (2006). PCB congeners and dechlorination in sediments of Sheboygan River, Wisconsin, determined by matrix factorization. *Environmental Science and Technology*, *40*(1), 120–129. https://doi.org/10.1021/es050083p

Carpenter, S. R., Cole, J. J., Essington, T. E., Hodgson, J. R., Houser, J. N., Kitchell, J. F., & Pace, M. L. (1998). Evaluating alternative explanations in ecosystem experiments. *Ecosystems*, *1*(4), 335–344. https://doi.org/10.1007/s100219900025

Carreon-Martinez, L. B., Walter, R. P., Johnson, T. B., Ludsin, S. A., & Heath, D. D. (2015).

Benefits of turbid river plume habitat for lake erie yellow perch (Perca flavescens) recruitment determined by Juvenile to larval genotype assignment. *PLoS ONE*, *10*(5), 1–19. https://doi.org/10.1371/journal.pone.0125234

Caswell, H. (2002). *Matrix Population Models* (Second). Retrieved from https://www.whoi.edu/cms/files/mpm2e_tableofcontents_116984.pdf

Chapra, S. C. (1975). *Comment on "An Empirical Method of Estimating the Retention of Phosphorus in Lakes" by W. B. Kirchner and P. J. Dillon*. *11*(6), 1033–1034.

Chapra, S. C. (1977). Total Phosphorus Model For The Great Lakes. *Journal of the Environmental Engineering Division*, *103*(April), 147–161.

Chapra, S. C., & Dolan, D. M. (2012). Great Lakes total phosphorus revisited: 2. Mass balance modeling. *Journal of Great Lakes Research*, *38*(4), 741–754. https://doi.org/10.1016/j.jglr.2012.10.002

Chen, C., Liu, H., & Beardsley, R. C. (2003). An unstructured grid, finite-volume, three-dimensional, primitive equations ocean model: Application to coastal ocean and estuaries. *Journal of Atmospheric and Oceanic Technology*, *20*(1), 159–186. https://doi.org/10.1175/1520-0426(2003)020<0159:AUGFVT>2.0.CO;2

Claxton, W. T., Wilson, A. B., Mackie, G. L., & Boulding, E. G. (1998). A genetic and morphological comparison of shallow- and deep-water populations of the introduced dreissenid bivalve Dreissena bugensis. *Canadian Journal of Zoology*, *76*(7), 1269–1276. https://doi.org/10.1139/z98-064

DePinto, J. V., Young, T. C., & Martin, S. C. (1981). Algal-Available Phosphorus in Suspended Sediments from Lower Great Lakes Tributaries. *Journal of Great Lakes Research*, *7*(3), 311–325. https://doi.org/10.1016/S0380-1330(81)72059-8

Di Toro, D. M., Thomas, N. A., Herdendorf, C. E., Winfield, R. P., & Connolly, J. P. (1987). A Post Audit of a Lake Erie Eutrophication Model. *Journal of Great Lakes Research*, *13*(4), 801–825. https://doi.org/10.1016/S0380-1330(87)71692-X

Diggins, T. P. (2001). A seasonal comparison of suspended sediment filtration by quagga (Dreissena bugensis) and zebra (D. polymorpha) mussels. *Journal of Great Lakes Research*, *27*(4), 457–466. https://doi.org/10.1016/S0380-1330(01)70660-0

Dillon, P. J., & Rigler, F. H. (1974a). A Test of a Simple Nutrient Budget Model Predicting the Phosphorus Concentration in Lake Water. *Journal of the Fisheries Research Board of Canada*, *31*(11), 1771–1778. https://doi.org/10.1139/f74-225

Dillon, P. J., & Rigler, F. H. (1974b). The phosphorus-chlorophyll relationship in lakes. *Limnology and Oceanography*, *19*(September), 767–773.

Dolan, D. M., & Chapra, S. C. (2012). Great Lakes total phosphorus revisited: 1. Loading analysis and update (1994-2008). *Journal of Great Lakes Research*, *38*(4), 730–740.

https://doi.org/10.1016/j.jglr.2012.10.001

Dolan, D. M., Yui, A. K., & Geist, R. D. (1981). Evaluation of River Load Estimation Methods for Total Phosphorus. *Journal of Great Lakes Research*, *7*(3), 207–214. https://doi.org/10.1016/S0380-1330(81)72047-1

Dow, B. (2018). *Assessment and Mapping of the Milwaukee Estuary Habitat by* (University of Wisconsin-Milwaukee). Retrieved from https://dc.uwm.edu/etd/1785%0A

Eadie, B. J., Chambers, R. L., Gardner, W. S., & Bell, G. L. (1984). Sediment Trap Studies in Lake Michigan: Resuspension and Chemical Fluxes in the Southern Basin. *Journal of Great Lakes Research*, *10*(3), 307–321. https://doi.org/10.1016/S0380-1330(84)71844-2

Eadie, B. J., Robbins, J. A., Val Klump, J., Schwab, D. J., & Edgington, D. N. (2008). Winter-spring storms and their influence on sediment resuspension, transport, and accumulation patterns in southern Lake Michigan. *Oceanography*, *21*(SPL.ISS. 4), 118–135. https://doi.org/10.5670/oceanog.2008.09

El-Shaarawi, A. H., & Dolan, D. M. (1989). Maximum Likelihood Estimation of Water Quality Concentrations from Censored Data. *Canadian Journal of Fisheries and Aquatic Sciences*, *46*(6), 1033–1039. https://doi.org/10.1139/f89-134

Elser J. J., & Hassett R. P. (1994). A stoichiometric analysis of the zooplankton-phytoplankton interaction in marine and freshwater ecosystems. *Nature*, *370*, 211–213.

Emery-Butcher, H. E., Beatty, S. J., & Robson, B. J. (2020). The impacts of invasive ecosystem engineers in freshwaters: A review. *Freshwater Biology*, (October 2017), 999–1015. https://doi.org/10.1111/fwb.13479

Esra Dökümcüoğlu, V., & Yılmaz, M. (2020). Assessment of Cell Counting Method Based on Image Processing for a Microalga Culture. *MedFAR*, *3*(2), 75–81.

Evans, M. S., Quigley, M. A., & Wojcik, J. A. (1990). Comparative Ecology of Pontoporeia Hoyi Populations in Southern Lake Michigan: the Profundal Region versus the Slope and Shelf Regions. *International Journal of Great Lakes Research*, *16*(1), 27–40.

FAO, & IWMI. (2017). *Water pollution from agriculture: a global review Executive summary. Food and Agriculture Organization of the United Nations and the International Water Management Institute*. 35. Retrieved from http://www.fao.org/3/a-i7754e.pdf

Fillingham, J. H. (2015a). *Modeling Lake Michigan Nearshore Carbon and Phosphorus Dynamics*. University of Wisconsin-Milwaukee.

Fillingham, J. H. (2015b). MODELING LAKE MICHIGAN NEARSHORE CARBON AND PHOSPHORUS DYNAMICS (University of Wisconsin-Milwaukee; Vol. 8). https://doi.org/10.1017/CBO9781107415324.004

Froelich, P. N. (1988). Kinetic control of dissolved phosphate in natural rivers and estuaries: A

primer on the phosphate buffer mechanism. *Limnology*, *33*(July).

Gallardo, B., Clavero, M., Sánchez, M. I., & Vilà, M. (2016). Global ecological impacts of invasive species in aquatic ecosystems. *Global Change Biology*, *22*(1), 151–163. https://doi.org/10.1111/gcb.13004

Grayson, R. B., Finlayson, B. L., Gippel, C. J., & Hart, B. T. (1996). The potential of field turbidity measurements for the computation of total phosphorus and suspended solids loads. *Journal of Environmental Management*, *47*(3), 257–267. https://doi.org/10.1006/jema.1996.0051

Hamzah, F. B., Mohd Hamzah, F., Mohd Razali, S. F., Jaafar, O., & Abdul Jamil, N. (2020). Imputation methods for recovering streamflow observation: A methodological review. *Cogent Environmental Science*, *6*(1), 1745133. https://doi.org/10.1080/23311843.2020.1745133

Hanneman, R. a, & Riddle, M. (2005). Introduction to Social Network Methods. *Riverside, CA: University of California, Riverside. On-Line Textbook*, *46*(7), 5128–5130. https://doi.org/10.1016/j.socnet.2006.08.002

Hawley, N., & Zyren, J. E. (1990). Transparency Calibrations for Lake St. Clair and Lake Michigan. *International Journal of Great Lakes Research*, *16*(1), 113–120. Retrieved from https://www.glerl.noaa.gov/pubs/fulltext/1990/19900001.pdf

Hebert, P. D. N., Muncaster, B. W., & Mackie, G. L. (1989). Ecological and genetic studies on Dreissena polymorpha (Pallas): a new mollusc in the Great Lakes. *Canadian Journal of Fisheries and Aquatic Sciences*, *46*(9), 1587–1591. https://doi.org/10.1139/f89-202

Hecky, R., & DePinto, J. (2020). *Understanding declining productivity in the offshore regions of the Great Lakes*. Retrieved from https://ijc.org/sites/default/files/2020-07/SAB-SPC_DecliningProductivityReport_2020.pdf

Hecky, R. E., Smith, R. E. H., Barton, D. R., Guildford, S. J., Taylor, W. D., Charlton, M. N., & Howell, T. (2004, July). The nearshore phosphorus shunt: A consequence of ecosystem engineering by dreissenids in the Laurentian Great Lakes. *Canadian Journal of Fisheries and Aquatic Sciences*, Vol. 61, pp. 1285–1293. https://doi.org/10.1139/F04-065

Herb, W., Janke, B., Mohseni, O., & Stefan, H. (2008). Thermal Pollution of Streams by Runoff From Paved Surfaces. *Hydrological Processes*, *22*, 987–999. https://doi.org/10.1002/hyp.6986

Higgins, Scott N.; Hecky, Robert E.; Guildford, S. J. (2006). Environmental Controls of Cladophora Growth Dynamics in Eastern Lake Erie: Application of the Cladophora Growth Model (CGM). *Journal of Great Lakes Research*, *32*, 629–644. https://doi.org/10.3394/0380-1330(2006)32

Hijmans, R. J. (2020). *raster: Geographic Data Analysis and Modeling*. Retrieved from

https://cran.r-project.org/package=raster

Horgan, M. J., & Mills, E. L. (1997). Clearance rates and filtering activity of zebra mussel (Dreissena polymorpha): Implications for freshwater lakes. *Canadian Journal of Fisheries and Aquatic Sciences*, *54*(2), 249–255. https://doi.org/10.1139/f96-276

Howell, E. T., & Benoit, N. (2020). Nutrient footprints on the Toronto-Mississauga waterfront of Lake Ontario. *Journal of Great Lakes Research*, (xxxx). https://doi.org/10.1016/j.jglr.2020.11.009

Huang, C., Kuczynski, A., Auer, M. T., O'Donnell, D. M., & Xue, P. (2019). Management transition to the Great Lakes nearshore: Insights from hydrodynamic modeling. *Journal of Marine Science and Engineering*, *7*(5). https://doi.org/10.3390/jmse7050129

Hui, Y., Zhu, Z., Atkinson, J. F., & Saharia, A. M. (2021). Impacts of phosphorus loading temporal pattern on benthic algae growth in Lake Ontario. *Journal of Hydrology*, *598*, 126449. https://doi.org/10.1016/j.jhydrol.2021.126449

Hwang, H.-M., Fiala, M. J., Park, D., & Wade, T. L. (2016). Review of pollutants in urban road dust and stormwater runoff: part 1. Heavy metals released from vehicles. *International Journal of Urban Sciences*, *20*(3), 334–360. https://doi.org/10.1080/12265934.2016.1193041

James, W. F., & Barko, J. W. (2005). Biologically labile and refractory phosphorus loads from the agriculturally-managed upper eau galle river watershed, wisconsin. *Lake and Reservoir Management*, *21*(2), 165–173. https://doi.org/10.1080/07438140509354426

Ji, R., Chen, C., Budd, J. W., Schwab, D. J., Beletsky, D., Fahnenstiel, G. L., … Bundy, M. (2002). Influences of suspended sediments on the ecosystem in Lake Michigan: A 3-D coupled bio-physical modeling experiment. *Ecological Modelling*, *152*(2–3), 169–190. https://doi.org/10.1016/S0304-3800(02)00027-3

Jones, C. G., Lawton, J. H., & Shachak, M. (1994). Organisms as Ecosystem Engineers. *Oikos*, *69*(3), 373–386. Retrieved from http://www.jstor.org/stable/3545850

Kerr, J. M., DePinto, J. V., McGrath, D., Sowa, S. P., & Swinton, S. M. (2016). Sustainable management of Great Lakes watersheds dominated by agricultural land use. *Journal of Great Lakes Research*, *42*(6), 1252–1259. https://doi.org/10.1016/j.jglr.2016.10.001

Kleinman, P. J. A., Sharpley, A. N., McDowell, R. W., Flaten, D. N., Buda, A. R., Tao, L., … Zhu, Q. (2011). Managing agricultural phosphorus for water quality protection: Principles for progress. *Plant and Soil*, *349*(1–2), 169–182. https://doi.org/10.1007/s11104-011-0832-9

Kovalenko, K. E., Pelicice, F. M., Kats, L. B., Kotta, J., & Thomaz, S. M. (2021). Aquatic invasive species: introduction to the Special Issue and dynamics of public interest. *Hydrobiologia*, *848*(9), 1939–1953. https://doi.org/10.1007/s10750-021-04585-y

Kuczynski, A., Auer, M. T., Brooks, C. N., & Grimm, A. G. (2016). The cladophora resurgence in

Lake Ontario: Characterization and implications for management. *Canadian Journal of Fisheries and Aquatic Sciences*, *73*(6), 999–1013. https://doi.org/10.1139/cjfas-2015-0460

Lam, D. C. L., & Schertzer, W. M. (1987). Lake Erie Thermocline Model Results: Comparison with 1967–1982 Data and Relation to Anoxic Occurrences. *Journal of Great Lakes Research*, *13*(4), 757–769. https://doi.org/10.1016/S0380-1330(87)71689-X

Lam, D. C. L., Schertzer, W. M., & Fraser, A. S. (1987). A Post-Audit Anaylsis of the NWRI Nine-Box Water Quality Model for Lake Erie. *Journal of Great Lakes Research*, *13*(4), 782–800. https://doi.org/10.1016/S0380-1330(87)71691-8

Landi, P., Minoarivelo, H. O., Brännström, Å., Hui, C., & Dieckmann, U. (2018). Complexity and stability of ecological networks: a review of the theory. *Population Ecology*, *60*(4), 319–345. https://doi.org/10.1007/s10144-018-0628-3

Larson, J. H., Evans, M. A., Fitzpatrick, F. A., Frost, P. C., Bailey, S., Kennedy, R., … Reneau, P. C. (2019). Water column nutrient processing rates in rivermouths of Green Bay (Lake Michigan). *Biogeochemistry*, *142*(1), 73–93. https://doi.org/10.1007/s10533-018-0517-z

Larson, J. H., Frost, P. C., Vallazza, J. M., Nelson, J. C., & Richardson, W. B. (2016). Do rivermouths alter nutrient and seston delivery to the nearshore? *Freshwater Biology*, *61*(11), 1935–1949. https://doi.org/10.1111/fwb.12827

Larson, J. H., Trebitz, A. S., Steinman, A. D., Wiley, M. J., Mazur, M. C., Pebbles, V., … Seelbach, P. W. (2013). Great Lakes rivermouth ecosystems: Scientific synthesis and management implications. *Journal of Great Lakes Research*, *39*(3), 513–524. https://doi.org/10.1016/j.jglr.2013.06.002

Lee, G., Jones, R., & Rast, W. (1980). Availability of phosphorus to phytoplankton and its implications for phosphorus management strategies. *Phosphorus Management Strategies for Lakes.*, 1–42. Retrieved from http://www.gfredlee.com/Nutrients/Avail-P.pdf

Lei, J., Payne, B. S., & Wang, S. Y. (1996). Filtration dynamics of the zebra mussel, *Dreissena polymorpha*. *Canadian Journal of Fisheries and Aquatic Sciences*, *53*(1), 29–37. https://doi.org/10.1139/cjfas-53-1-29

Leontief, W. W. (1936). Quantitative Input and Output Relations in the Economic Systems of the United States. *The Review of Economics and Statistics*, *18*(3), 105–125. Retrieved from http://www.jstor.org/stable/1927837

Li, J., Ianaiev, V., Huff, A., Zalusky, J., Ozersky, T., & Katsev, S. (2020). *Benthic invaders control the phosphorus cycle in the world's largest freshwater ecosystem*. (16). https://doi.org/10.1073/pnas.2008223118

Li, M., Whelan, M. J., Wang, G. Q., & White, S. M. (2013). Phosphorus sorption and buffering mechanisms in suspended sediments from the Yangtze Estuary and Hangzhou Bay, China. *Biogeosciences*, *10*(5), 3341–3348. https://doi.org/10.5194/bg-10-3341-2013

Lin, P., & Guo, L. (2016). Dynamic changes in the abundance and chemical speciation of dissolved and particulate phosphorus across the river-lake interface in southwest Lake Michigan. *Limnology and Oceanography*, *61*(2), 771–789. https://doi.org/10.1002/lno.10254

Logan, T., Verhoff, F. H., & Depinto, J. V. (1979). *Biological Availability of Total Phosphorus*. Retrieved from https://apps.dtic.mil/sti/pdfs/ADA083694.pdf

MacLellan-Hurd, R.-A. (2020). *Quagga Mussel Induced Phosphorus Cycling Changes in Lake Michigan* (University of Wisconsin - Milwaukee). Retrieved from https://dc.uwm.edu/etd/2557

Madenjian, C. P., Pothoven, S. A., Schneeberger, P. J., Ebener, M. P., Mohr, L. C., Nalepa, T. F., & Bence, J. R. (2010). Dreissenid mussels are not a " dead end " in Great Lakes food webs. *Journal of Great Lakes Research*, *36*, 73–77. Retrieved from https://digitalcommons.unl.edu/usdeptcommercepub/402

Madon, S. P., Schneider, D. W., Stoeckel, J. A., & Sparks, R. E. (1998). Effects of inorganic sediment and food concentrations on energetic processes of the zebra mussel, *Dreissena polymorpha*: implications for growth in turbid rivers. *Canadian Journal of Fisheries and Aquatic Sciences*, *55*(2), 401–413. https://doi.org/10.1139/cjfas-55-2-401

Marcarelli, A. M., Coble, A. A., Meingast, K. M., Kane, E. S., Brooks, C. N., Buffam, I., … Stottlemyer, R. (2019). Of Small Streams and Great Lakes: Integrating Tributaries to Understand the Ecology and Biogeochemistry of Lake Superior. *Journal of the American Water Resources Association*, *55*(2), 442–458. https://doi.org/10.1111/1752-1688.12695

McDowell, R. W., Worth, W., & Carrick, S. (2021). Evidence for the leaching of dissolved organic phosphorus to depth. *Science of the Total Environment*, *755*, 142392. https://doi.org/10.1016/j.scitotenv.2020.142392

Mills, E. L., Dermott, R. M., Roseman, E. F., Dustin, D., Mellina, E., Conn, D. B., & Spidle, A. P. (1993). Colonization, ecology, and population structure of the "Quagga" mussel (Bivalvia: Dreissenidae) in the lower Great Lakes. *Canadian Journal of Fisheries and Aquatic Sciences*, *50*(11), 2305–2314. https://doi.org/10.1139/f93-255

Montenero, M. P., Dilbone, E. K., & Waples, J. T. (2017). Using medically-derived iodine-131 to track sewage effluent in the Laurentian Great Lakes. *Water Research*, *123*, 773–782. https://doi.org/10.1016/j.watres.2017.07.022

Mosley, C., & Bootsma, H. (2015). Phosphorus recycling by profunda quagga mussels (Dreissena rostriformis bugensis) in Lake Michigan. *Journal of Great Lakes Research*, *41*, 38–48. https://doi.org/10.1016/j.jglr.2015.07.007

Naddafi, R., & Rudstam, L. G. (2013). Predator-induced behavioural defences in two competitive invasive species: The zebra mussel and the quagga mussel. *Animal Behaviour*, *86*(6), 1275–1284. https://doi.org/10.1016/j.anbehav.2013.09.032

Nalepa, T. F. (2010). An Overview of the Spread, Distribution, and Ecological Impacts of the Quagga Mussel, Dreissena rostriformis bugensis, with Possible Implications to the Colorado River System. *Proceedings of the Colorado River Basin Science and Resource Management Symposium, November 18–20, 2008, Scottsdale, Arizona: Coming Together: Coordination of Science and Restoration Activities for the Colorado River Ecosystem*, 113–121. Retrieved from https://www.glerl.noaa.gov/pubs/fulltext/2010/20100039.pdf

Newcomer Johnson, T. A., Kaushal, S. S., Mayer, P. M., Smith, R. M., & Sivirichi, G. M. (2016). Nutrient retention in restored streams and rivers: A global review and synthesis. *Water (Switzerland)*, *8*(4), 1–28. https://doi.org/10.3390/w8040116

Newton, R. J., & McLellan, S. L. (2015). A unique assemblage of cosmopolitan freshwater bacteria and higher community diversity differentiate an urbanized estuary from oligotrophic Lake Michigan. *Frontiers in Microbiology*, *6*(SEP). https://doi.org/10.3389/fmicb.2015.01028

Paerl, H. W., Fulton, R. S., Moisander, P. H., & Dyble, J. (2001). Harmful freshwater algal blooms, with an emphasis on cyanobacteria. *TheScientificWorldJournal*, *1*, 76–113. https://doi.org/10.1100/tsw.2001.16

Paul, M. J., & Meyer, J. L. (2001). STREAMS IN THE URBAN LANDSCAPE. *Annual Review of Ecology and Systematics*, *21*(1), 333–365. https://doi.org/10.1146/annurev.ecolsys.32.081501.114040

Pebesma, E. (2018). Simple Features for R: Standardized Support for Spatial Vector Data. *The R Journal*, *10*(1), 439–446. https://doi.org/10.32614/RJ-2018-009

Pilcher, D. J., McKinley, G. A., Kralj, J., Bootsma, H. A., & Reavie, E. D. (2017). Modeled sensitivity of Lake Michigan productivity and zooplankton to changing nutrient concentrations and quagga mussels. *Journal of Geophysical Research: Biogeosciences*, *122*(8), 2017–2032. https://doi.org/10.1002/2017JG003818

Prestigiacomo, A. R., Effler, S. W., Gelda, R. K., Matthews, D. A., Auer, M. T., Downer, B. E., … Walter, M. T. (2016). Apportionment of bioavailable phosphorus loads entering Cayuga Lake, New York. *Journal of the American Water Resources Association*, *52*(1), 31–47. https://doi.org/10.1111/1752-1688.12366

R Core Team. (2020). *R: A Language and Environment for Statistical Computing*. Retrieved from https://www.r-project.org/

Rainey, R. H. (1967). Natural displacement of pollution from the Great Lakes. *Science*, *155*(3767), 1242–1243. https://doi.org/10.1126/science.155.3767.1242

Ready, K. R., Kadlec, R. H., Flaig, E., & Gale, P. M. (1999). Phosphorus retention in streams and wetlands: A review. *Critical Reviews in Environmental Science and Technology*, *29*(1), 83–146. https://doi.org/10.1080/10643389991259182

Reisinger, A. J., Tank, J. L., Rosi-Marshall, E. J., Hall, R. O., & Baker, M. A. (2015). The varying role of water column nutrient uptake along river continua in contrasting landscapes. *Biogeochemistry*, *125*(1), 115–131. https://doi.org/10.1007/s10533-015-0118-z

Richardson, C. J. (1985). Mechanisms Controlling Phosphorus Retention. *Science*, *228*, 1424–1427.

Robertson, D. M., & Saad, D. A. (2011). Nutrient Inputs to the Laurentian Great Lakes by Source and Watershed Estimated Using SPARROW Watershed Models. *Journal of the American Water Resources Association*, *47*(5), 1011–1033. https://doi.org/10.1111/j.1752-1688.2011.00574.x

Robinson, C. (2015). Review on groundwater as a source of nutrients to the Great Lakes and their tributaries. *Journal of Great Lakes Research*, *41*(4), 941–950. https://doi.org/10.1016/j.jglr.2015.08.001

Rowe, M. D., Anderson, E. J., Wang, J., & Vanderploeg, H. A. (2015). Modeling the effect of invasive quagga mussels on the spring phytoplankton bloom in Lake Michigan. *Journal of Great Lakes Research*, *41*, 49–65. https://doi.org/10.1016/j.jglr.2014.12.018

Rowe, Mark D., Anderson, E. J., Vanderploeg, H. A., Pothoven, S. A., Elgin, A. K., Wang, J., & Yousef, F. (2017). Influence of invasive quagga mussels, phosphorus loads, and climate on spatial and temporal patterns of productivity in Lake Michigan: A biophysical modeling study. *Limnology and Oceanography*, *62*(6), 2629–2649. https://doi.org/10.1002/lno.10595

Scavia, D. (1980). AN ECOLOGICAL MODEL OF LAKE ONTARIO. *Ecological Modelling*, *8*(162), 49–78. Retrieved from http://scavia.seas.umich.edu/wp-content/uploads/2009/11/scavia_1980.pdf

Scavia, D., & Fahnenstiel, G. L. (1987). Dynamics of Lake Michigan Phytoplankton: Mechanisms Controlling Epilimnetic Communities. *Journal of Great Lakes Research*, *13*(2), 103–120. https://doi.org/10.1016/S0380-1330(87)71635-9

Scheffer, M., Carpenter, S., Foley, J. A., Folke, C., & Walker, B. (2001). Catastrophic shifts in ecosystems. *Nature*, *413*(6856), 591–596. https://doi.org/10.1038/35098000

Schindler, D W. (1971). CARBON, NITROGEN, AND PHOSPHORUS AND THE EUTROPHICATION OF FRESHWATER LAKES1. *Journal of Phycology*, *7*(4), 321–329. https://doi.org/10.1111/j.1529-8817.1971.tb01527.x

Schindler, D W. (2006). Recent advances in the understanding and management of eutrophication. *Limnology and Oceanography*, *51*, 356–363. https://doi.org/10.12688/f1000research.15081.1

Schindler, David W., Carpenter, S. R., Chapra, S. C., Hecky, R. E., & Orihel, D. M. (2016). Reducing phosphorus to curb lake eutrophication is a success. *Environmental Science and*

Technology, *50*(17), 8923–8929. https://doi.org/10.1021/acs.est.6b02204

Schneider, C. A., Rasband, W. S., & Eliceiri, K. W. (2012). NIH Image to ImageJ: 25 years of image analysis. *Nature Methods*, *9*(7), 671–675. https://doi.org/10.1038/nmeth.2089

Schwab, D. J., Beletsky, D., & Lou, J. (2000). The 1998 coastal turbidity plume in Lake Michigan. *Estuarine, Coastal and Shelf Science*, *50*(1), 49–58. https://doi.org/10.1006/ecss.1999.0531

Schwab, David J, & Beletsky, D. (1998). Lake Michigan Mass Balance Study: Hydrodynamic Modeling Project. *NOAA Technical Memorandum ERL GLERL*, 1–53. Retrieved from https://www.glerl.noaa.gov//pubs/tech_reports/glerl-108/tm-108.pdf

Sharpley, A. N. (2003). Soil Mixing to Decrease Surface Stratification of Phosphorus in Manured Soils. *Journal of Environmental Quality*, *32*(4), 1375–1384. https://doi.org/https://doi.org/10.2134/jeq2003.1375

Sharpley, A. N., Smith, S. J., Jones, O. R., Berg, W. A., & Coleman, G. A. (1992). The Transport of Bioavailable Phosphorus in Agricultural Runoff. *Journal of Environmental Quality*, *21*(1), 30–35. https://doi.org/10.2134/jeq1992.00472425002100010003x

Shen, C. (2016). Modeling of dreissenid mussel impacts on Lake Michigan. Retrieved from https://dc.uwm.edu/etd/1309

Shen, C., Liao, Q., & Bootsma, H. A. (2020). Modelling the influence of invasive mussels on phosphorus cycling in Lake Michigan. *Ecological Modelling*, *416*(June 2019), 108920. https://doi.org/10.1016/j.ecolmodel.2019.108920

Shen, C., Liao, Q., Bootsma, H. A., Troy, C. D., & Cannon, D. (2018). Regulation of plankton and nutrient dynamics by profundal quagga mussels in Lake Michigan: a one-dimensional model. *Hydrobiologia*, *815*(1), 47–63. https://doi.org/10.1007/s10750-018-3547-6

Smith, B. J., & Simpkins, D. G. (2018). Influence of river plumes on the distribution and composition of nearshore Lake Michigan fishes. *Journal of Great Lakes Research*, *44*(6), 1351–1361. https://doi.org/10.1016/j.jglr.2018.08.012

Smith, D. R., Francesconi, W., Livingston, S. J., & Huang, C. hua. (2015). Phosphorus losses from monitored fields with conservation practices in the Lake Erie Basin, USA. *Ambio*, *44*(2), 319–331. https://doi.org/10.1007/s13280-014-0624-6

Smith, V. H., & Schindler, D. W. (2009). Eutrophication science: where do we go from here? *Trends in Ecology and Evolution*, *24*(4), 201–207. https://doi.org/10.1016/j.tree.2008.11.009

Stone, S. J. L. and S. F. (2005). *National Center for Environmental Economics - The Economic Impacts of Aquatic Invasive Species : A Review of the Literature*.

Strayer, D. L., Caraco, N. F., Cole, J. J., Findlay, S., & Pace, M. L. (1999). Transformation of freshwater ecosystems by bivalves: A case study of zebra mussels in the Hudson River.

BioScience, *49*(1), 19–27. https://doi.org/10.2307/1313490

Tang, H., Vanderploeg, H. A., Johengen, T. H., & Liebig, J. R. (2014). Quagga mussel (Dreissena rostriformis bugensis) selective feeding of phytoplankton in Saginaw Bay. *Journal of Great Lakes Research*, *40*(S1), 83–94. https://doi.org/10.1016/j.jglr.2013.11.011

Thomann, R V. (1974). *Systems Analysis and Water Quality Management*. Retrieved from https://books.google.com/books?id=XeVRAAAAMAAJ

Thomann, Robert V, Di Toro, D. M., Winfield, R. P., & O'Connor, D. J. (1975). *Mathematical modelling of phytoplankton in Lake Ontario*. (EPA-660/3-75-005).

Tomlinson, L. M., Auer, M. T., Bootsma, H. A., & Owens, E. M. (2010). The Great Lakes Cladophora Model: Development, testing, and application to Lake Michigan. *Journal of Great Lakes Research*, *36*(2), 287–297. https://doi.org/10.1016/j.jglr.2010.03.005

Turschak, B. A., & Bootsma, H. A. (2015). Lake Michigan trophic structure as revealed by stable C and N isotopes. *Journal of Great Lakes Research*, *41*(May), 185–196. https://doi.org/10.1016/j.jglr.2015.04.004

Turschak, B. A., Bunnell, D., Czesny, S., Höök, T. O., Janssen, J., Warner, D., & Bootsma, H. A. (2014). Nearshore energy subsidies support Lake Michigan fishes and invertebrates following major changes in food web structure. *Ecology*, *95*(5), 1243–1252. https://doi.org/10.1890/13-0329.1

USGS. (1999). A New Evaluation of the USGS Streamgaging Network. *US Geological Survey: A Report to Congress*. Retrieved from http://water.usgs.gov/streamgaging/report.pdf

V., T. R., & J., S. M. (1964). Estuarine Water Quality Management and Forecasting. *Journal of the Sanitary Engineering Division*, *90*(5), 9–38. https://doi.org/10.1061/JSEDAI.0000505

Valipour, R., León, L. F., Depew, D., Dove, A., & Rao, Y. R. (2016). High-resolution modeling for development of nearshore ecosystem objectives in eastern Lake Erie. *Journal of Great Lakes Research*, *42*(6), 1241–1251. https://doi.org/10.1016/j.jglr.2016.08.011

Vanderploeg, H. A., Bunnell, D. B., Carrick, H. J., & Höök, T. O. (2015). Complex interactions in Lake Michigan's rapidly changing ecosystem. *Journal of Great Lakes Research*, Vol. 41, pp. 1–6. https://doi.org/10.1016/j.jglr.2015.11.001

Vanderploeg, H. A., Liebig, J. R., Carmichael, W. W., Agy, M. A., Johengen, T. H., Fahnenstiel, G. L., & Nalepa, T. F. (2001). Zebra mussel (*Dreissena polymorpha*) selective filtration promoted toxic *Microcystis* blooms in Saginaw Bay (Lake Huron) and Lake Erie. *Canadian Journal of Fisheries and Aquatic Sciences*, *58*(6), 1208–1221. https://doi.org/10.1139/cjfas-58-6-1208

Vanderploeg, H. A., Liebig, J. R., Nalepa, T. F., Fahnenstiel, G. L., & Pothoven, S. A. (2010). Dreissena and the disappearance of the spring phytoplankton bloom in Lake Michigan. *Journal of Great Lakes Research*, *36*, 50–59. https://doi.org/10.1016/J.JGLR.2010.04.005

Vollenweider, R.A. (1969). Moglichkeiten und Grenzen elementarer Modelle der Stoffbiilanz von Seen. *Hydrobiologia*, *66*, 1–36.

Vollenweider, Richard A. (1975). Input-output models - With special reference to the phosphorus loading concept in limnology. *Schweizerische Zeitschrift Für Hydrologie*, *37*(1), 53–84. https://doi.org/10.1007/BF02505178

Wang, Y., Hammes, F., Boon, N., & Egli, T. (2007). Quantification of the filterability of freshwater bacteria through 0.45, 0.22, and 0.1 µm pore size filters and shape-dependent enrichment of filterable bacterial communities. *Environmental Science and Technology*, *41*(20), 7080–7086. https://doi.org/10.1021/es0707198

Waples, J. T., Bootsma, H. A., & Klump, J. V. (2017). How are coastal benthos fed? *Limnology and Oceanography Letters*, *2*(1), 18–28. https://doi.org/10.1002/lol2.10033

Warner, D. M., & Lesht, B. M. (2015). Relative importance of phosphorus, invasive mussels and climate for patterns in chlorophyll a and primary production in Lakes Michigan and Huron. *Freshwater Biology*, *60*(5), 1029–1043. https://doi.org/10.1111/fwb.12569

Wilkins, M. B. 1984. Advance Plant Physiology. Pitman Publishing, Ltd., London.

Woolley, J. P., McGowan, M. L., Teare, H. J. A., Coathup, V., Fishman, J. R., Settersten, R. A., … Juengst, E. T. (2016). Citizen science or scientific citizenship? Disentangling the uses of public engagement rhetoric in national research initiatives Donna Dickenson, Sandra Soo-Jin Lee, and Michael Morrison. *BMC Medical Ethics*, *17*(1), 1–17. https://doi.org/10.1186/s12910-016-0117-1

Wu, J., Sunda, W., Boyle, E. A., & Karl, D. M. (2000). Phosphate depletion in the Western North Atlantic Ocean. *Science*, *289*(5480), 759–762. https://doi.org/10.1126/science.289.5480.759

Wuebbles, D., Cardinale, B., Cherkauer, K., Davidson-Arnott, R., Hellmann, J., Infante, D., … Ballinger, A. (2019). An Assessment of the Impacts of Climate Change on the Great Lakes. *The Environmental Law & Policy Center*, 74. Retrieved from http://elpc.org/wp-content/uploads/2019/03/Great-Lakes-Climate-Change-Report.pdf

Yuan, F., Li, H., Kakarla, R., Kasden, C., Yao, S., Xue, B., & Sun, Y. (2020). Variability of sedimentary phosphorus fractions in the western and Sandusky basins of Lake Erie. *Journal of Great Lakes Research*, *46*(4), 976–988. https://doi.org/10.1016/j.jglr.2020.05.013

Zhou, X., Auer, M. T., & Xue, P. (2021). Open lake phosphorus forcing of cladophora growth: Modeling the dual challenge in great lakes trophic state management. *Water (Switzerland)*, *13*(19). https://doi.org/10.3390/w13192680

Appendix: Links to Data Sources, Web Applications, and Tutorials

Raw data files and source code for apps are available on my github page
https://github.com/natevanee

Web based GUIs for matrix modeling and data exploration tools are available on my Shiny Server. These tools provide options for interactive plotting and data table creation as well as plot and data download options.

NutriModeler: https://nvanee.shinyapps.io/NutrientLoadingModel/

LimnoExplorer: https://nvanee.shinyapps.io/LimnoExplorer/

BuoyApp_2020: https://nvanee.shinyapps.io/BuoyApp_2020/

Additional R Markdown tutorials, including examples of automating data retrieval from federal servers, are available on my RPubs page: https://rpubs.com/nvanee